UNIVERSITY OF OSLO
Department of Geosciences
MetOs section

Modelling effects of exhaust from diesel and gasoline vehicles on tropospheric chemistry

Master thesis in Geosciences Meteorology and oceanography

Karianne Ødemark

02.03.2009

Abstract

Automobile emissions are known to contribute to local air pollution and to be a considerable sized source of CO_2. The impact on tropospheric chemistry is investigated in this thesis, for road traffic as a whole and for gasoline and diesel emissions separately. Also, estimates of radiative forcings imposed by the two fuel types are done.

A chemical-transport model, OsloCTM2, is applied to examine the effects from several model runs with different emission scenarios. The effect of emission legislations, Euro4 and Euro5 is investigated, in addition to surface ozone concentrations in populated areas, bearing in mind the health treath ozone poses to humans. In the Euro4 and Euro5 model runs, total fuel consumption are sat to either gasoline or diesel emissions, and to satisfy emission factors based on the EU legislation emission limits. Estimates of radiative forcings from road traffic induced alterations in CH_4, O_3, black carbon and CO_2 are performed.

The results show that summertime surface ozone concentrations due to gasoline emissions increase 5-13 ppb in the most urbanized regions in the Northern Hemisphere, while in more remote areas, the increase is up to 3 ppb. In winter a decrease of 4 ppb is found north of 30° N in industrialized regions. For diesel, increased levels in the range of 1-3 ppb are found over Europe in summer, while in winter there is a decrease of 2 ppb. The corresponding ozone-related forcings are 39.6 mWm^{-2} from gasoline and 2.6 mWm^{-2} from diesel. In the Euro4 case, increase in surface ozone levels are in the range of 1-4 ppb for gasoline and 2-6 ppb for diesel. In Euro5, the levels are reduced compared to Euro4, for gasoline the concentrations are from 0.5-2.5 ppb and for diesel 1-4 ppb. The ozone induced forcings in these cases are 7.6, 16.1, 6.0 and 13.2 mWm^{-2} for Euro4 gasoline, Euro4 diesel, Euro5 gasoline and Euro5 diesel, respectively.

Radiative forcings from alterations in CH_4 give negative values for the various model runs. Change in burden in black carbon, leads to a higher forcing from diesel than from gasoline, as opposed to forcings from CO_2. For radiative forcings due to O_3, CH_4, BC and CO_2 added up in the Euro4 case, the results show that while diesel has a larger forcing than gasoline in a time frame of 20 years, in time frames of 100 and 500 years, forcing from gasoline surpasses the forcing from diesel. All the components added up in the Euro5 case, show that the stricter legislations considerably decrease the estimated forcings. On a time frame of 20 years, diesel still has the largest forcing, while in 100 years, it is slightly less than gasoline. On a time frame of 500 years, gasoline is the major contributor to radiative forcing of the two fuel

types.

Levels of surface ozone obtained every hour in three different regions, show that road traffic contribute to the highest occurring levels of ozone by a fear shear. In USA, Europe and Asia, respectively 9, 8 and 4 % of concentrations between 40 and 100 ppb is due to road traffic. The results show that a transfer from Euro4 to Euro5 reduces the occurrences of the highest ozone levels, thus a larger shear of the health intiminating levels is expected to decrease when transferring from Euro4 to Euro5 legislation emission limits.

Acknowledgements

First of all I would like to thank my supervisor, Terje Berntsen for a interesting and exciting topic to work with, and for inspiring and uplifting guidance. I would also like to thank Jens Borken at DLR (Deutsches Zentrum für Luft- und Raumfahrt) for providing the emission data through the EU project QUANTIFY.

A big thank you also goes out to Amund Søvde, for helping me with all kinds of computer- and model related problems. And Ole Kristian Kvissel, for getting me started with the model, and for being there with answers throughout the working process. I would also like to thank Stig B. Dalsøren for helping me with getting the emission data safely into the model. Also, a thank you goes out to Ragnhild Bieltvedt Skeie for the snow-code for the Black Carbon model runs. Last, but not least, I want to thank my fellow students for making the time spent in the study hall much more fun! Especially Nina Kristiansen, with whom I shared the finishing stage. Thank you for making it much more easy to keep up the spirit.

Contents

Chapter 1

Introduction

Earth's climate is warming due to anthropogenic emissions, and carbon dioxide (CO_2) is identified as the main, though not the only, cause for the observed warming (IPCC, 2001). CO_2 is one of six greenhouse gases included in the Kyoto Protocol, consequently CO_2 emissions are regulated. However, the tropospheric ozone precursors carbon monoxide, CO, hydrocarbons, $NMVOC$, nitrogen oxides, NO_x, and the aerosol precursor black carbon, organic carbon and SO_2, not included in the Kyoto Protocol, also play significant roles in climate change (Rypdal et al., 2005). NO_x, VOC and CO are however regulated for air pollution in e.g Europe.

The primary emission source of CO_2 is fossil fuel combustion, and emissions from road transport constitute a significant and growing share of the greenhouse gas emission (Berntsen et al., 2009). This has lead to a taxation of cars emitting CO_2. Automobiles with diesel engines emit $\sim$ 20 % less CO_2 per km than a similar car with gasoline engine (Mazzi and Dowlatabadi, 2006). The exhaust emission inventory from Borken et al. (2007) used in this thesis and presented in chaper 3.2 estimates diesel to emit 28 % less CO_2 than gasoline. A climate migitation policy that focuses on CO_2 emission is expected to lead to an increase of automobiles with diesel engines; in Norway the fraction of diesel passenger cars increased by 10 % from 2000 to 2006.

However, car exhaust consists of more than CO_2; components with an indirect greenhouse effect through chemical reactions or with an influence on the Earth's albedo are also emitted. NO_x, CO and hydrocarbons lead to chemical production of ozone (O_3) as well as changes in the concentration of the OH radical, the main oxidant of the atmosphere (Niemeier et al., 2006; Matthes et al., 2007). Changes in OH affect the lifetime of methane (CH_4), thus emissions of NO_x, CO and $NMVOC$ change the abundance of the greenhouse gases ozone and methane (Wild et al., 2001). Automobiles, and in particular cars with diesel engines, emit aerosols, more precisely carbonaceous particles (BC and OC). BC particles absorb sunlight, change the albedo of snow and ice if deposited on these surfaces, and may also change

cloud properties (Lohmann and Feichter, 2005). Ozone and aerosol concentrations have changed significantly since pre-industrial times and have thus contributed to the changes in radiative forcing (RF) (see figure 1.1) resulting in changes in development and patterns of climate parameters (IPCC, 2001).

Automobiles with diesel engines emit more particulate matter and NO_x while gasoline cars emit more CO and hydrocarbons (Mazzi and Dowlatabadi, 2006). When all exhaust components have been taken into consideration, an important task is to decide whether substitution of gasoline with diesel is a good option to mitigate global warming. Also is the question of relative weight given to short-term air pollution compared to possible harmful effects of more long-term climate change, a question that involves value judgement, and is an important and difficult dilemma for policymakers to resolve.

Another aspect with implications for policy designs is whether or not/to what extent the climate effect of the species depends on where they are emitted. For short-lived components like ozone precursors, the chemical processes that produces O_3 can be non-linear (Matthes et al., 2007), so that the rate of formation and the total amount of the secondary pollutant depends on the background levels of the precursor species. Ozone is formed when NO_x, CO, CH_4 and $NMHCs$ is processed by sunlight (Granier et al., 2006), described more in-depth in the theory chapter, chapter 2.1. In addition to producing ozone, these non-linear processes also change the oxidizing capacity of the atmosphere, by changing OH concentrations. An important role of OH is to remove methane from the atmosphere. In most environments, NO_x emissions increase OH concentration, thus leading to an increased removal of methane. On the contrary, will CO and $NMHC$ reduce the concentration of OH, leading to a reduction in methane removal. The short atmospheric lifetime, and thus the heterogeneous distribution of O_3 makes incorporation of this radiatively active species into international climate legislation a challenge. For CO_2, which is a long-lived greenhouse gas, the resultant radiative forcing is not sensitive to the location of the primary emission, as it is for ozone and its precursors. Different residence times for the different components in exhaust imply that the relative climate effect from the species is not constant, but varies over time. A comparison between gasoline and diesel is thus dependent on what time perspective is regarded.

The climatic effects from road traffic emissions are important considerations, but also important is the health threat air pollution poses to humans. Road transport is particularly important regarding air pollution, in that the emissions are released in very close proximity to humans (Colvile et al., 2001). CO is a toxic component because of its ability to bond more efficiently to the haemoglobin than oxygen (Ernst and Zibrak, 1998), and thus hinder the blood from transporting oxygen to vital organs from the lungs. NO_x alone is not regarded as a health hazard for other than sensitive groups. Ozone, however, adversely affects human health (West et al., 2006), and can cause

reduced lung function, intolerance in respiratory passages and cause cough, chest pain, increased mucus production and has been associated with increased mortality rate. There are large differences in sensitivity to ozone from person to person, and persons with asthma are regarded as particularly vulnerable (U.S. Environmental Protection Agency, 2007). Ozone is in addition considered to cause great amount of damage to vegetation (Reich and Amundson, 1985).

Emissions of particulate matter and soot also cause adverse effects to humans. In their study, Pope III et al. (1995) reviewed epidemiological research that evaluated health effects of particulate air pollution, and they concluded that particulate air pollution is an important contributing factor to respiratory disease. Observed health effects include increased respiratory symptoms, decreased lung function, increased hospitalizations and other health care visits for respiratory and cardiovascular disease, increased respiratory morbidity as measured by absenteeism from work or school or other restrictions in activity, and increased cardiopulmonary disease mortality.

With more than 500 millions automobiles and trucks operating in the world (Niemeier et al., 2006), road vehicles emit significant amounts of chemical compounds in the atmosphere. Previous studies, such as Niemeier et al. (2006), found that road traffic increased summertime ozone concentrations by typically 1-5 ppb in the remote areas, and by 5-20 ppb in industrialized regions of the Northern Hemisphere, and found a corresponding ozone-related radiative forcing of 0.05 Wm^{-2}. Unger et al. (2008) found a global annual mean radiative forcing (at 2030, by O_3, sulfate, black and organic carbon, and indirect CH_4 effects) from the transportation sector to be 0.067 Wm^{-2}. Fuglestvedt et al. (2008) found that since pre-industrial time, transport has contributed 15 % and 30 % of the total man made CO_2 and O_3 forcing, respectively, and road transport is the main contributing subsector. Jacobson et al. (2004) concluded in their study that the replacement of gasoline with modern diesel vehicles in the U.S may drive up photochemical smog including total column ozone, near surface ozone, and nitrogen-containing species over the U.S.

However, not many studies have treated different fuel types from road traffic separately, and the objective of this study is to examine the different atmospheric effects from gasoline- and diesel exhaust emissions. A global chemistry transport model, OsloCTM2 (Sundet, 1997), has been used to calculate ozone production, change in ozone precursors, together with transport and deposition of black carbon (BC) particles. The simulations have been done with a horizontal resolution of 2.8 $\times$ 2.8°and several model runs with different emission scenarios have been executed. Borken et al. (2007) have provided the fuel-type emission data set, generated in association with the EU project QUANTIFY. Differences between gasoline and diesel have been investigated, as well as the effect from legislation limits (Euro4 and Euro5)

on exhaust emissions. To see the effect from these legislation from a heath perspective, hourly-levels of ozone from three different populated areas have been studied. Radiative forcings from ozone, change in CH_4 levels, black carbon and CO_2 were calculated using simplified formulas, for each of the model runs.
The underlying theory associated with atmospheric chemistry, with a focus on ozone production and its precursors is presented in chapter 2, followed by a description of the model used in this thesis in chapter 3. The results are presented and discussed in chapter 4, before chapter 5 gives a summary and some concluding remarks of this thesis.

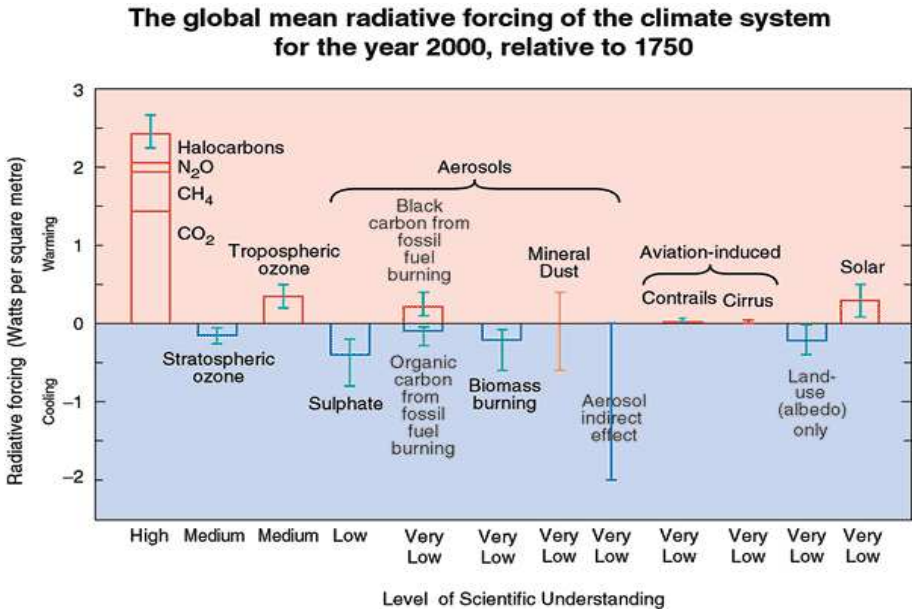

Figure 1.1: *The global mean radiative forcings for different compounds, for the year 2000, relative to 1750. From IPCC (2001), section "Summary for Policymakers", figure 3.*

Chapter 2

Theory

Nitrogen oxides ($NO_2 + NO = NO_X$), carbon monoxide (CO) and volatile organic compounds (VOCs), which are emitted by combustion engines contribute to photochemical production of ozone and other secondary pollutants. Ozone is a greenhouse gas, and an increase in the ozone abundance can lead to additional radiative forcing (Niemeier et al., 2006). Ozone is additionally a health hazard, causing human respiratory problems, damaging plants and is expected to reduce crop productivity (Sitch et al., 2007). The anthropogenic emissions from road traffic will furthermore alter the oxidizing potential of the atmosphere, by altering the abundance of OH, and thereby the abundance of methane (CH_4), which also is a greenhouse gas. In addition to the already mentioned gases emitted by combustion engines, the emission of aerosol particles is substantial, with transport being an important source of man-made emissions of black carbon (BC), 14 % (Fuglestvedt et al., 2008), and road transport being the largest contributor in the transport sector. Aerosol emissions have impact on the atmosphere and climate system through several indirect effects which will be described in more detail later in this chapter.

This chapter will first give an overview of atmospheric chemistry in general, before describing key components affected by and from road vehicle emission, and the way in which they modify the chemistry of the troposphere. The theory is mainly based on Brasseur et al. (1999) and Jacob (1999).

2.1 Atmospheric chemistry

There are in general four types of processes that control the concentration of a chemical component in the atmosphere:

- *Emission.* A variety of sources, anthropogenic and biogenic, emit chemical species into the atmosphere.

- *Chemistry.* Species can be formed or removed from the atmosphere by chemical reactions.

- *Transport.* Horizontal and vertical motions transport species away from its place of origin.

- *Deposition.* Chemical compounds can be deposited to the Earth's surface either by wet or dry deposition, involving scavenging by precipitation or direct reaction or absorption to the surface respectively.

Lifetime

A components abundance is determined by the importance of the above processes relative to each other. In figure 2.1 these processes are demonstrated in a one-box model, which can be an atmospheric domain of choice. It describes how a chemical species X is determined by transport, noted by a flow of X into the box, F_{in}; and out of the box F_{out}; chemical production, P; chemical loss, L; emission E; and deposition, D. F_{in}, chemical production and emission are regarded as *sources* of X, and F_{out}, chemical loss and deposition as *sinks*.

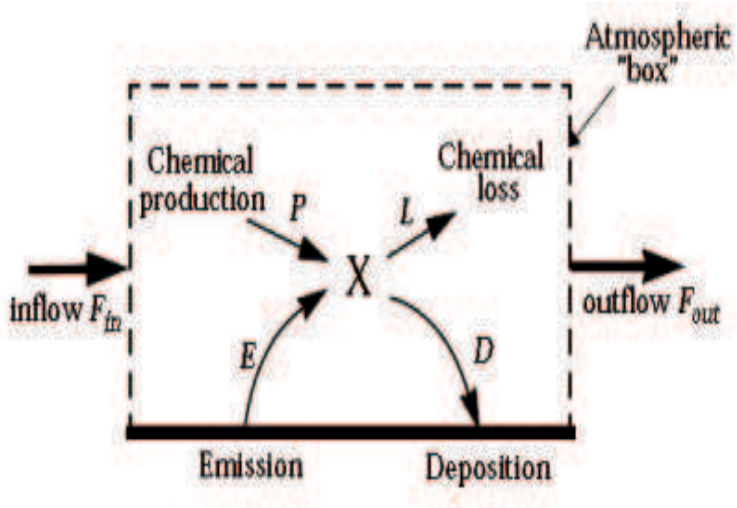

Figure 2.1: *The abundance of X depends on transportation into and out of the box, chemical production and loss, and emission and deposition. From Jacob (1999).*

Within a grid box in a numerical model, the rate of change with time must equal the difference between sources and sinks. With c being the concentration of the species X, the change of c with time can be written

$$\frac{dc}{dt} = \Sigma sources - \Sigma sinks = E + P + F_{in} - L - D - F_{out} \qquad (2.1)$$

The atmospheric lifetime τ of a species is the average time it takes for a molecule to diminish by a factor $1/e$ and is thus called e-folding time. τ is helpful for measuring the time it takes for a system to reach steady state, and can be calculated as

$$\tau = \frac{c}{\Sigma sinks} = \frac{c}{F_{out} + L + D} = \frac{1}{k} \tag{2.2}$$

where k is the overall rate constant for the loss processes. The chemical lifetime of a species is a determining factor on its distribution. If the lifetime is shorter than the time it takes for a component to be transported over long distances, its distribution in the atmosphere will be heterogeneous, with concentrations limited to its place of origin, as can be seen for the components investigated in the result chapter.

2.2 Key constituents in tropospheric chemistry

2.2.1 The hydroxyl radical (OH)

The hydroxyl radical, OH, is the neutral form of the hydroxide ion, and is highly reactive and consequently short-lived (order of one second). OH concentrations in the atmosphere are highly variable because of its short lifetime, and thus respond rapidly to changes in its sources and sinks. For the same reason, the hydroxyl radical is often referred to as the troposphere's detergent, since it reacts with many pollutants and acts as the first step to their removal.

The primary source of OH in the troposphere is the reaction of excited oxygen atoms, $O(^1D)$, with water vapour

$$O(^1D) + H_2O \rightarrow 2OH \tag{2.3}$$

This process is most effective where water vapour mixing ratio is high i.e. at low altitudes. $O(^1D)$ is made available through photolysis of ozone

$$O_3 + h\nu \rightarrow O(^1D) + O_2 \tag{2.4}$$

The prevailing sinks of OH are reactions with CO and CH_4, and these components therefore play an important role in driving the radical chemistry in the atmosphere.
The presence of NO_x regenerates OH consumed in the oxidation of CO and other hydrocarbons, and at the same time provides a source of O_3 in the troposphere to generate additional OH, as shown in the following.
CO is oxidized and the result is a H atom which rapidly reacts with O_2 to give CO_2 and HO_2:

$$CO + OH \xrightarrow{O_2} CO_2 + HO_2 \tag{2.5}$$

HO_2 reacts with NO, when present, and in addition to regenerating OH, produces NO_2 which in turn photolysis and creates O_3

$$HO_2 + NO \rightarrow OH + NO_2 \tag{2.6}$$

$$NO_2 + h\nu \xrightarrow{O_2} NO + O_3 \tag{2.7}$$

The resulting net reaction is

$$net : CO + 2O_2 \rightarrow CO_2 + O_3 \tag{2.8}$$

CO and $NMHC$ is thus OH sinks, while NO_x can regenerate the radical and produce O_3, as also described in the following subchapters, and exemplified in the result chapter.

2.2.2 Nitrogen oxides (NO_X)

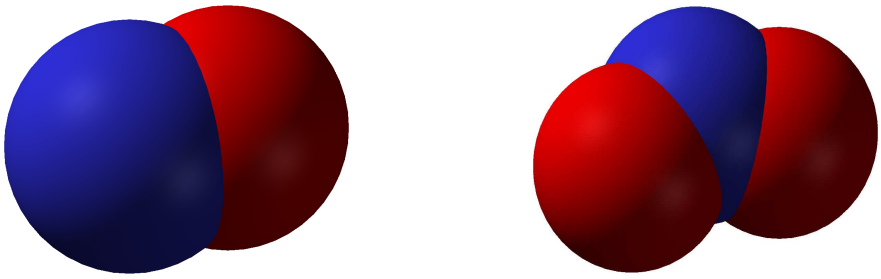

(a) **(b)**

Figure 2.2: *a) NO and b) NO_2*

Fossil fuel combustion accounts for about half of the global source of NO_x (Jacob, 1999), and transport is the most important source among anthropogenic emissions (37% of total antropogenic emission) (Fuglestvedt et al., 2008). Table 2.1 shows present-day sources of tropospheric NO_x. Part of the combustion source is due to oxidation of the organic nitrogen present in fuel. An additional source in combustion engines is the thermal decomposition of air supplied to the combustion chamber. At the high temperature of the combustion chamber oxygen thermolyzes and O reacts with N_2 to produce NO

$$O_2 \Leftrightarrow O + O \tag{2.9}$$

$$O + N_2 \Leftrightarrow NO + N \tag{2.10}$$

$$N + O_2 \Leftrightarrow NO + O \tag{2.11}$$

NO_x is primarily emitted as NO, but because of rapid interconversion between NO and NO_2 the two species are often groped together and considered under the budget of the NO_x family as a whole. Figure 2.2 shows the molecular structure of NO and NO_2. The main sink of NO_x is oxidation to HNO_3 in the daytime

$$NO_2 + OH + M \rightarrow HNO_3 + M \tag{2.12}$$

and at night

$$NO_2 + O_3 + M \rightarrow NO_3 + O_2 \tag{2.13}$$

$$NO_3 + NO_2 + M \rightarrow NO_2O_5 + M \tag{2.14}$$

$$NO_2O_5 + H_2O \rightarrow 2HNO_3 \tag{2.15}$$

The lifetime of NO_x is approximately one day, and because of this short lifetime, it is not transported very far away from its place of origin. An efficient mechanism for transporting anthropogenic NO_x to the global troposphere is however through the formation of the reservoir species, peroxyacetylnitrate ($CH_3C(O)OONO_2$), PAN. PAN is produced by photochemical oxidation of carbonyl compounds in the presence of NO_x. PAN can thus indirectly transport NO_x over long distances, when PAN releases NO_x again, further away from its place of origin.

Source	$TgNyr^-1$
Fossil fuel	33.0
Biomass burning	7.1
Soils	5.6
Lightning	5.0
NH_3 oxidation	-
Aircraft	0.7
Transport from stratosphere	<0.5
Total	**51.9**

Table 2.1: *Estimated present-day sources of tropospheric NO_x in Tg(N/yr), from IPCC (2001)*

2.2.3 Ozone (O_3)

Since 1750, the total amount of tropospheric ozone is estimated to have increased by 36% (IPCC, 2001), and the corresponding radiative forcing is $0.35Wm^{-2}$ (figure 1.1). The reason for this enlargement in O_3 concentration, is primarily due to antropogenic emissions of several O_3-forming gases. As mentioned in the preceding sections, tropospheric ozone is produced by the oxidation of CO and hydrocarbons by OH in the presence of NO_x. Ozone is called a secondary pollutant, since it is not emitted directly into the atmosphere, but produced from chemical reactions with other components. Regions with high emissions of CO, hydrocarbons and NO_X thus produce O_3 rapidly. Both hydrocarbons and NO_x are present in automobile exhaust.

Tropospheric ozone is of environmental importance because of its capacity as a greenhouse gas, but also as being a health hazard. If exposed to high levels it can cause lung and respiratory difficulties, such as scratchy throats, cough, hoarseness, shortness of breath and headache.

Tropospheric ozone has an average lifetime of the order of weeks (IPCC, 2001) dependent on season, in the summertime it ranges from five days to a few weeks, and at mid-latitudes in wintertime it can be more than three months. This relatively short lifetime implies that the spatial distribution of ozone will be heterogeneous, with higher concentrations near its sources, as the results in chapter 4 shows.

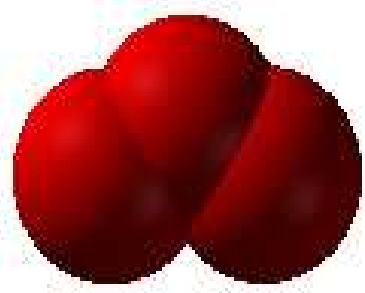

Figure 2.3: Ozone

Ozone consists of three oxygen molecules, see figure 2.3. The production of O_3 is the photochemical reactions with NO_x and CO, described in reactions 2.5 to 2.7. However, ozone can also be produced by other hydrocarbons than CO, such as methane, CH_4, or so-called non-methane-hydrocarbons, $NMHCs$. There are several hundreds of different hydrocarbons emitted by automobiles causing an immensely complex photochemistry. However, researchers have suggested the following to be the most important reactions for O_3 formation (Brasseur et al., 1999).

The production is a chain of several steps, initiated by production of HO_x ($HO_x = H + OH + HO_2$),

$$H_2O + O(^1D) \rightarrow 2OH \tag{2.16}$$

and continues by OH reacting with $NMHC$ (notation RH, where R is an organic group).

$$RH + OH \xrightarrow{O_2} RO_2 + H_2O \tag{2.17}$$

$$RO_2 + NO \rightarrow RO + NO_2 \tag{2.18}$$

$$RO + O_2 \rightarrow HO_2 + R'CHO \tag{2.19}$$

$$HO_2 + NO \rightarrow OH + NO_2 \tag{2.20}$$

$$2(NO_2 + h\nu \rightarrow NO + O) \tag{2.21}$$

$$2(O + O_2 + M \rightarrow O_3 + M) \tag{2.22}$$

$$NET : RH + 4O_2 + h\nu \rightarrow R'HCO + H_2O + 2O_3 \tag{2.23}$$

RO_2 produced in 2.17 reacts with NO to yield an organic radical, RO, and NO_2, which photolyses, creating O_3. In the above reactions $NMHC$ are consumed, while NO_x play the role as a catalyst. $NMHC$ and NO_x are often referred to as ozone precursors, however, at the same time as the above reactions, other reactions in the atmosphere consume NO_x by converting it to HNO_3 or nitrate, which are removed from the atmosphere by deposition.

In regions where concentrations of $NMHC$ are low, such as in remote areas away from pollution sources, the ozone production is dominated by oxidation of CO and CH_4 instead of $NMHC$, with the reaction scheme similar to the previous (2.17 - 2.23). For all three reaction chains, there are only interconversion of NO and NO_2, so again there is no net loss of NO_x, while $NMHC$, CO and CH_4 are consumed.

The efficiency of the photochemical O_3 production depends on the concentration of NO_x, being inefficiently with high NO_x levels, efficiently with low NO_x levels and not at all efficient with very low NO_x concentrations.
When NO_x is low reaction 2.16 is followed by

$$OH + CO \rightarrow CO_2 + H \tag{2.24}$$

$$H + O_2 + M \rightarrow HO_2 + M \tag{2.25}$$

$$HO_2 + O_3 \rightarrow OH + 2O_2 \tag{2.26}$$

which destroy O_3, and is thus a O_3 sink. Another of the main O_3 sinks is reaction 2.4. These two sinks are approximately of the same size, see table 2.2 for global budget of ozone. Dry deposition on the Earth's surface is also an ozone sink, but relatively minor compared to chemical loss.

The following reactions which cycles NO_x between NO and NO_2 have no effect on O_3, and is thus called a *null cycle*:

$$NO + O_3 \rightarrow NO_2 + O_2 \tag{2.27}$$

$$NO_2 + h\nu \rightarrow NO + O \tag{2.28}$$

$$O + O_2 + M \rightarrow O_3 + M \tag{2.29}$$

However, in polluted areas where emission of NO_x is high, mixing ratios of NO often exceed O_3 mixing ratio and reaction 2.27 may diminish O_3, which will be exemplified in chapter 4. In urban air NO can also be converted to NO_2 by reaction 2.18, so that $NMHCs$ is consumed in the conversion instead of O_3, and the effect is O_3 production when $MNHCs$ are present. Figure 2.4 of ozone concentration as a function of NO_x and hydrocarbon emissions, show the nonlinear relationship between ozone mixing ratios and different values of NO_x and hydrocarbons. When the initial mixing ratio of NO_x is low, an increase in the abundance of hydrocarbons does not affect the amount of ozone, so the concentration of ozone is insensitive to hydrocarbons, but increase with increasing NO_x. When NO_x levels are high, the ozone production rate is limited by the supply of hydrocarbons, and ozone concentration increases with increasing hydrocarbons, a so called *hydrocarbon-limited regime*. At low levels of hydrocarbons we see from figure 2.4 that an increase in NO_x could decrease ozone concentrations, because reaction 2.27 is the main mechanism converting NO to NO_2, and at night when there is no sunlight, reaction 2.28 stops, and there is an O_3 loss. When hydrocarbon levels are high, ozone production increase with increasing NO_x and is insensitive to changes in hydrocarbons, this is the *NO_x-limited regime*.

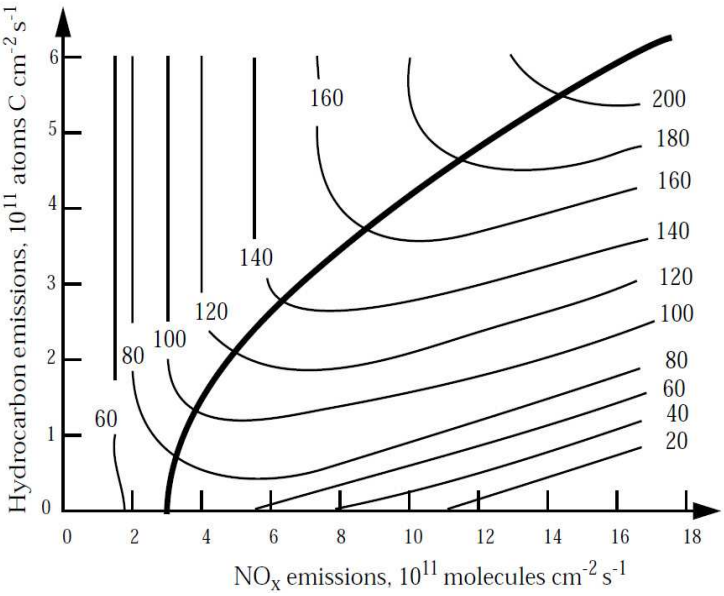

Figure 2.4: *Ozone concentration [ppb] as a function of NO_x and hydrocarbon emissions. The thick line separates the NO_x-limited (top left) and hydrocarbon-limited (bottom right) regimes. From (Jacob, 1999).*

Figure 2.5 shows the relative enhancements of NO_x, CO, O_3 and OH concentrations from preindustrial times to today. The increase of NO_x and CO has contributed to an enhancement of ozone concentrations, particularly in the Northern Hemisphere.

	(TgO_3yr^{-1})
SOURCES	**3400-5700**
Chemical production	3000-4600
$HO_2 + NO_2$	(70%)
$CH_3O_2 + NO$	(20%)
$RO_2 + NO$	(10%)
Transport from the stratosphere	400-1100
SINKS	**3400-5700**
Chemical loss	3000-4200
$O(^1D) + H_2O$	(40%)
$HO_2 + O_3$	(40%)
$OH + O_3$	(10%)
Others	(10%)

Table 2.2: Global budget of O_3 (Jacob, 1999)

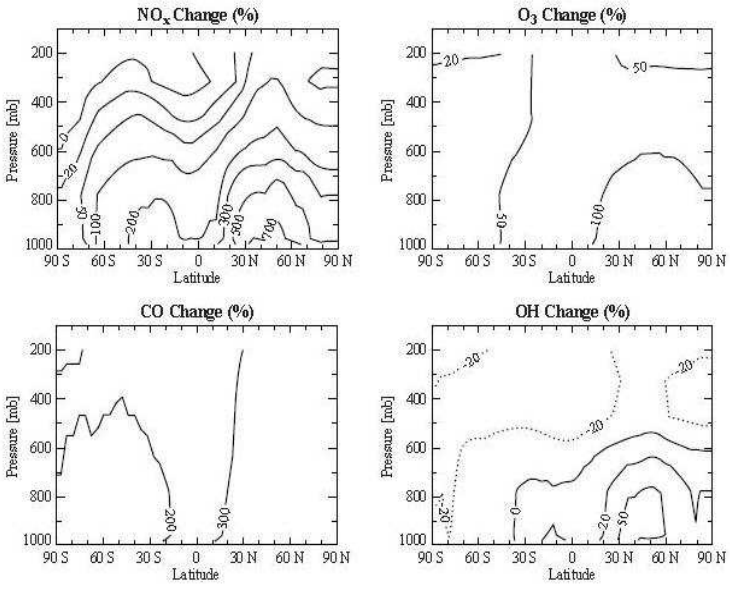

Figure 2.5: *Relative enhancements of NO_X, CO, O_3 and OH concentrations from preindustrial times to today (Jacob, 1999).*

2.2.4 Carbon monoxide (CO)

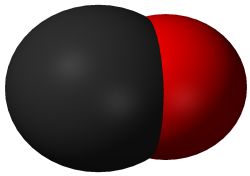

Figure 2.6: Carbon monoxide

In addition to production by oxidation of methane and other hydrocarbons, carbon monoxide is released at the Earth's surface by incomplete combustion associated with biomass burning and fossil fuels. Human activities account for about 50-60 percent of the CO emission (Brasseur et al., 1999). A global budget of the sources and sinks of CO is presented in table 2.3. As a result of human activities being the major emission source of carbon monoxide, the Northern Hemisphere contains about twice as much CO as the Southern Hemisphere (IPCC, 2001). Because of its relatively short lifetime and prominent emission patterns, the distribution of CO has large gradients in the atmosphere. CO is not a strong enough absorber of terrestrial infrared radiation to be regarded as a direct greenhouse gas, but because of its reaction with the OH radical, CO plays an important role in tropospheric chemistry as an oxidant sink, and it is also a tropospheric ozone precursor. Molecular structure of CO is shown in figure 2.6.

	Range of estimates ($TgCOyr^{-1}$)
SOURCES	
Fossil & domestic fuel	650
Biomass burning	700
Vegetation	150
Oceans	50
Oxidation of Methane	800
Oxidation of Isoprene	270
Oxidation of Terpene	~ 0
Oxidation of industrial NMHC	110
Oxidation of biomass NMHC	30
Oxidation of Acetone	20
SINKS	
OH reaction	1500-2700
Surface deposition	250-640

Table 2.3: *Global tropospheric budget of CO in Tg(CO/yr). From IPCC (2001)*

2.2.5 Hydrocarbons

A hydrocarbon is an organic compound consisting of hydrogen and carbon, with the general molecular formula C_nH_m. The atmospheric budget of hydrocarbons is controlled by emissions, anthropogenic and natural (most often biogenic), and atmospheric destruction, in most cases by photochemical reactions with atmospheric oxidants, such as OH, NO_3 and O_3. Methane is the simplest form of hydrocarbon, and has the highest atmospheric abundance, about 1.8 ppm in 1994 (Brasseur et al., 1999). Because of its long lifetime, approximately 8-10 years (Brasseur et al., 1999), it is globally distributed through the lower atmosphere. Other hydrocarbons, non-methane hydrocarbons (NMHCs) have smaller emission rates than methane, and are in addition more reactive, leading to much smaller atmospheric concentrations, except very near their emission sources. However, the chemistry of these NMHCs play an important role in many regions of the troposphere, as they are precursors of tropospheric ozone.

SOURCES	$Emissions, TgCyr^{-}1$
ANTHROPOGENIC	
Transportation	22
Stationary source fuel combustion	4
Industrial processes including natural gas production	17
Biomass burning, forest fires, incineration	45
Organic solvents	15
Anthropogenic subtotal	*103*
NATURAL	
Oceanic	
Light hydrocarbons	5-10
$C_9 - C_{28} n - alkane$	1-26
Terrestrial	
Microbial production	6
Emissions from vegetation	
isoprene	500
monoterpenes	125
other	$\sim$ 520
Natural subtotal	$\sim$ *1170*
Total emissions	$\sim$ **1273**

Table 2.4: *Estimates of global NMHC emissions. From Brasseur et al. (1999)*

Table 2.4 gives a global estimation of NMHC emissions adapted from Brasseur et al. (1999). The distribution of different hydrocarbon species depends on the strength and location of their sources, their reactivity, and on the pro-

cess that distribute them. However, the impact of the shorter-lived NMHCs extends over the entire troposphere due to the formation of longer-lived intermediates like CO, and various carbonyl and carboxyl compounds (Poisson et al., 2000).

2.2.6 Aerosols

Aerosol particles such as sulphate and carbonaceous aerosols have considerably increased the global mean burden of aerosol particles from preindustrial times to the present-day (Lohmann and Feichter, 2005). Aerosols affect the atmosphere by scattering and absorbing radiation, and as acting as cloud condensation nuclei and ice nuclei, referred to as indirect effect. The indirect effect changes cloud-properties and thus altering cloud albedo, lifetime and precipitation efficiency. Clouds are an important regulator of the Earth's radiation budget, and about 60 % of the Earth's surface is covered with clouds (Lohmann and Feichter, 2005). Clouds cool the Earth-atmosphere system on a global average basis at the top-of-atmosphere, with losses of $48 Wm^{-2}$ in the solar spectrum, which is only partially compensated by trapped infrared radiation ($30 Wm^{-2}$)(Lohmann and Feichter, 2005).

The indirect effects consist of several mechanisms (Lohmann and Feichter, 2005):

- *The Twomey effect*: the enhanced reflection of solar radiation due to the more but smaller cloud droplets in a cloud.

- *Cloud lifetime or 2nd indirect effect:* more but smaller cloud droplets reduce the precipitation efficiency, and thereby increase the cloud lifetime, and in that way the reflectivity also increases.

- *Semi-direct effect:* absorption of solar radiation by aerosols leads to an increase in temperature which in turn leads to evaporation of cloud droplets.

- *Thermodynamic effect:* Smaller cloud droplets delay the onset of freezing.

- *Glaciation effect:* More ice nuclei increase the precipitation efficiency.

- *Riming indirect effect:* Smaller cloud droplets decrease the riming efficiency.

- *Surface energy budget effect:* Increased aerosol and cloud optical thickness decrease the net solar surface radiation.

Both the Twomey and the cloud lifetime effect tend to cool the Earth-atmosphere system by increasing cloud optical depth and cloud cover. Carbonaceous aerosols and dust exert a positive forcing at the top-of-atmosphere (TOA), at least in regions with high surface albedo, and can in this way directly warm the atmosphere. If absorption of solar radiation of these particles also occurs within the cloud droplets, this effect will not only be amplified, but the temperature enhancement may lead to evaporation of the cloud droplets. The reduced cloud optical depth and cloud cover further enlarges warming of the Earth-atmosphere system. The radiative effect is different for scattering aerosols, SO_4 and OC, and absorbing aerosols, BC.

Black carbon

In addition to the effects mentioned above, black carbon (BC) affects the climate forcing when deposited on snow. Very small quantities of BC reduce snow reflectance because of multiple scattering in the snow pack and because of the vast gap between mass absorption coefficients of BC and ice (Flanner et al., 2007). The reflectance of snow is strongly sensitive to the snow grain effective radius, which is determined by the rate of snow aging, where aged snow absorbs stronger than fresh snow (Flanner et al., 2007). Small changes in solar absorption in snow can modify snow melt timing, and Flanner et al. shows that additional BC forcing in snow shifts snow melt earlier. BC in snow packs can aggravate a disproportionately large climate response since the forcing tends to overlap with the beginning of snow melt, therefore triggering more rapid removal of snow, and a change in snow-albedo feedback, with diminishing snow leading to higher surface albedo.

Since BC is an absorbing aerosol, its presence in the atmosphere leads to a reduction of the planets albedo by absorbing the solar radiation reflected by the surface-atmosphere-cloud system (Ramanathan and Carmichael, 2008). But for the same reason, i.e absorbing solar radiation, BC also absorbs direct solar radiation, and thus reducing the solar radiation reaching the surface. This effect is referred to as dimming, and contributes negatively to the radiative forcing from black carbon. However, the resulting top-of-atmosphere direct forcing is positive, and IPCC (2001) estimated it to be within the range of 0.1 to $0.4 W m^{-2}$. Thus black carbon is an important contributor to radiative forcing, however, the level of scientific understanding regarding black carbon is very low, see figure 1.1, and more research is essential.

2.3 Road vehicles legislation

The European Union regards air quality as a major task, and since the early 1970s, the EU has been working to improve air quality by controlling emissions of harmful substances into the atmosphere, improving fuel quality, and by integrating environmental protection requirements into the transport and energy sectors (`http://ec.europa.eu/environment/air`). For light-duty vehicles, the emission standard currently in force is the Euro 4, while Euro 5 and Euro 6 will take affect in 2010 and 2014 respectively. The main effect of Euro 5 is to reduce the emission of particulate matter from diesel cars from 25 mg/km to 5 mg/km and to reduce the emission of NO_X from 25 mg/km to 18 mg/km (table 2.5).

	in [kg/km]	CO_2	BC	OC	CO	HC	NO_x
Euro 3	Diesel	0.144	2.8E-05	9.0E-06	6.4E-04	9.8E-05	5.0E-04
(2000)	Gasoline	0.173	2.0E-06	2.1E-06	2.3E-03	1.8E-04	1.5E-04
Euro 4	Diesel	0.139	1.4E-05	4.5E-06	5.0E-04	4.9E-05	2.5E-04
(2005)	Gasoline	0.167	2.0E-06	2.1E-06	1.0E-03	9.0E-05	8.0E-05
Euro 5	Diesel	0.134	2.8E-06	9.0E-07	5.0E-04	4.9E-05	2.0E-04
(2009)	Gasoline	0.161	1.4E-06	1.5E-06	1.0E-03	6.8E-05	6.0E-05

Table 2.5: *European emission standards for passenger cars, kg/km. NO_x is given in kg NO_2/km. From Berntsen et al. (2009)*

Chapter 3

Model description and setup

3.1 OsloCTM2

3.1.1 General description

The model used in this thesis, OsloCTM2, is a three-dimensional global chemistry transport model. Originally OsloCTM2 was used for the troposphere only, but later stratospheric chemistry was added, along with modules for sulphur chemistry, sea salt, mineral dust, nitrate and secondary organic aerosols, thus being a very comprehensive and complete model (Sundet, 1997; Berntsen and Isaksen, 1997).

OsloCTM2 is equipped with various choices for horizontal and vertical resolution; the horizontal being T21; $5,625° \times 5,625°$, T42; $2,81° \times 2,81°$, T63; $1,875° \times 1,875°$, and $1° \times 1°$ (figure 3.1) and the vertical 19, 40 or 60 layers. The simulations executed in this thesis use the T42 horizontal resolution with 40 vertical layers. In the vertical the model uses a hybrid co-ordinate system, and moving upward in the troposphere the weight shifts from sigma formulation to pressure (figure 3.2) The model also has several options for model modules, type of chemistry and number of chemical components included. It is an off-line model with meteorological data from the European Centre for Medium-Range Weather Forecasts Integrated Forecast System model. The meteorological input data are updated every 3 hour. It is produced for each day by a 36 hour IFS model run where the first 12 hours are spin-up and the last 24 hours are sampled for use in OsloCTM2.

Advection is solved using the Second Order Momentum method (Prather, 1986), which is computer demanding, but very accurate. Convection is calculated by a mass flux scheme by Tiedtke (Tiedtke, 1989), where mass flux updrafts, mass flux downdrafts, mass flux entrainment and mass flux detrainment are given by the IFS.

The chemical scheme is adopted from the CTM-1 (Berntsen and Isaksen, 1997). The basic time step of the CTM2 is one hour, but this time step is

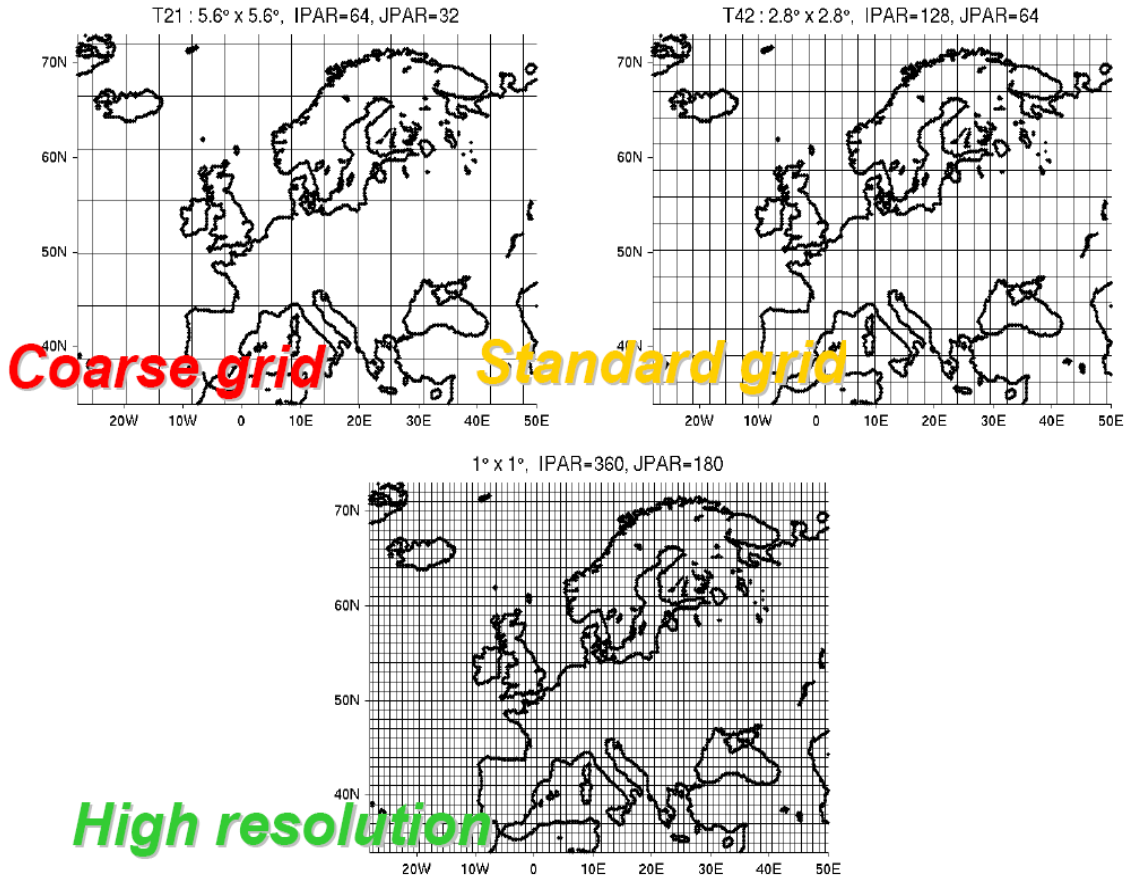

Figure 3.1: *OsloCTM2 horizontal model grid over Europe for several resolutions (Gauss, 2003).*

too long for the chemistry module, which currently runs with a time step of five minutes (Gauss, 2003). Numerous chemical species and thermal and photolytic reactions are included. The mass balance equation

$$\frac{dC_i}{dt} = P_i - L_i C_i \tag{3.1}$$

where C is the concentration of the species i, P_i is the chemical production and L_i chemical loss, is solved by the QSSA (Quasi Steady State Approximation) integration technique (Hesstvedt et al., 1978). Because of the dependency of the production and loss terms on other species, a coupled equation system for all the species of interest will be nonlinear. When all the production and loss terms are known, and constant, equation 3.1 can be solved to yield

$$C_i(t) = C_i(0)exp(-\frac{t}{\tau}) + \tau P_i(1 - exp\frac{-t}{\tau}) \tag{3.2}$$

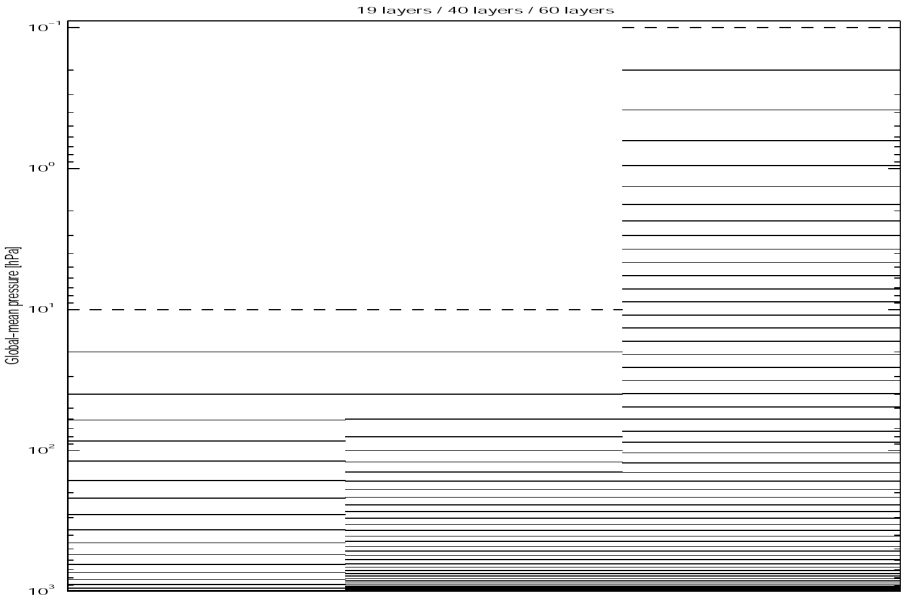

Figure 3.2: *OsloCTM2 vertical resolution, with 19, 40 and 60 layers (Gauss, 2003)*

Emission inventory for the standard simulation can be chosen from either the EU project RETRO (Reanalysis of the tropospheric chemical composition over the last 40 years), which covers the period 1960 - 2000, or the EU project POET (Present and future surface emissions of the atmospheric compounds) (Olivier et al., 2003), which is the default, covering the period 1990 to 2001. The latter inventory includes surface emissions of NO_x, CO, and $NMVC$, and also zonal averaged methane concentration at the surface based on observations. NO_x emission from lightning is set to 5 Tg (N) based on Price et al. (1997a,b) and Pickering et al. (1998). Aircraft emissions are based on a NASA inventory. The emission inventory from automobiles used to compare petrol- and diesel car exhaust in this thesis is described in next section.

3.2 Road transport exhaust emission inventory

The inventory (Borken et al., 2007) covers eight exhaust compounds emitted by five vehicle categories and fuel types each, and represents an emission inventory for direct greenhouse gases and air pollutants from road transportation for 216 countries and territories covering the whole world, on a $1 \times 1°$horizontal resolution. Calibration of the inventory to fuel balance in each country has been done.

Road transport is defined as any movement with motorized vehicles on public roads, either for passengers or freight transportation. Emissions from

aggregates with fuel systems for e.g. cooling, heating or loading are not accounted for, only fuel consumption for vehicle propulsion is included. Road vehicles are separated in five categories (using UN-ECE classifications): mopeds, motor-cycles and three-wheelers; passenger cars; busses and coaches; light duty trucks below 3,5 tons gross wight; and heavy duty trucks above 3,5 tons gross weight. The fuel is distinguished by gasoline, diesel, Liquefied petroleum gas (LPG) and Compressed natural gas (CNG), biodiesel and ethanol (bioalcohol). The exhaust emissions are calculated as tail-pipe mass of CO_2, SO_2, CO, $NMHC$, CH_4, NO_x, BC, OC and primary PM, given as totals for the year 2000, along with the corresponding fuel consumption and transport volumes. The fuel consumptions and emissions are calculated as the product of vehicle mileage and emission factor for each of the eight compounds, summed over all vehicle- and fuel categories in all 216 countries. Detailed data are usually only available for OECD (Organisation for Economic Co-operation and Development) countries, thus for most other countries a comprehensive data set was derived by Borken et al. (2007) to ensure consistency across regions and countries.

Road transportation emitted about 4280×10^6 tons fossil carbon dioxide, 110×10^6 tons carbon monoxide, 15×10^6 tons non-methane volatile compounds, 0.8×10^6 tons methane, 30×10^6 tons nitrogen oxides, 1.4×10^6 tons primary particulate matter and 1.9×10^6 tons sulphur dioxide worldwide in the year 2000 (Borken et al., 2007). About three quarters of global exhaust emissions resulted from only about 15 countries. These countries have high traffic volumes or old, unregulated, inefficient exhaust emission control, or both. The United States, Japan, Germany, France, United Kingdom, Canada and Italy, China, Brazil, Russia, Mexico and India figure among the top fifteen emitters for all pollutants covered in the inventory. In Iran and Saudi-Arabia petrol is so cheap that driving is very much abundant, often with outdated vehicles. The biggest emitting countries in Africa are South Africa, Egypt and Nigeria. The 150 countries and territories with the lowest emissions from road transport account altogether for not more than 6% to the global totals.

The focus of this study is the effects of gasoline- and diesel combustion only, therefore LPG-, CNG-, biodiesel- and ethanol exhaust are not included. Further are only emissions of CO, NO_X, $NMHC$ and BC included in the model runs. $NMHC$ were split into C_2H_4, C_2H_6, C_3H_6, C_3H_8, C_4H_{10}, C_6H_{14}, H_2CO, CH_3CHO, C_6HXR and *isoprene*, according to the emission factors for gasoline- and diesel propulsion from U.S Environmental Protection Agency, Technology Transfer Network Cleringhouse for Inventories & Emissions factors found at
`http://www.epa.gov/ttn/chief/software/speciate/index.html`. Programming in Fortran was used to read the inventory and inscribe the emissions into appropriate files, for each of the components, before interpolating from $1 \times 1^\circ$ to the T42 resolution used in the CTM. The emissions were

updated each month in the model, and assumed to take place in the first model layer. The emissions from road transport originally incorporated in the model were "turned off", so the model runs have only the road transport inventory described here included. Figure 3.5 shows the global distribution of CO, NO_X, $NMHC$ and BC from gasoline and diesel exhaust, while figures 3.3 and 3.4 shows the fuel consumptions for the year 2000 for gasoline and diesel, respectively.

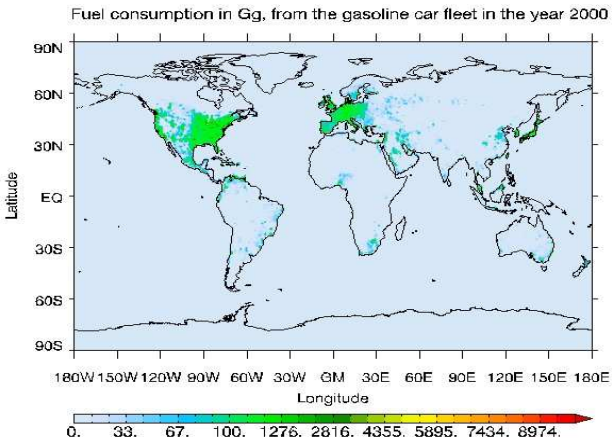

Figure 3.3: *Distribution of gasoline fuel consumption in Gg (10^9 g), per 1x1° for the year 2000.*

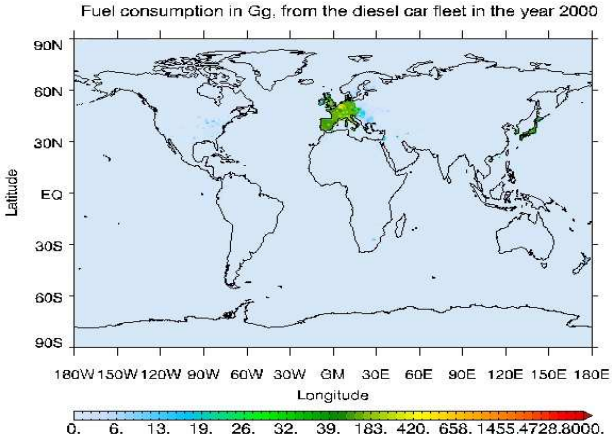

Figure 3.4: *Distribution of diesel fuel consumption in Gg (10^9 g), per 1x1° for the year 2000.*

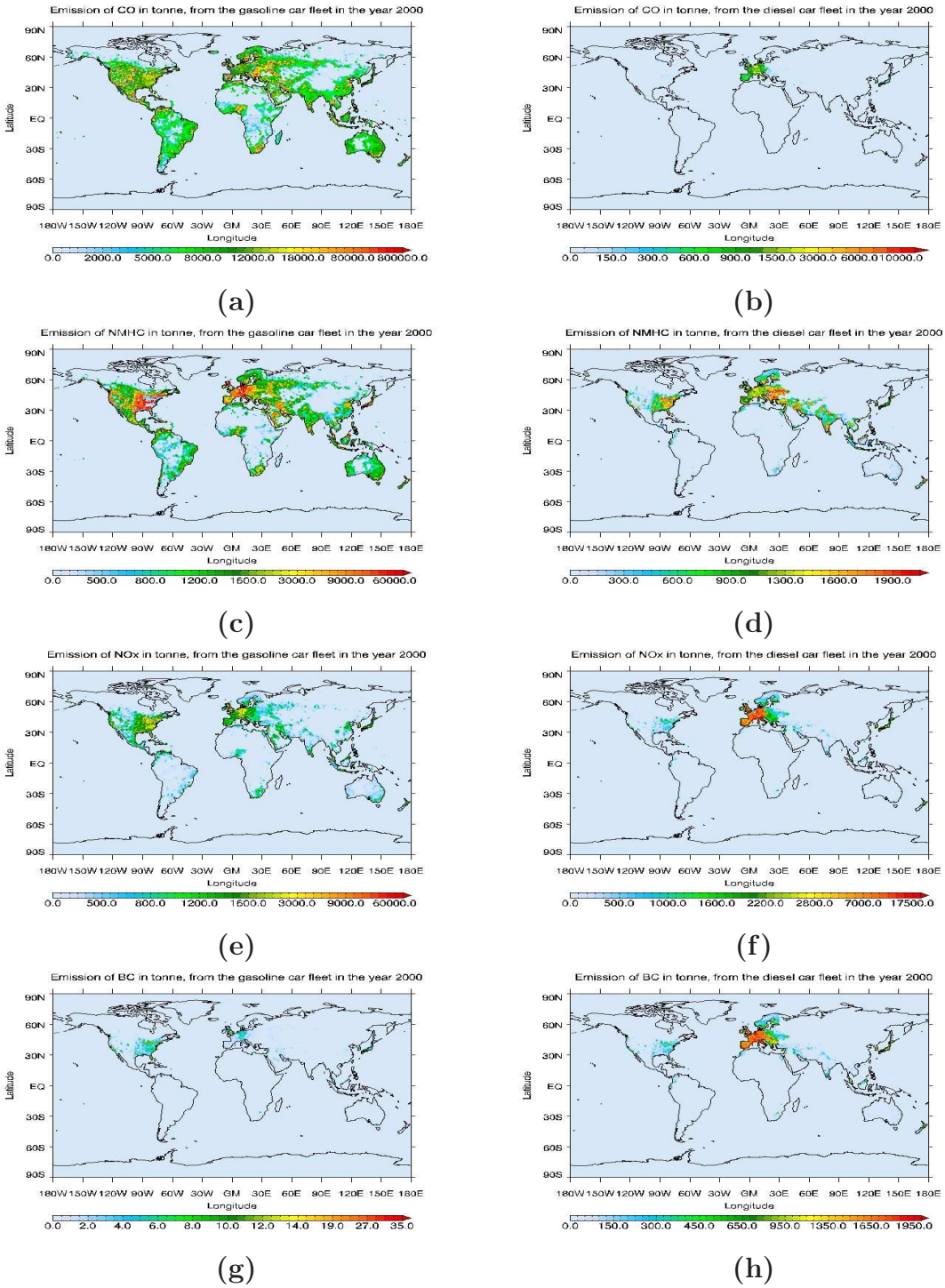

Figure 3.5: *Distribution of automobile emissions of a) CO from gasoline cars b) CO from diesel cars c) NMHC from gasoline cars d) NMHC from diesel cars e) NO_X from gasoline cars f) NO_X from diesel cars g) BC from gasoline cars and h) BC from diesel cars. All in tons per 1x1° in the year 2000.*

3.2.1 Model setup for this study and model scenarios

The tropospheric version of the model was run with T42 horizontal resolution and with 40 vertical layers. The model was run for 16 months, including four months spin-up, starting from 1st of August 2005, and finishing 31.st of December 2006. Spin-up is included to assure equilibrium in chemical processes (steady-state).
To investigate the impact of road traffic on the chemical composition of the global troposphere several model runs, with different scenarios, were carried out. Table 3.1 summarizes the different model cases.

Case Name	Case Description
Ref 1	Reference run with no traffic.
Ref 2	Reference run with present worldwide traffic.
Gasoline	Only gasoline traffic emission included.
Diesel	Only diesel traffic emission included.
E4 Gasoline	Total fuel consumed (i.e the sum of gasoline and diesel) were sat to be gasoline emissions, and sat to obey Euro 4 emission standards.
E4 Diesel	Same as the above, but with all fuel consumption sat to diesel, and Euro 4 standards.
E5 Gasoline	Total fuel consumption sat to gasoline emissions with Euro 5 standards.
E5 Diesel	Total fuel consumption sat to diesel emissions with Euro 5 standards.

Table 3.1: *Summary of model cases*

See table 2.5 for emission standards. $Ref1$, refers to a world with no emissions from road traffic. This and the $Ref2$ case are used as references to assess the difference in impacts from gasoline and diesel exhaust emissions. $Ref2$ minus $Diesel$ give the effect from gasoline emissions only, and $Ref2$ minus $Gasoline$ the effect from diesel only. To examine the Euro 4 and Euro 5 cases, $Ref1$ where subtracted from $E4Gasoline$, $E4Diesel$, $E5Gasoline$ and $E5Diesel$ in order to see the effect from exhaust alone. The Euro4

and Euro5 standards scenarios give the opportunity to quantify the effect of stricter emission regulations, in addition to investigate the hypothetical situations where the whole world's road traffic emissions are sat to be from either gasoline- or diesel automobiles. The results from the model runs are presented in the next chapter, "Results and discussion".

The Euro4 and Euro5 cases were calculated through converting total fuel consumption to corresponding kilometres, using mileage values of 10.6 km/l and 13.8 km/l for gasoline and diesel, respectively. Gasoline density of 737 g/l, and a diesel density of 856 g/l were used. Mileage and densities were found in Jacobson (2002).

To investigate the change in black carbon concentrations from car exhaust, additional model runs were executed. The chemistry in the OsloCTM2 was turned off, since the evolution of black carbon over time is independent of chemical reactions, but is only dependent on transportation and deposition. The model thus simulate transportation and deposition. To obtain this, a separate snow-code which expands the OsloCTM2 with a routine which generates snow layers and black carbon contents in these layers was used (pers. comm. Ragnhild B. Skeie at Cicero). Black carbon is emitted as 80% hydrophobic, and the remaining 20 % as hydrophilic, and is divided between black carbon from biomass burning and fossil fuel. Black carbon from fossil fuel is emitted only at the surface, with a diurnal cycle with 50 % higher emission during daytime. Emission data is updated at the beginning of every month. The BC particles are transferred to hydrophilic mode (oxidized or coated by a hydrophilic compound) at a constant rate of 24 % per day, a rate that is an estimate of the aging time for black carbon. A constant rate of aging is however not physically correct. Hydrophobic aerosols are transferred to hydrophilic mode, and lost through dry deposition. The hydrophilic particles are removed through both dry and wet deposition (Berntsen et al., 2006).
The black carbon model runs done in addition to the other model runs, were done with equivalent scenarios, given in table 3.1, except for the Euro4 runs. Since the only difference in the Euro4 and Euro5 runs is the size of the emissions, the distribution of black carbon would be equal, only a factor larger in Euro4 than in Euro5, given by the emission limits in table 2.5.

3.2.2 Validation of OsloCTM2

Observations adapted from Hauglustaine et al. (1998), where the global chemical transport model, MOZART, was evaluated, is presented here along with model results from OsloCTM2 used in this thesis. Surface concentrations of CO, O_3 and C_2H_6 from model setup "Ref 2", from different locations are shown in figure 3.6, figure 3.8, and figure 3.7, respectively. Model results are presented as monthly means during each month for a whole year, from January to December. The model calculations from OsloCTM2 are in

the left column in the figures, while in the right column are both observations (circles) and calculations from MOZART (boxes). The measurements are from Solberg et al. (1996), Greenberg et al. (1996), Novelli et al. (1992, 1994) and Oltmans and Levy (1994) and are represented by their monthly mean, and in the case of CO and O_3, their standard deviation over the period of record (up to 10 years).

For CO there is in most cases good agreement between OsloCTM2 and the observations, in terms of seasonal cycle, with maximum values during winter when the CO oxidation is smallest. The values for OsloCTM2 seems however generally slightly lower than the observations (figure 3.6).

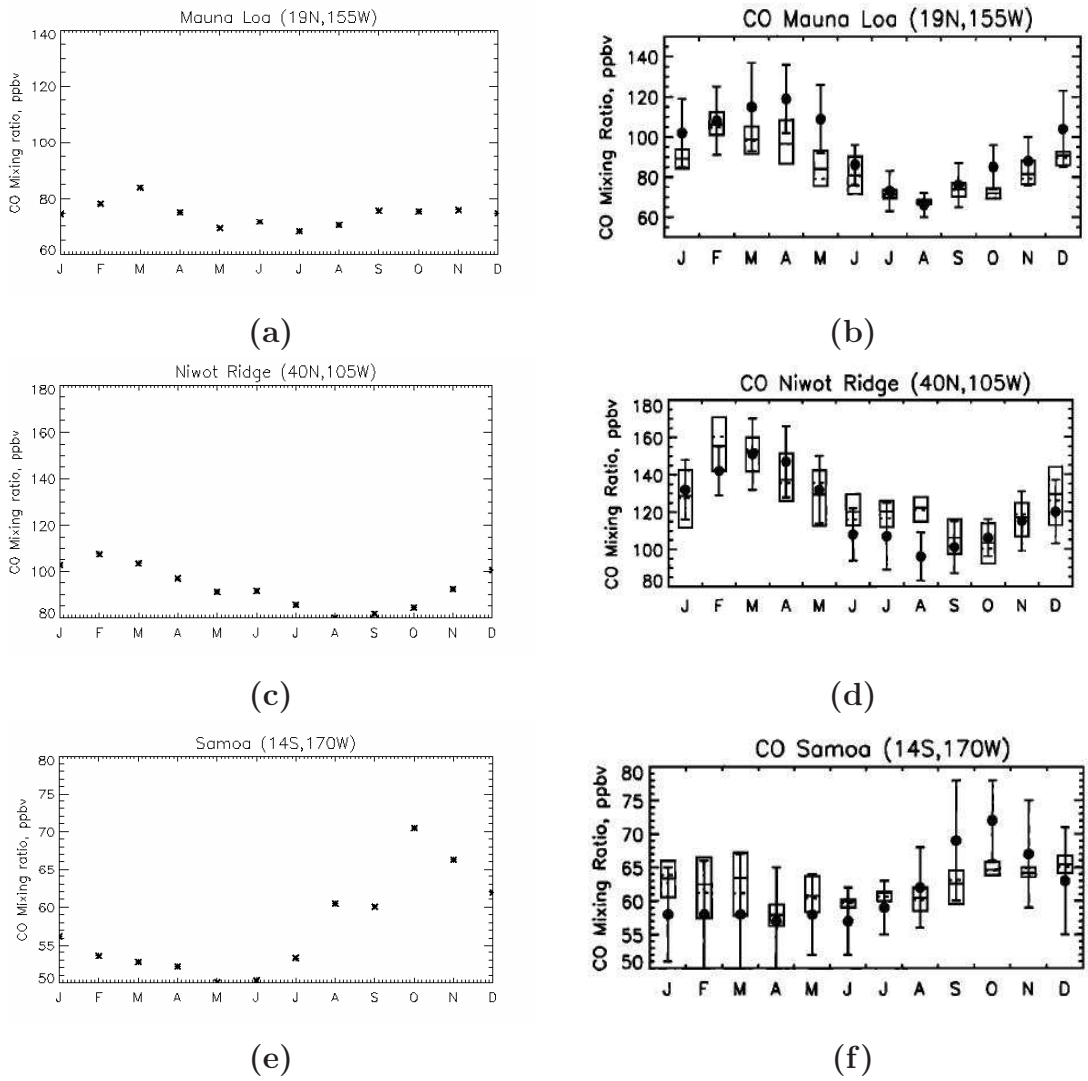

Figure 3.6: *(a), (c) and (e): Surface concentrations of CO [ppb] calculated with the OsloCTM2 model. (b), (d) and (f): Surface concentrations of CO observations (circles) and calculated by MOZART (boxes).*

The seasonal variation of ethane, C_2H_6, is also well reproduced in OsloCTM2,

though the concentrations seem to be somewhat underestimated (figure 3.7).

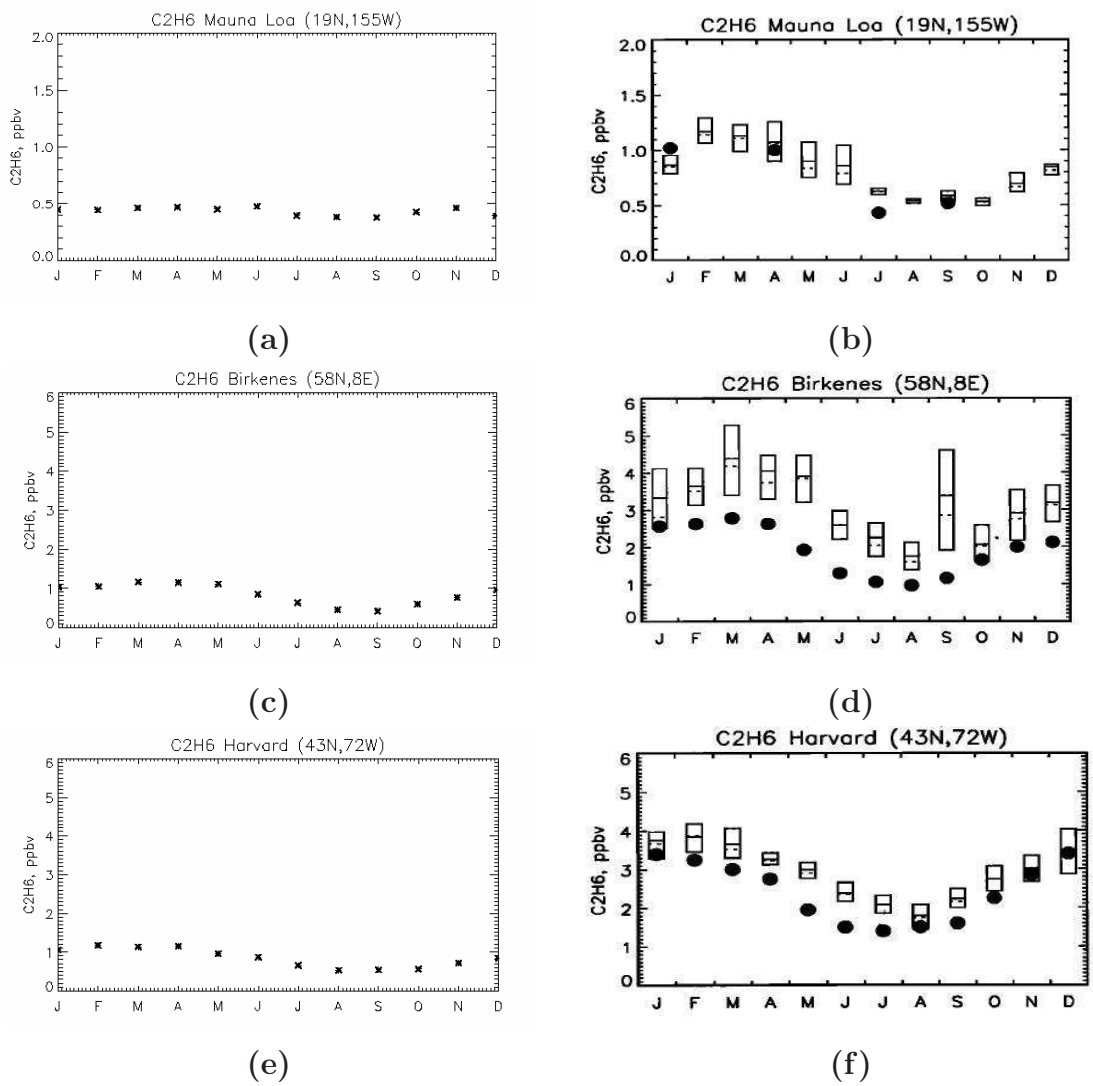

Figure 3.7: *(a), (c) and (e): Surface concentrations of C_2H_6, ethane [ppb], calculated with the OsloCTM2 model. (b), (d) and (f): Surface concentrations of C_2H_6 observations (circles) and calculated by MOZART (boxes).*

The seasonal cycle of surface O_3 mixing ratios calculated and observed are compared in figure 3.8. A weaker seasonal cycle is found in the calculations at Mauna Loa (figure 3.8 (a)). This underestimation of springtime maxima is also found in the MOZART model, and Hauglustaine et al. (1998) explains it to probably be associated with underestimation of transport of ozone from higher latitudes. At Niwot Ridge, in Colorado, OsloCTM2 produces a summertime maximum, caused by enhanced photochemical production, which is a little larger than the observed values. The simulations at Barrow, Alaska, are also somewhat higher than the observed mixing ratios. However, there is an overall good agreement between the observed and the modelled mixing

ratios, for the three components presented here, and I think one can conclude that OsloCTM2 represents the distribution of chemical components quite well. Thus, I trust the model to give reliable results also when it comes to the other model scenarios, which are presented later. Moreover, to yield the results, the differences between the various model runs and reference runs are investigated, which can be more accurate than examining one model run alone.

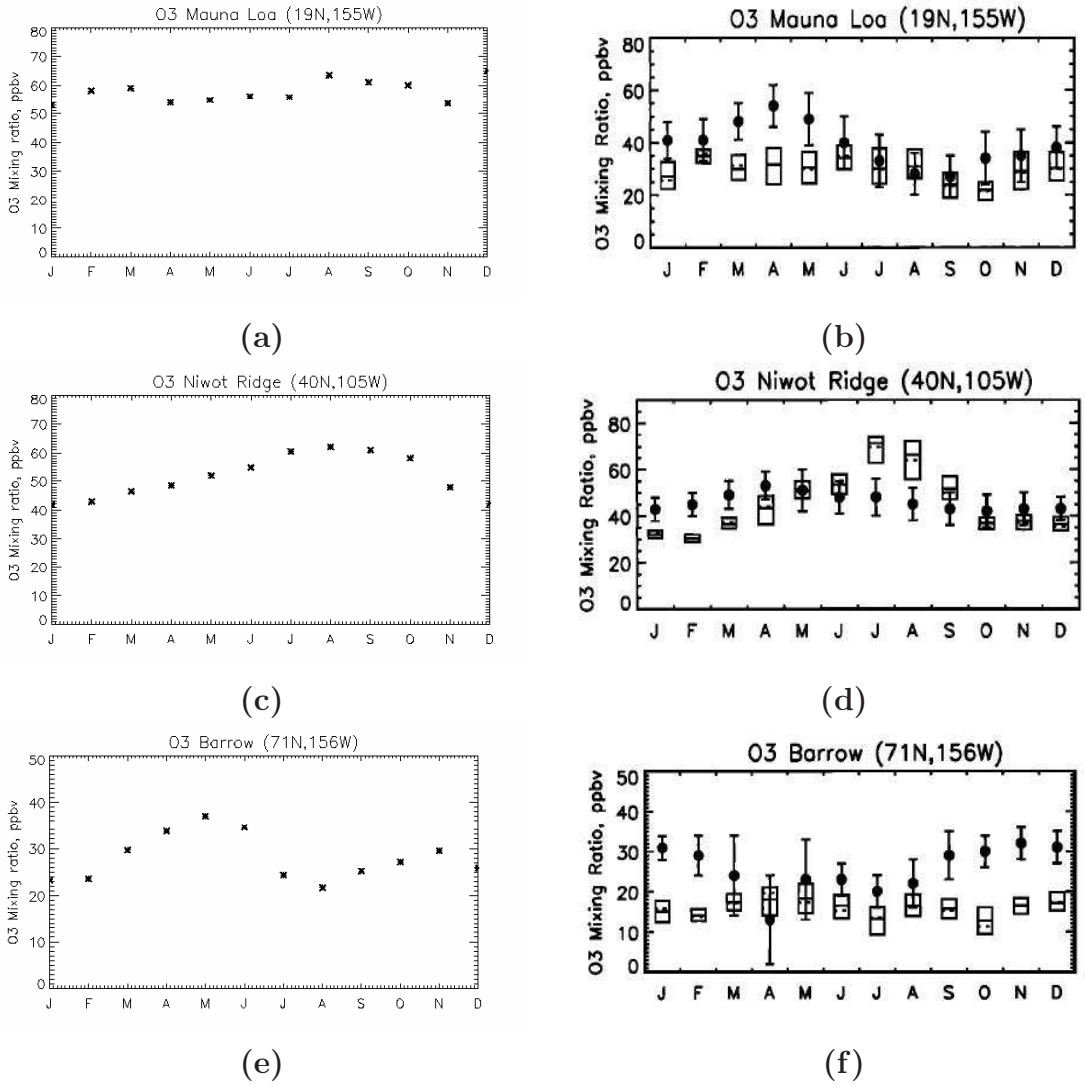

Figure 3.8: *(a), (c) and (e): Surface concentrations of O_3 [ppb] calculated with the OsloCTM2 model. (b), (d) and (f): Surface concentrations of O_3 observations (circles) and calculated by MOZART (boxes).*

Myhre et al. (2008) has investigated whether OsloCTM2 is able to reproduce observed daily variation in atmospheric aerosols, and in comparison to observations, the model performs well. For more detail on the validation on simulations of aerosols, see Myhre et al. (2008).

Chapter 4

Results and discussion

Results from the OsloCTM2 model runs will be presented and discussed in this chapter. The focus will be on change in ozone precursors, and differences in ozone production in the various model setups. The gasoline model run will be compared with diesel, and the Euro4 and Euro5 scenarios will be compared to investigate the effect of stricter car exhaust regulations, as well as a comparison on effects from different fuel type emissions. Black carbon model runs will also be presented and elaborated. Changes in ozone will be regarded not only from a climate-effect perspective, but also from a health-threat point of view. The results from each model run will be presented for the components CO, NO_x, O_3 and BC. Components representing hydrocarbons are not included, but their distribution resemble those of the other ozone precursors presented here. Radiative forcing calculated from changes in ozone, changes in methane and black carbon, and calculations based on emissions of CO_2 are presented in chapter 4.5.

4.1 Carbon monoxide (CO)

Figure 4.1 shows the surface distribution of CO from the "Ref 2" model run, with present worldwide traffic, minus "Ref 1", without traffic, so the effect of traffic alone is shown. The increase in CO from traffic extend over $20 - 140$ ppb in urban areas in North America, which corresponds to an increase of CO of $15 - 40\%$ (not shown), and up to 40 ppb in Europe. It should be noted that the T42 horizontal resolution, used in this thesis, can not resolve city areas, so the concentrations in city centers can be assumed to exceed what is calculated here. In remote regions, where traffic is of considerably smaller scale than in urbanized areas, an increase of around 10 ppb, or 5%, is found. In July, some plumes are more pronounced than in January, e.g in north-east United States. However, because of more sunlight in the summer, and thus more chemical activity, the areas over which the CO enhancements extent are smaller, as one can see in figure 4.1 b. In 4.1 a (January), CO enhancements are transported over the Atlantic ocean, eastward over the Eurasian continent, and also north to the Arctic.

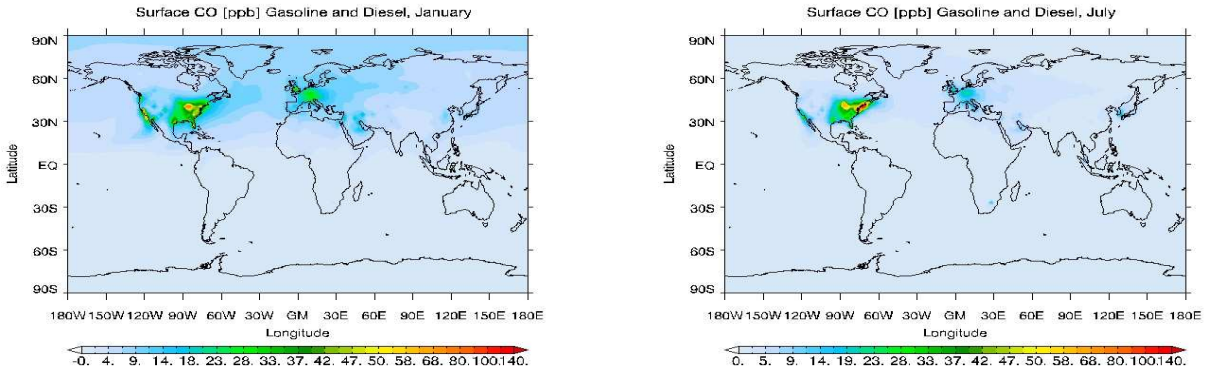

(a) **(b)**

Figure 4.1: *Distribution of surface CO [ppb] from both diesel and gasoline; "Ref2" (with present worldwide traffic) minus "Ref1" (without traffic). a) January and b) July*

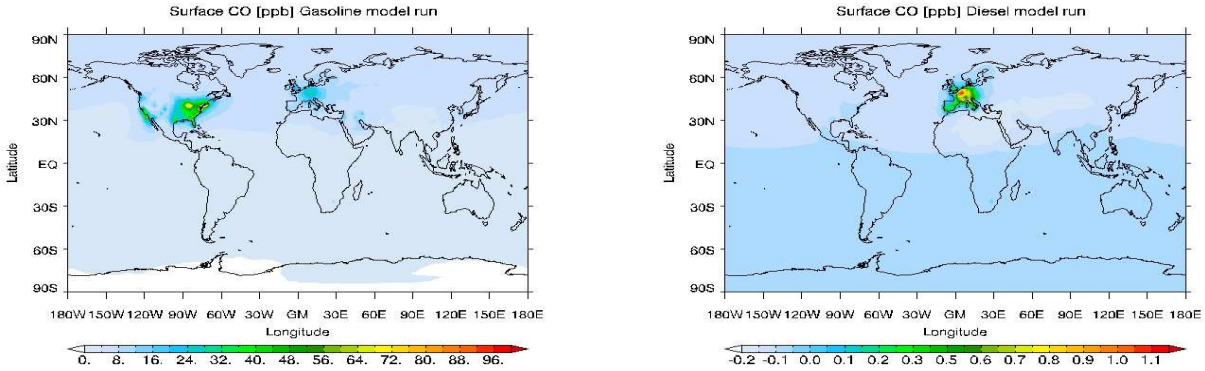

(a) **(b)**

Figure 4.2: *Distribution of surface CO [ppb] from a monthly average in the year the model was run a) gasoline and b) diesel, i.e "REF2" (with present worldwide traffic) minus Diesel and Gasoline model runs, respectively.*

Figure 4.2 shows the mean surface distribution of CO [ppb], averaged over the months the model was run for, i.e one year. The figure display enhancement from gasoline, left, and diesel, right, calculated from $Ref2$ (with present worldwide traffic) minus the model runs *Diesel* and *Gasoline*, respectively. The differences in emission patterns for the two fuel types are quite pronounced, with generally much higher emissions from gasoline, distributed mainly over North America and Europe. Diesel emissions have its source chiefly over south-west Europe. The mean CO contribution from gasoline is in the range of $30 - 100$ ppb in urbanized regions. Seasonal difference is shown in figure 4.3. In January (4.3 a), the increase in CO concentration from gasoline over north-eastern United States is 40-90 ppb (15-40 %), and in July (4.3 b) 50-140 ppb (20-50%), but over a smaller area. The increase in CO from diesel is much smaller, with only an increase of $\sim$1 ppb (0,9%)

over south-west Europe on average (figure 4.2 b), and similar situations in January and July (figure 4.3 c and d).

In figure 4.3 (d) there are areas where CO concentrations decrease. In the subsequent chapter 4.2, increase in NO_x from gasoline and diesel will be presented. Diesel has a higher emissions of NO_x than gasoline has, and thus diesel emissions can lead to a higher concentration in OH, and a high production of O_3, which in turn also increase the abundance of OH. With increased OH abundance, more CO is oxidised, by reaction 2.5, which can explain the reductions found in figure 4.3 (d).

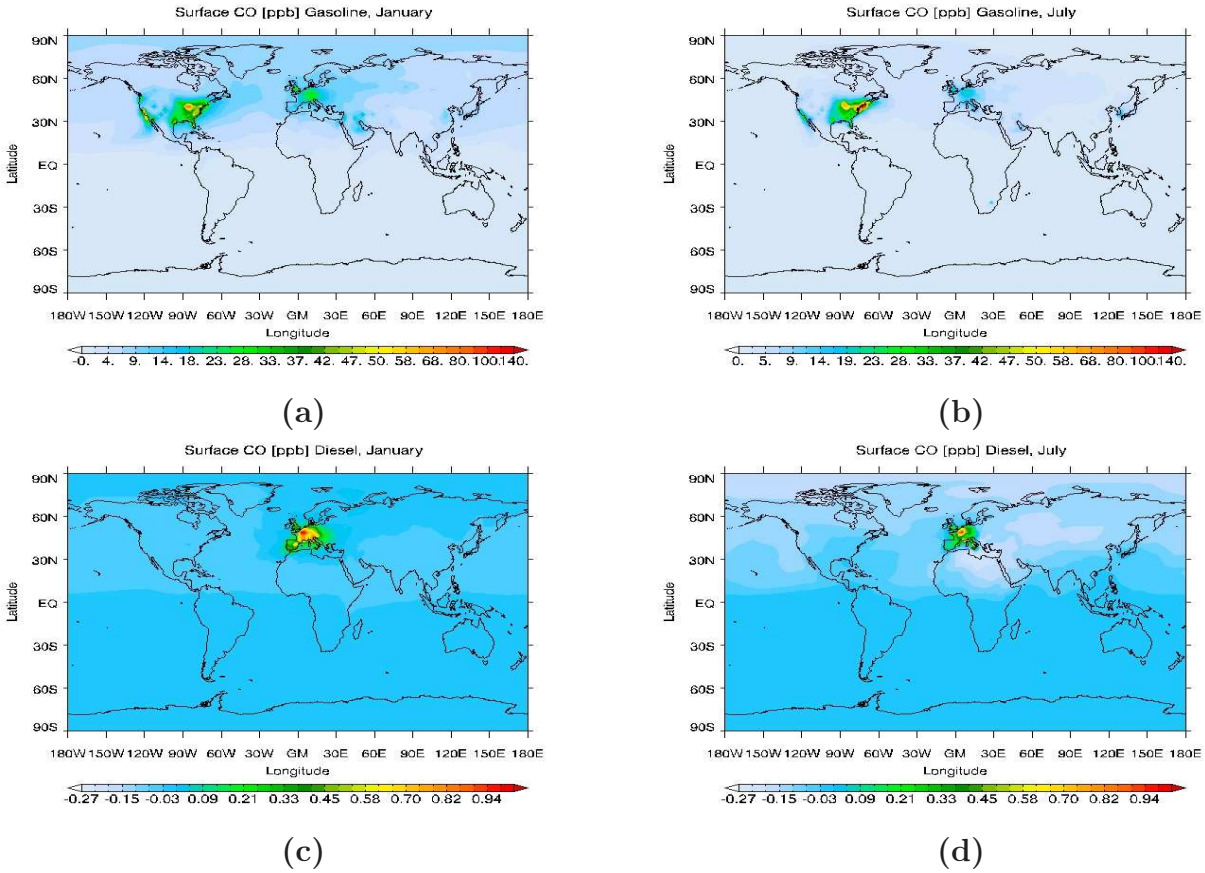

Figure 4.3: *Distribution of surface CO [ppb] from gasoline in a) January and b) July, and diesel in c) January and d) July calculated from "Ref2" model run (present worldwide traffic) minus Diesel model run, to get the effect of gasoline only, and equivalent "Ref2" minus Gasoline model run to get the effect of diesel only.*

Because there is a substantially higher number of cars with gasoline engines, plots with CO emission per a distance driven, 10^9 km (calculated from fuel consumption), were made, shown in figure 4.4. In January, the CO burden per 10^9 km, from gasoline emissions is in the range of 1 ppb to 8 ppb (figure

4.4 a) and in July about the same. For diesel, concentrations in the range of $0.1 - 1$ ppb per 10^9 km are found, but in a limited area, over south-west Europe, figure 4.4 c) and d). It is noticeable from the figure that gasoline has a higher emission of CO per driven distance than diesel, about by a factor 10 more. This has influence on the O_3 chemistry, as described in 2.2.3, and as will be exemplified later, in subchapter 4.3

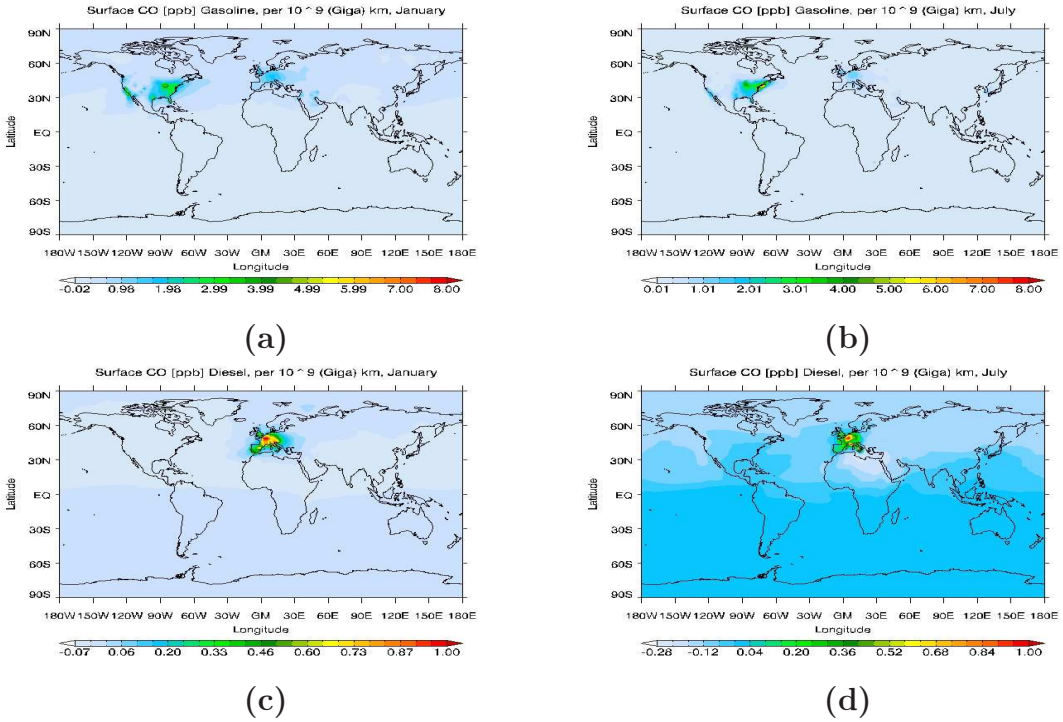

Figure 4.4: *Distribution of surface CO [ppb] from gasoline in a) January and b) July, and for diesel in c) January and d) July per distance driven. Here, the increase in CO from the two fuel types (minus "Ref2", without traffic) is plotted per* 10^9 *kilometre, calculated from the respective fuel consumptions.*

4.1.1 *CO* Euro4 and Euro5

The Euro4 and Euro5 model runs were performed with total fuel consumption sat to equal gasoline or diesel emissions, and to satisfy the legislation emission standards given in table 2.5. In the case of Euro4, the enhancement in surface CO from gasoline in January, figure 4.5 a, is most pronounced over north-eastern United States, but also a plume over California is present. The increase in these areas is in the range of 8-15 ppb (10 -14 %, not shown). The increase over Europe is somewhat smaller, in the range of 5-12 ppb (6-9 %). There are also some spots north in Saudi-Arabia, with an increase of about 5 ppb (5%). In July, figure 4.5 b, there are larger enhancements in the vicinity of Washington D.C., New York and Boston, with plumes of 14

ppm (17%). The transition from Euro4 to Euro5 involves no change in the case of CO (see table 2.5), and from figure 4.5 c and d, the Euro5 gasoline run from January and July, respectively, no change in the emission pattern is detectable. However, differences in emissions of NO_x and $NMHC$ when moving from Euro4 to Euro5 are expected to alter the abundance of OH, which in turn can change the CO distribution. In Euro5, there is less emission of NO_x, which leads to a smaller increase in OH, which yield an increase of CO over some regions (plots of difference between Euro5 and Euro4 not shown), but only of 0.05 ppb. In regions where emissions are particularly high, e.g. east coast of the United States, a decrease of 0.02 ppb is found.

Enhancement in CO from diesel with Euro4 emission limits (figure 4.5 e-h) shows the same emission patterns, which is natural, since total fuel consumption is sat either to gasoline or diesel. The increase is, however, of smaller scale, with the values over north-east United States being 4-7 ppb (3-6%), abouth half of the values from gasoline, in the winter for the Euro4 model run (figure 4.5 e). Over Europe, the increase is about 4 ppb (3%), and is most pronounced in the UK and central Europe. North and east Europe together with Spain have smaller values, only up to 2 ppb. In the summer (figure 4.5 f) New York and Boston have the largest enhancements, with 7 ppb (6%), and around 4 ppb is found otherwise in north-east U.S. California shows increases in the size of $\sim$3 ppb, about the same as Europe. The CO emissions legislation are for diesel, as it was for gasoline, the same for Euro4 and Euro5 (table 2.5), and the figures from Euro5 diesel model runs, figure 4.5 g and h, show no detectable differences in the distribution or size in CO enhancements. Nevertheless, following the same reasoning as before, a decrease in NO_x leads to a smaller abundance in OH, and a small increase in CO for the Euro5 run. In January, the increase is in the range of 0.1-0.15 ppb in the Northern Hemisphere, and 0.01 ppb in Southern Hemisphere. In July, the increase is in the range of 0.1-0.2 ppb in NH, and 0.05 in SH (not shown).

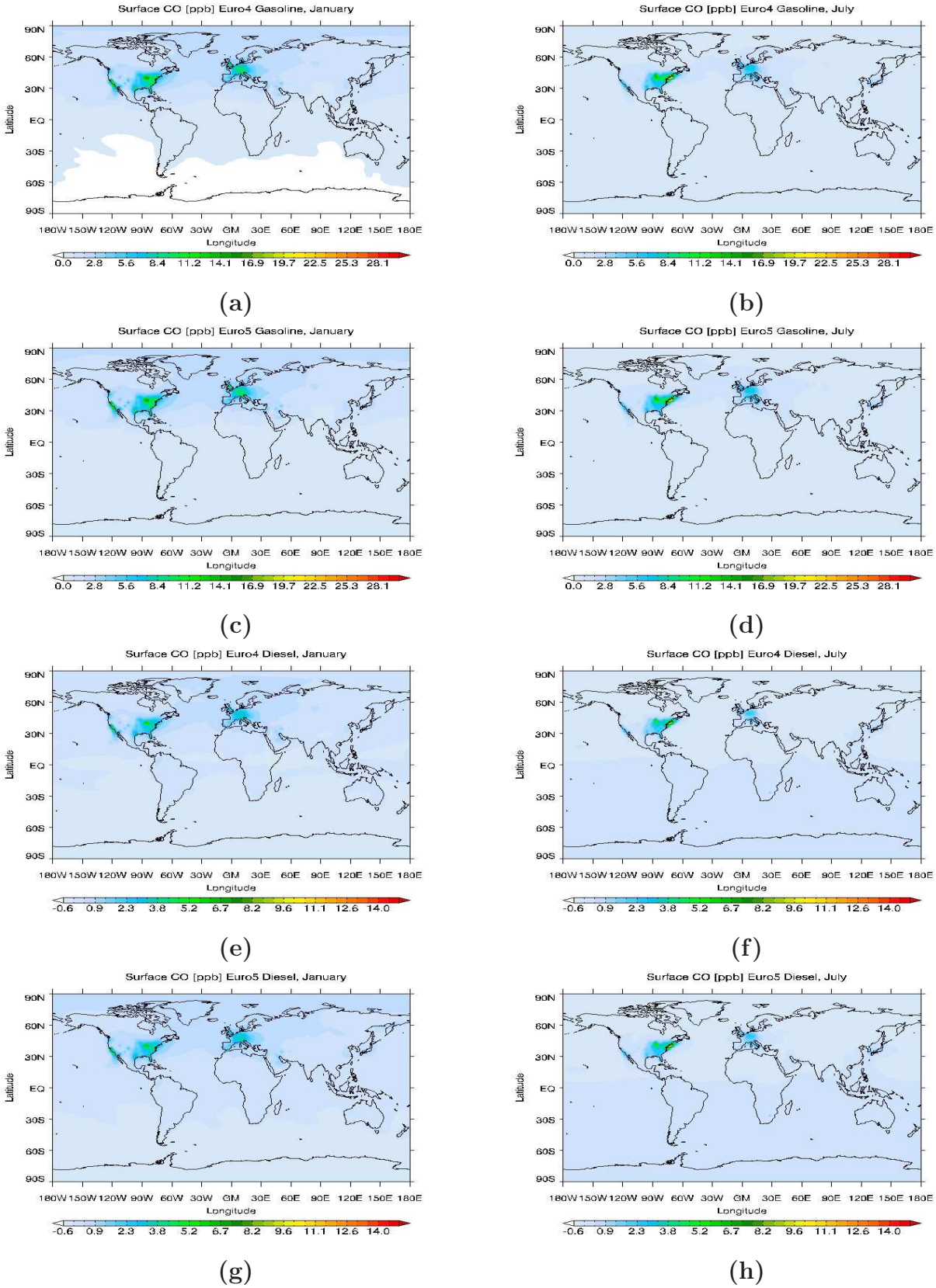

Figure 4.5: *Distribution of surface CO [ppb] from gasoline Euro4 model run in a) January and b) July, and Euro5 model in c) January and d) July and diesel Euro4 model run in e) January and f) July. Diesel Euro5 in g) January and f) July. The results are presented as the difference between the respective model runs, and "Ref1" (without any traffic).*

4.2 Nitrogen oxides (NO_x)

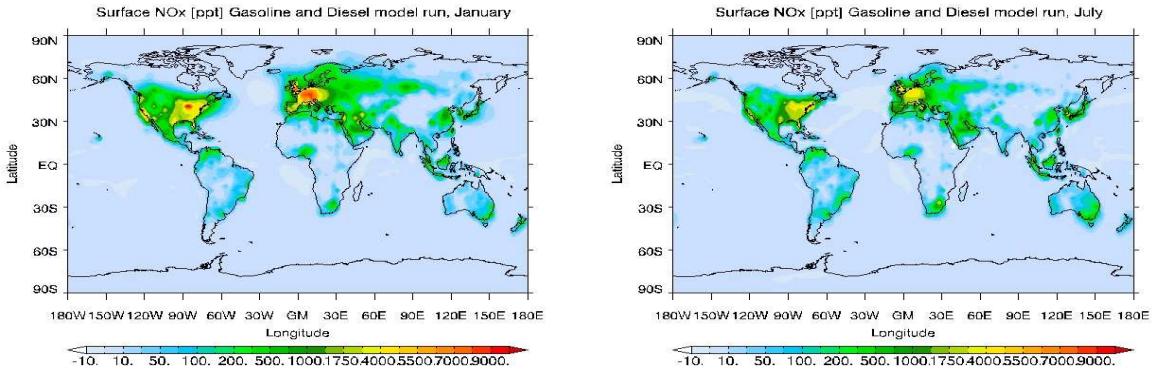

(a) (b)

Figure 4.6: *Distribution of surface NO_x [ppt] from both diesel and gasoline model run, "Ref2" (with present worldwide traffic) minus "Ref1" (with no traffic emission) in a) January and b) July*

The addition in surface NO_x from road traffic is shown in figure 4.6, for January to the left, and July to the right. It is the "Ref 1" model run scenario, with no traffic emission, subtracted from the model run scenario "Ref 2" with present worldwide traffic emission, so the effect on NO_x from traffic only can be investigated. The largest increase in NO_x are found over the same regions as for carbon monoxide, namely North-America and Europe. Here are the mixing ratios of NO_x ranging from 1200-8000 ppt in January, corresponding to 35-80 % (not shown), and 1200-5500 ppt (35-65 %) in July. Increasements over some parts of South-America, South-Africa, Nigeria, Saudi-Arabia, Eastern Europe, Norway, Russia, India, China, Japan and Korea, Thailand and parts of Australia also show an enhancement in NO_x, where the concentrations are found in the interval 300-850 ppt (20-35%) in January and around 600 ppt (25 %) in July. In the vicinity of Hawaii, NO_x levels of about 100 ppt is found, where dominant easterly winds transport the plume over the ocean west of the island, though not very far due to the relatively short lifetime of NO_x.

The monthly average of NO_x over the year the model was run for, from gasoline and diesel separately (figure 4.7) shows that NO_x is emitted over larger parts of the world from gasoline than diesel. Diesel (figure 4.7 b) has only a plume of emissions over south-west Europe, with concentrations of 1500 - 3000 ppt (20-35 %, not shown). NO_x emissions from gasoline are found over more, and bigger, parts of the Earth's surface. Emissions are concentrated over urbanized areas, with emissions especially pronounced over large areas of North America (1750-6000 ppt, 25-65 %), Middle America (100-500 ppt, ∼20%), Venezuela, Argentina, Brazil (500-1000 ppt, ∼10%), South Africa (∼1750 ppt, 25 %), Nigeria (500 ppt, 20%), the Middle East (1750-3000 ppt,

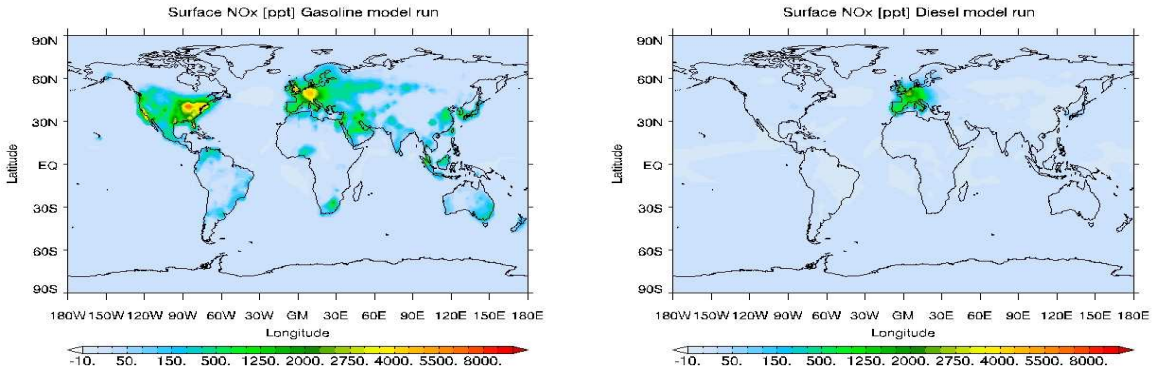

(a) **(b)**

Figure 4.7: *Distribution of surface NO_x [ppt] averaged over all months the model was run for (1 year). From a) Gasoline model run and b) Diesel model run, i.e "Ref2" (with present worldwide traffic) minus diesel traffic model run and gasoline traffic model run, respectively.*

~30%), Europe (1750-5000 ppt, 25-50%), Saudi-Arabia (1750-3000 ppt, 25-50%), India, China, Korea, Japan, Malaysia and south-east Australia (~1500 ppt, 20%).

The seasonal differences in NO_x contributions from gasoline and diesel are shown in figure 4.8. The difference from January to July is not striking, but for gasoline, there is about 3000 ppt higher concentrations in urbanized, industrialized areas, such as North America and Europe in January. The difference in diesel between January and July is around 1000 ppt where the emission is highest, in central Europe. In the outskirts of the emission hot-spot in Europe, the difference is less, about 100 ppt.

The impact of NO_x emissions compared to CO is much more confined to the vicinity of the source regions as the atmospheric lifetime of NO_x is about one order of magnitude shorter than the lifetime of CO (1-2 days and on the order of months, respectively). However, the relative enhancement of NO_x in areas outside the emission source, e.g in the Arctic over Spitsbergen, is 20 % from gasoline (not shown) and 8 % from diesel. Emissions of NMHC from road traffic, leading to enhanced formation of PAN can explain the increase in NO_x outside the emissions hot-spots, since PAN can be transported through the hemisphere and decompose in subsidence regions, as mentioned in the subsection about Nitrogen oxides, in the theory, section 2.2.2. This represents an indirect transport of NO_x.

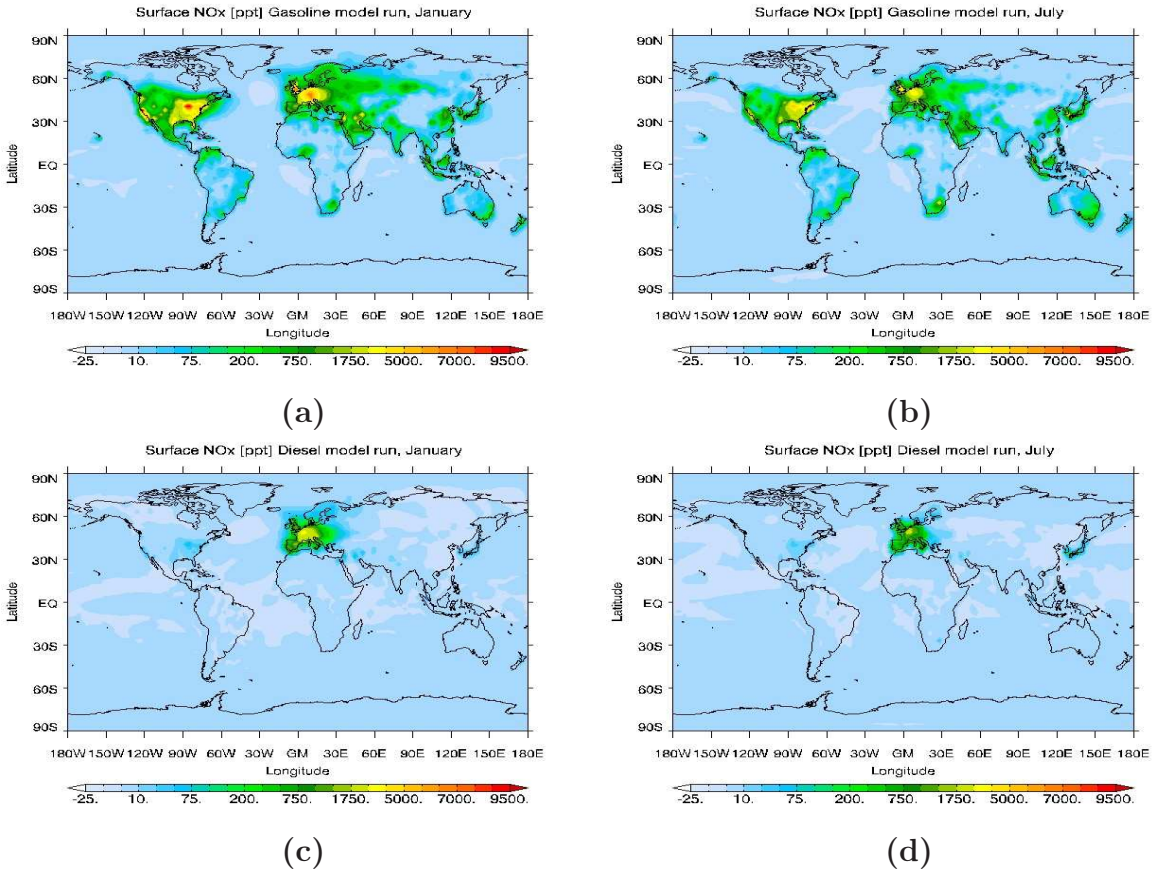

Figure 4.8: *Distribution of surface NO_x [ppt] from gasoline in a) January and b) July, and diesel in c) January and d) July. Calculated from "Ref2" (with current worldwide emissions) minus the model runs for Diesel and Gasoline, respectively.*

Figure 4.9 show NO_x emissions per distance driven, equivalent to figure 4.4, for CO. Both fuel types show a larger burden pr km in January (a and c), because of the longer lifetime when there is less sunlight. Over North America 50 - 500 ppt is found, and 50 - 350 ppt in Europe, per distance driven (10^9 kilometres) with gasoline engine (a and b). With diesel engine (c and d), up to 2750 ppt per distance driven is found in central Europe, with a sharp gradient of lower increase away from where the maximum burden is found. 50 - 200 ppt is calculated in North America.

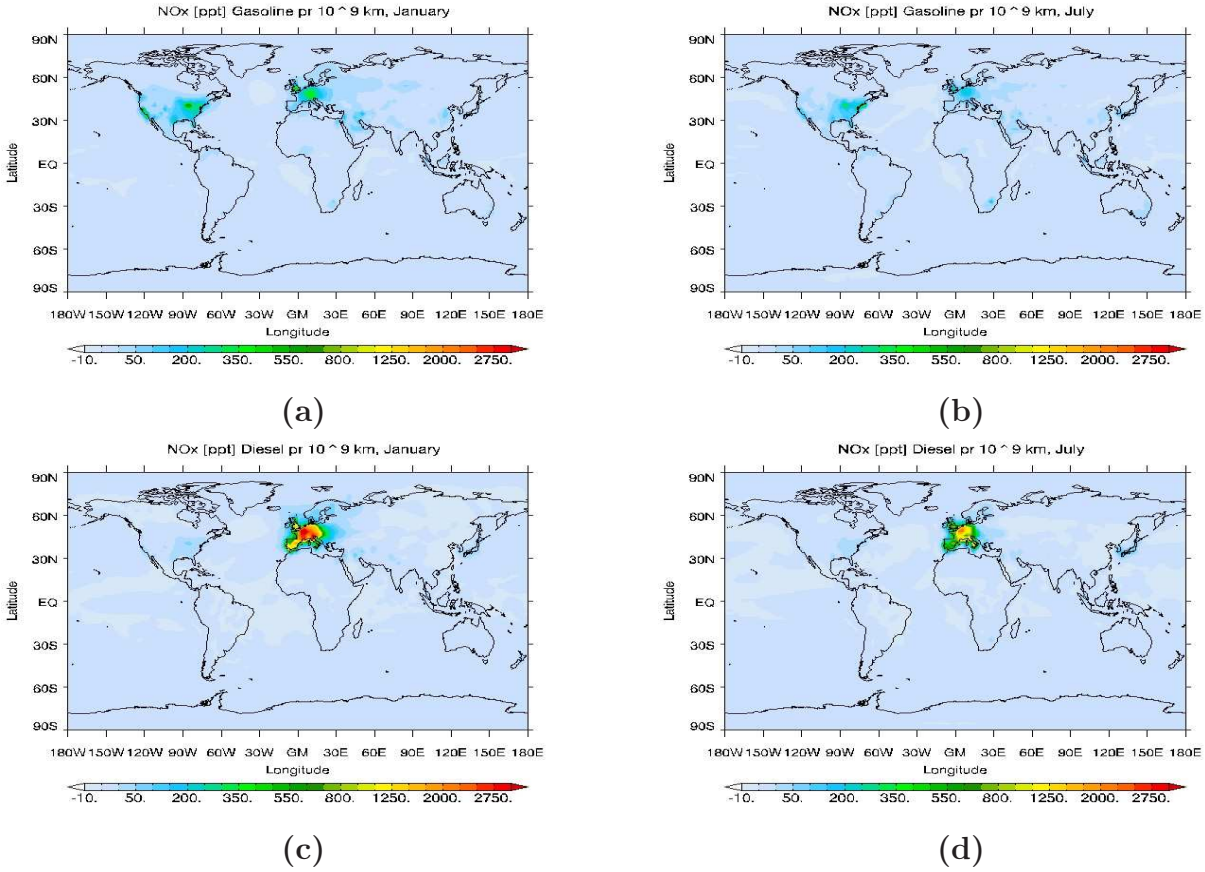

Figure 4.9: *Distribution of surface NO_x [ppt] from gasoline in a) January and b) July, and diesel in c) January and d) July per distance driven. In this figure, the increase in NO_x from the two fuel types (minus "Ref1", without traffic) is plotted per 10^9 kilometre, calculated from the respective fuel consumptions.*

4.2.1 NO_x Euro4 and Euro5

Figure 4.10 shows NO_x enhancements from traffic when all automobiles are sat equivalent to gasoline emissions, and to satisfy Euro4 (figure 4.10 a and b) and Euro5 (figure 4.10 c and d) legislation emission limits. The emission legislation limits are found in table 2.5. In northern United States in January, the NO_x concentrations in the Euro4 model run range from 50 ppt to a maximum of 2250 ppt (50 %) (only over a limited area, however), and in Europe $500 - 1100$ ppt (13-25 %). In July, emissions in other regions are slightly more prominent than in January, such as South-Africa, Saudi-Arabia and Japan as well as parts of South-America, but the maximum values in North America and Europe are somewhat smaller, only 1500 (30 %) and 700 (15 %) ppt, respectively. Euro5 (figure 4.10 c and d) standards reduce the maximum concentrations in North America and Europe to 1500 and 750 ppt, in January, and in July to 800 and 600 ppt.

Surface distribution of NO_x when all automobile exhaust emissions are sat to equal diesel exhaust is shown in figure 4.10 (e) - (h). NO_x maximum in January (e), is with Euro4 standards 4500 ppt, located in the same places as the maximum values in the gasoline Euro4 and Euro5 runs. East in Europe concentrations are calculated to be around 500 ppt, the same as in Saudi Arabia and a region in China. Japan shows concentrations of about 225 ppt. In July (4.10 f), the extent of NO_x concentrations are more confined. The concentrations are also of smaller scale, over North America the mixing ratios have a maximum of about 3000 ppt, and in Europe 1500 ppt.

Transferring to Euro5 standards leads to a reduction in the range of 400 - 1000 ppt east in North America (in January), with a maximum reduction on the location of maximum emission. In Europe the reduction is in the range of 400-600 ppt. In July, the reduction is of smaller scale, in the range of 250 to 550 ppt in the USA, and 250 ppt in Europe. Thus, the transition to Euro5 standards from Euro4 leads to a relatively large reduction in surface NO_x concentrations.

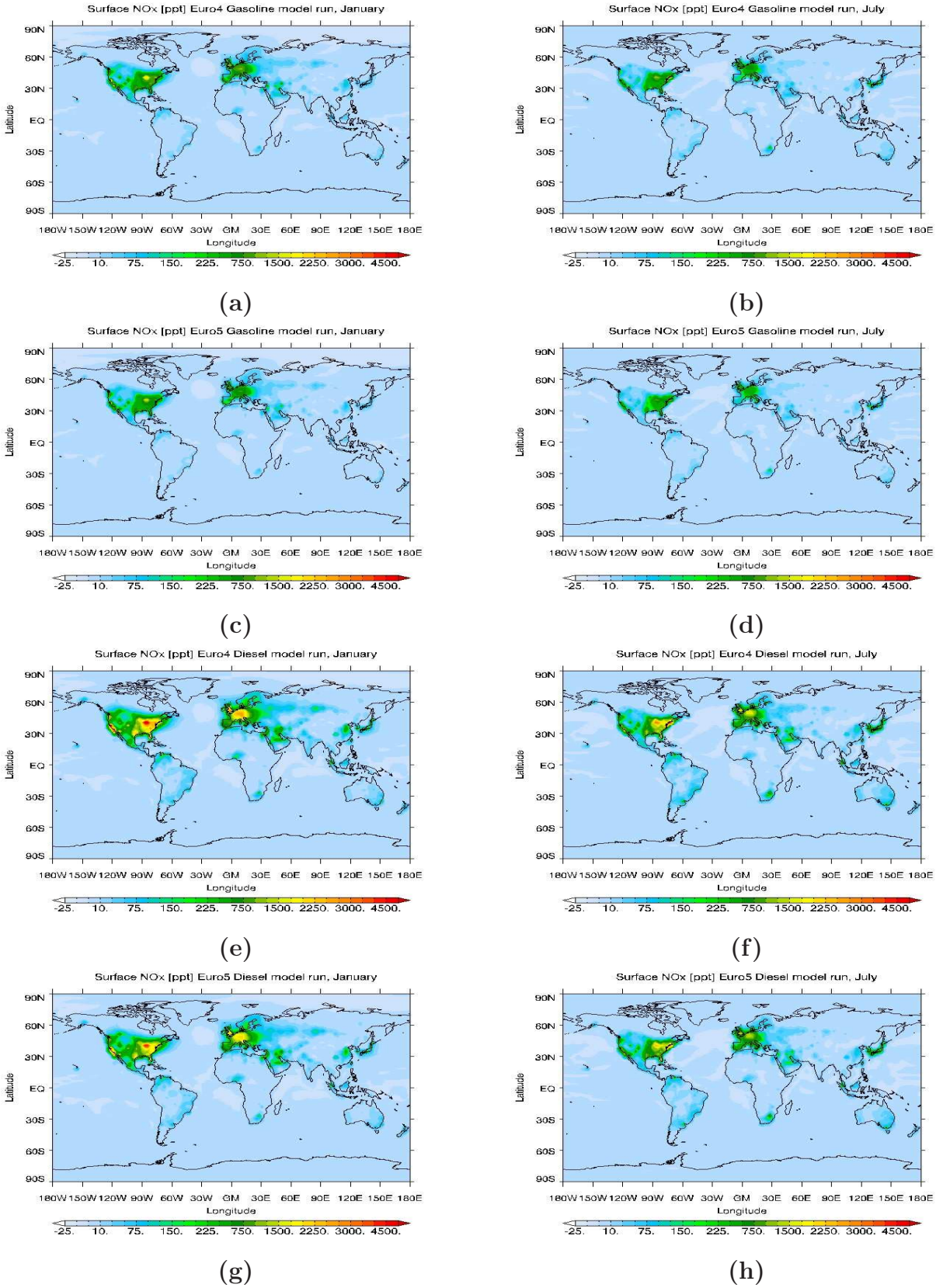

Figure 4.10: *Distribution of surface NO_x [ppt] from Euro4 gasoline model run for a) January and b) July, and Euro5 gasoline model run for c) January and d) July. From Euro4 diesel model run for e) January and f) July and Euro5 diesel model run for g) January and h) July. Here, total fuel consumption was sat to either gasoline or diesel, and to satisfy Euro4 and Euro5 legislation emission limits. The results are presented as the difference between the respective model runs, and "Ref1" (without any traffic). For emission limits, see table 2.5.*

4.3 Ozone (O_3)

In this section, the effect road traffic emissions exerts on tropospheric ozone levels is presented, first from road traffic as a whole, and then for the effects from gasoline and diesel individually. Further, the effects from Euro4 and Euro5 legislation emissions on gasoline and diesel are investigated, before examining if road traffic contribute to health threatening ozone levels, at the end of the subchapter.

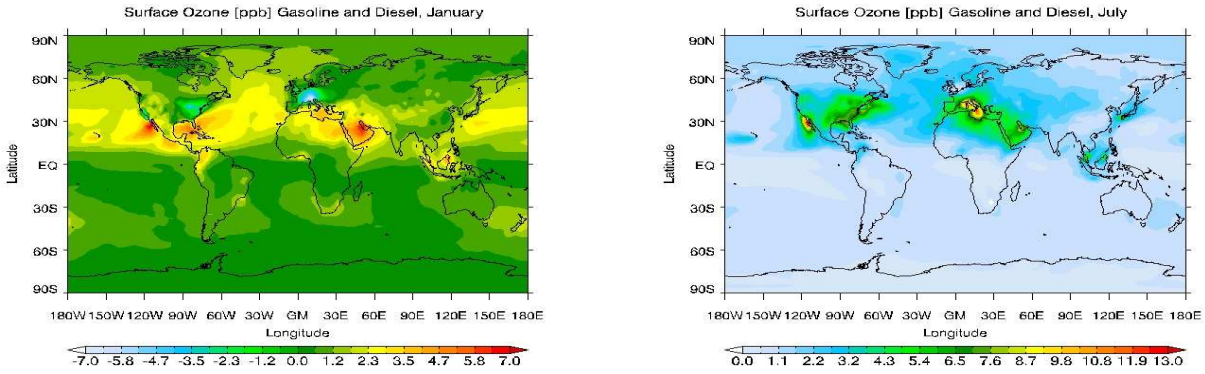

(a) **(b)**

Figure 4.11: *Distribution of surface Ozone [ppb] from both diesel and gasoline model run in a) January and b) July. Presented as the difference between "Ref2" (with present worldwide traffic) and "Ref1" (with no traffic).*

Changes in ozone concentrations due to road traffic are shown in figure 4.11 for January and July. During winter (4.11 a), in the highly polluted industrialized and urbanized regions of the Northern Hemisphere, negative ozone values are obtained, due to ozone titration. This ozone titration is associated with increased levels of NO_x concentrations (as seen in figure 4.6 which shows NO_x enhancement from road traffic). Thus the surface ozone concentration is decreased in response to road traffic, with approximately 2-7 ppb (∼30 %) in Europe and a slightly less reduction in northeast United States. Outside these areas, the changes in the concentration are slightly positive, with increases of the order of 4 ppb (8 %), north of 30 °N. Largest increase is found in the latitudinal band around 20-30 °N, where there is sufficient sunlight for photochemical reactions in January. Ozone increases of 5-10 ppb (10 to 15 %) are calculated in these regions. Hot-spots, with high ozone production in the urbanized areas are evident in the surface distribution of ozone levels in July (4.11 b). Automobile exhaust increases the concentration by 4-10 ppb (10-20 %) in North America, Europe, North Africa, Saudi-Arabia, east and south Asia, and reach 15 ppb (25%) in California and in the Mediterranean region. The ozone calculations for road traffic agree well with what Niemeier et al. (2006) calculated in their work.

The changes in ozone levels from gasoline and diesel emissions separately, for January and July are shown in figure 4.12, gasoline in (a) and (b) and diesel

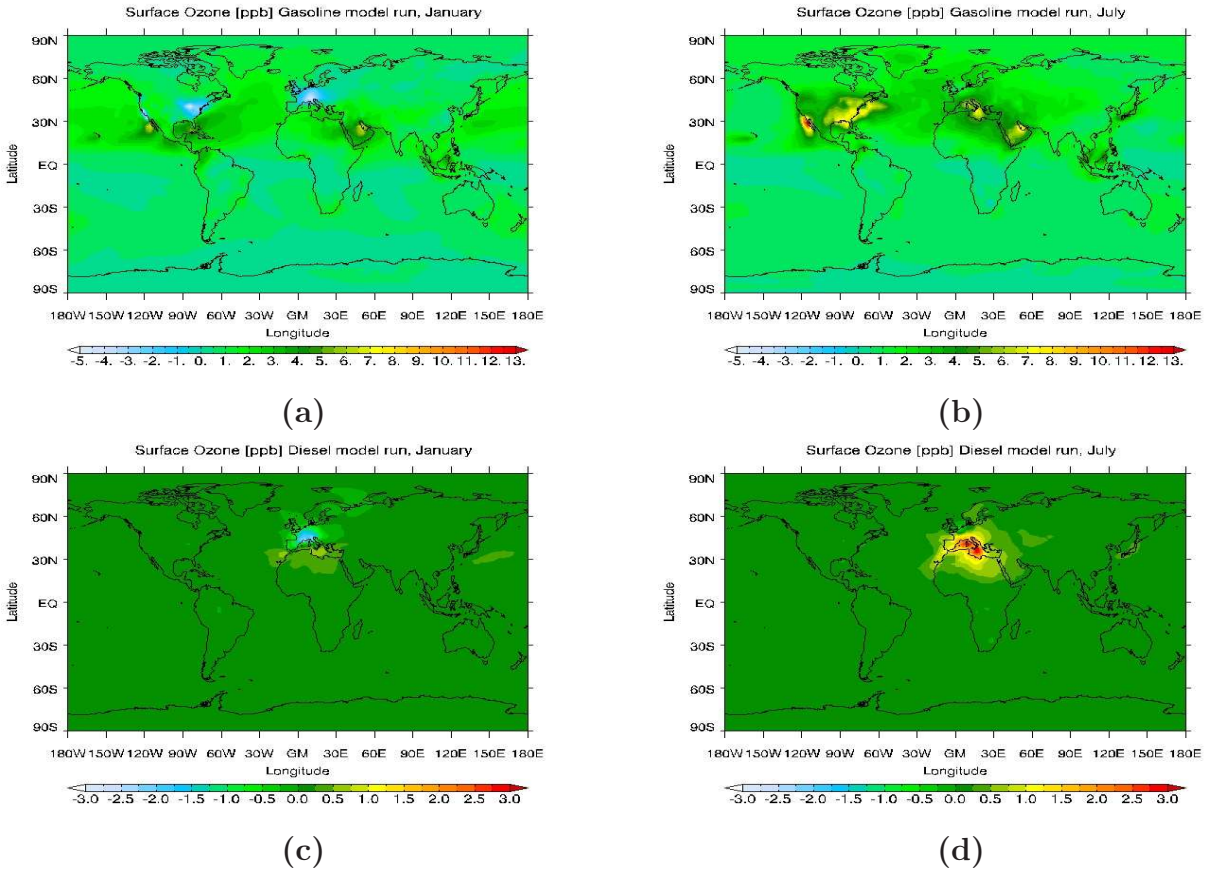

Figure 4.12: *Distribution of surface Ozone [ppb] from gasoline in a) January and b) July, and diesel in c) January and d) July. Here, differences between "Ref2" (with present worldwide traffic) and diesel and gasoline model runs, respectively, are shown.*

in (c) and (d). The surface distribution for the gasoline model run shows many of the same features as for total road traffic, however with not as large perturbations. Changes in ozone levels calculated from the diesel model run (4.12 c and d), are limited to Europe, with a decrease in ozone in January, of about 3 ppb or 10 % (not shown) in central Europe. In the Mediterranean an increase of 1 ppb or 4 % is found. In the summer (4.12 d), ozone levels due to diesel in central Europe are in the range of 1-3 ppb, or 5-10 %.

When changes in ozone are plotted per driven distance (10^9 kilometres), gasoline produces a reduction of 0.5 ppb in January in Europe and northeast U.S as well as in California (figure 4.13 a), per distance driven, and an increase of about the same size in Saudi-Arabia and south of California. In July, the contribution to surface ozone per driven distance with gasoline fuel is 1 ppb in California, and about 0.5 ppb in northeast U.S., south Europe and Saudi-Arabia (figure 4.13 b). The induced ozone change due to diesel per distance driven (figure 4.13 c and d, January and July, respectively) is of 2-3 ppb reduction in south Europe in January, and an increase of about

0.7 ppb in the Mediterranean region. In July, 2-4 ppb enhancement of ozone levels are calculated.

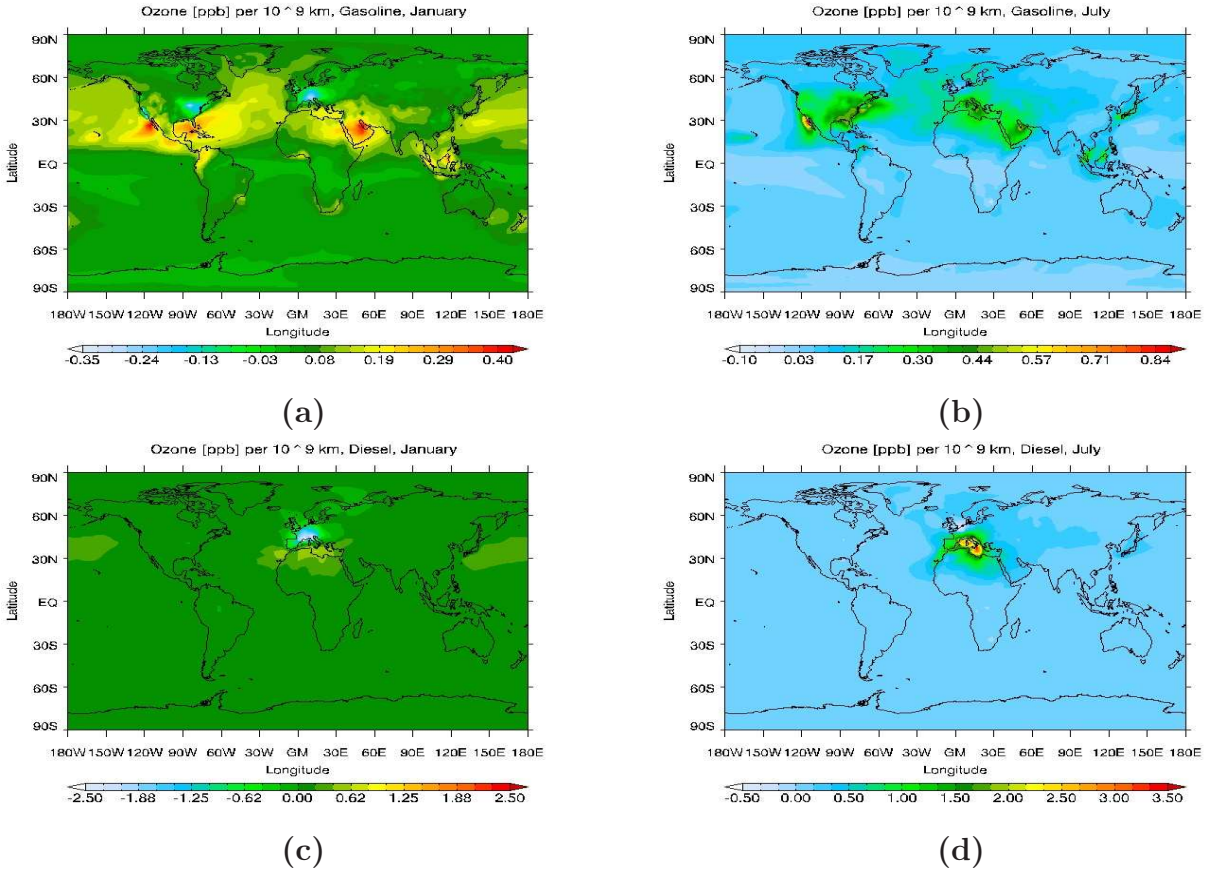

Figure 4.13: *Distribution of surface Ozone [ppb] from gasoline in a) January and b) July, and diesel in c) January and d) July, i.e "Ref2" (with present worldwide traffic) minus Diesel and Gasoline model runs, respectively, plotted per distance driven* (10^9 *km).*

Ozone is as described in the theory chapter (chapter 2) a secondary pollutant, produced in the atmosphere by reactions involving NO_x and CO. The two latter are on the contrary primary compounds, thus the distribution of ozone generally reflects the source regions of NO_x and CO, as can be seen when comparing the figures of CO, NO_x, and O_3, for example figures 4.1, 4.6 and 4.11. Road traffic (both gasoline and diesel) induced ozone increase in the summer outside the major source regions, is however of relatively considerable size; in the range of 1.5 - 3 ppb, or 5 - 10 % (not shown), for examlpe over Greenland (figure 4.11). In subchapter 4.2, it was discussed how NO_x can be transported to rural areas despite its relative short lifetime by the conversion to PAN. In this way NO_x from road traffic can be "re-emitted" outside the emission hot-spots in the urbanized regions. Here the concentrations of background trace gases are low, especially nitrogen oxides (Matthes

et al., 2007). As productivity of ozone formation decreases with increasing NO_x concentrations, NO_x emissions from road traffic are much more effective when emitted in remote areas. In industrialized regions ozone production takes place at high NO_x concentrations, and is, as discussed in association with figure 2.4, dependent on the supply of hydrocarbons.

When the high NO_x concentrations increase in the already highly polluted industrialized and urbanized regions of the Northern Hemisphere during winter, ozone is titrated, and its surface concentration is reduced in response to road traffic. O_3 concentrations are depressed through reaction with NO:

$$NO + O_3 \rightarrow NO_2 + O_2 \tag{4.1}$$

During summer, when there is sufficient sunlight, this reaction is normally balanced by photolysis of NO_2 (reactions 4.2, 4.3).

$$NO_2 + h\nu \rightarrow NO + O \tag{4.2}$$

$$O + O_2 + M \rightarrow O_3 + M \tag{4.3}$$

(also described in subchapter 2.2.3, reactions 2.27 to 2.29) and a net ozone production takes place when HO_2 reacts with NO

$$NO + HO_2 \rightarrow NO_2 + OH \tag{4.4}$$

in reaction 4.1's place, so that HO_2 is consumed in the conversion of NO to NO_2, and not O_3. These conditions apply above a threshold in the NO mass mixing ratio (typically above 10-30 ppt (Matthes et al., 2007)). HO_2 is formed during oxidation of CO and $NMHC$s, so their emissions influence the ozone production, as mentioned in subchapter 2.2.3.

NO_2 can also react with ozone to yield NO_3:

$$NO_2 + O_3 \rightarrow NO_3 + O_2 \tag{4.5}$$

When there is light present, NO_3 is photolysed back to NO_2 and O, but under conditions with no light, NO_3 reacts with NO_2:

$$NO_3 + NO_2 + M \rightarrow N_2O_5 + M \tag{4.6}$$

N_2O_5 then reacts with H_2O (liquid)

$$N_2O_5 + H_2O(l) \rightarrow 2HNO_3 \tag{4.7}$$

which is washed out, i.e removed by wet deposition. Thus, when there is no light present, two O_3 particles are removed (one from reaction 4.1, and one from 4.5), in addition to two NO_2 particles (from reactions 4.5 and 4.6).

Zonal mean distributions of ozone increase due to gasoline emissions are shown in figure 4.14, for January, April, July and October. While maximum

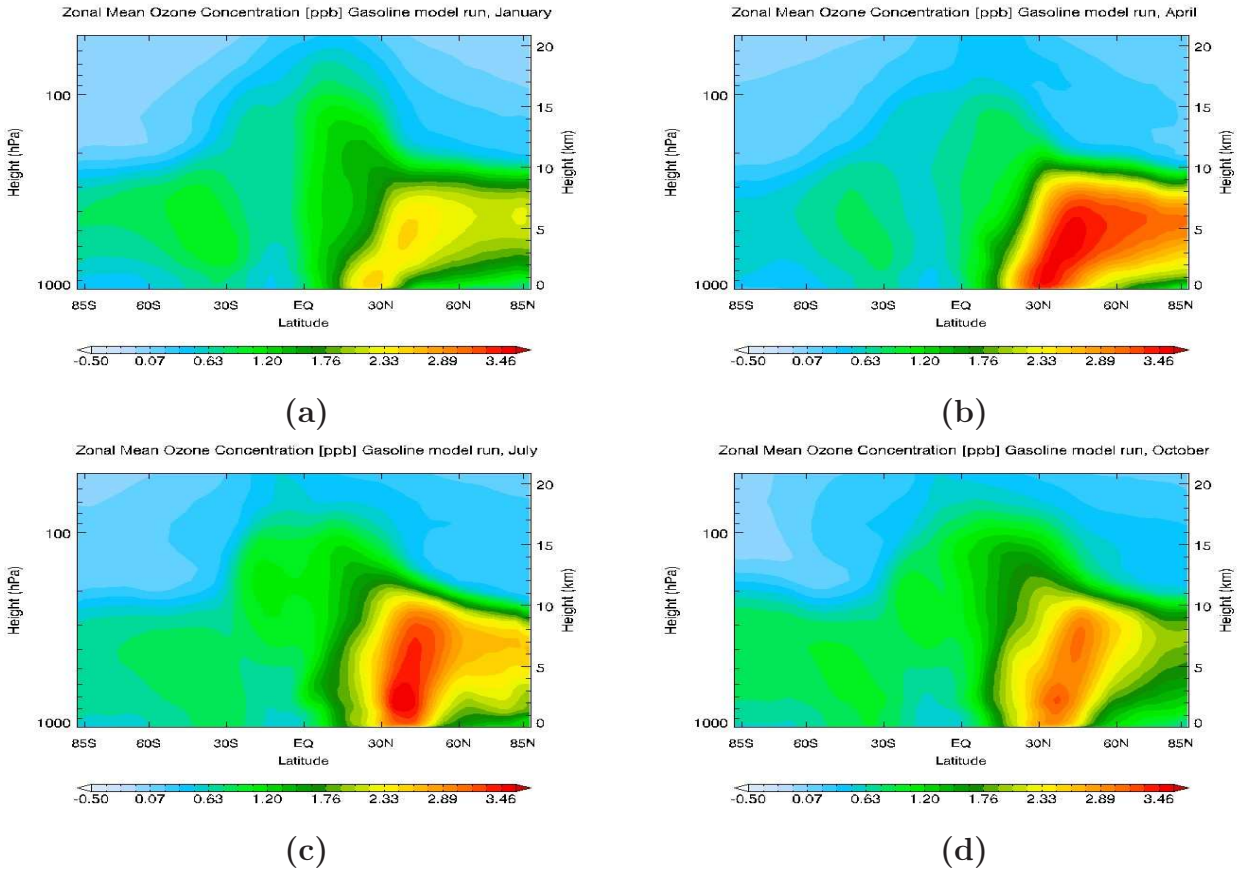

Figure 4.14: *Distribution of zonal mean ozone concentrations [ppb] from gasoline emissions, "Ref2" (with present worldwide traffic) minus diesel model run. In (a) January, (b) April, (c) July and (d) October*

surface ozone values occur during summer, the zonal mean shows a maximum in April. During winter, due to generally longer lifetime because of less chemical activity in lack of sunlight, the ozone precursors accumulate, which leads to a maximum in ozone concentrations in Northern Hemisphere in springtime, with values of 8 ppb. Maximum enhancement is around 30 ° N, where the ozone is lifted and transported north towards the Arctic regions. The maximum height with enhanced concentrations is reached over the tropics, where vertical exhange by convection is strong. About 1 ppb is calculated in 15 km height. Further north the enhancement is no higher than about 10 km.

In figure 4.15 the zonal mean concentrations in ozone from diesel are presented. The increase in ozone due to diesel is more confined than due to gasoline. However, the seasonal evolution is similar, with maximum in April, but with smaller abundances in all four months (in the range of 0.15 to 0.4 ppb). The figure shows that for diesel also, a plume of ozone reaches the Arctic. In January (4.15 a), the boundary layer in the Arctic is clean, while in the other three months, ozone concentrations reach the surface.

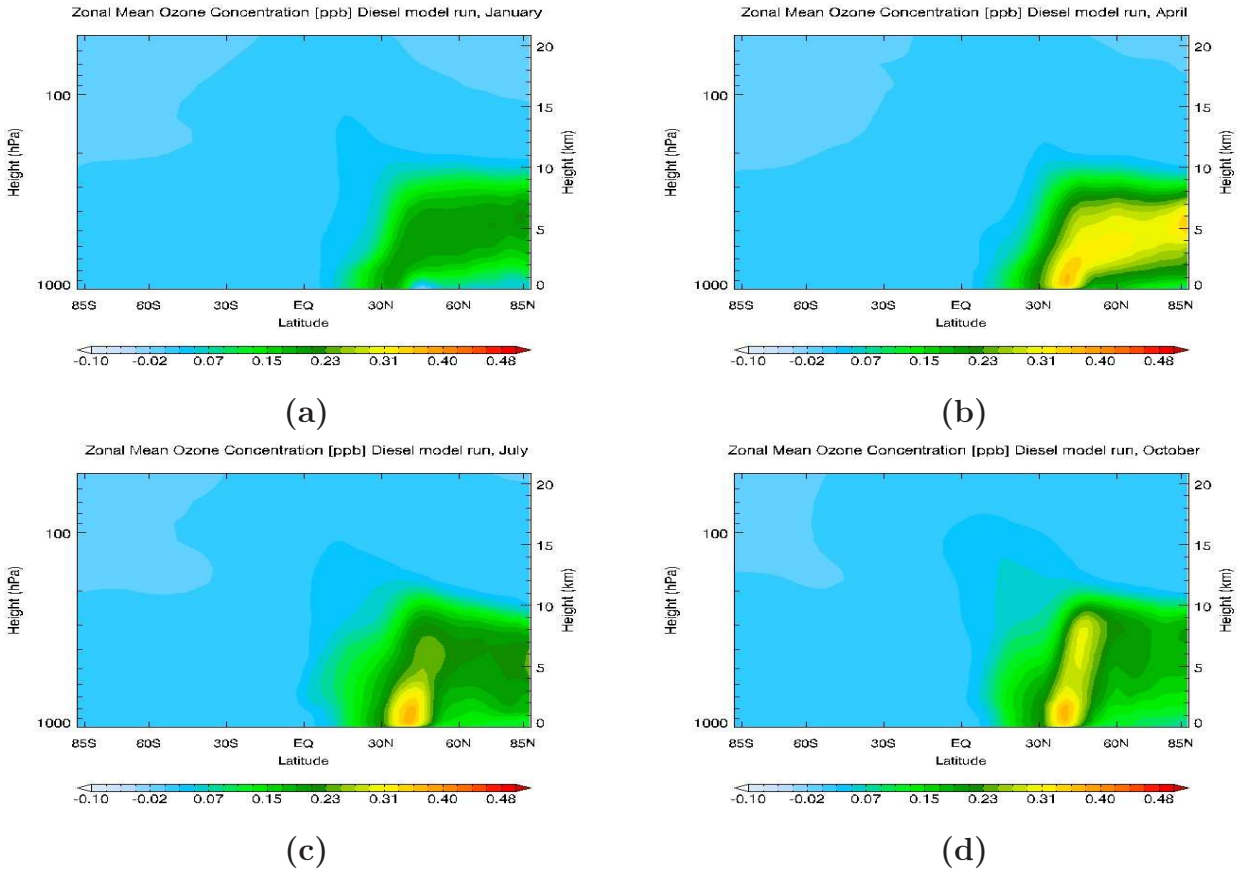

Figure 4.15: *Distribution of zonal mean ozone concentrations [ppb] from diesel emissions, "Ref2" (with present worldwide traffic) minus gasoline model run. In (a) January, (b) April, (c) July and (d) October*

Because of higher CO emissions from gasoline, which has a longer lifetime than NO_x, which is a more dominant component in diesel emissions, there is a larger ozone enhancement in the Southern Hemisphere in the gasoline model runs. CO can be transported longer than NO_x, and thus ozone can be produced further from the source of origin. This is implied in the two figures of zonal distribution, where small enhancement is detectable from the gasoline model run (1.25 ppb). However, the model was run for a shorter period of time than it takes for emissions from the Northern Hemisphere to be transported to the Southern Hemisphere, which is about 1 - 2 years. Longer model runs have to be performed to make a more certain statement on the contribution from gasoline in SH.

4.3.1 O_3 Euro4 and Euro5

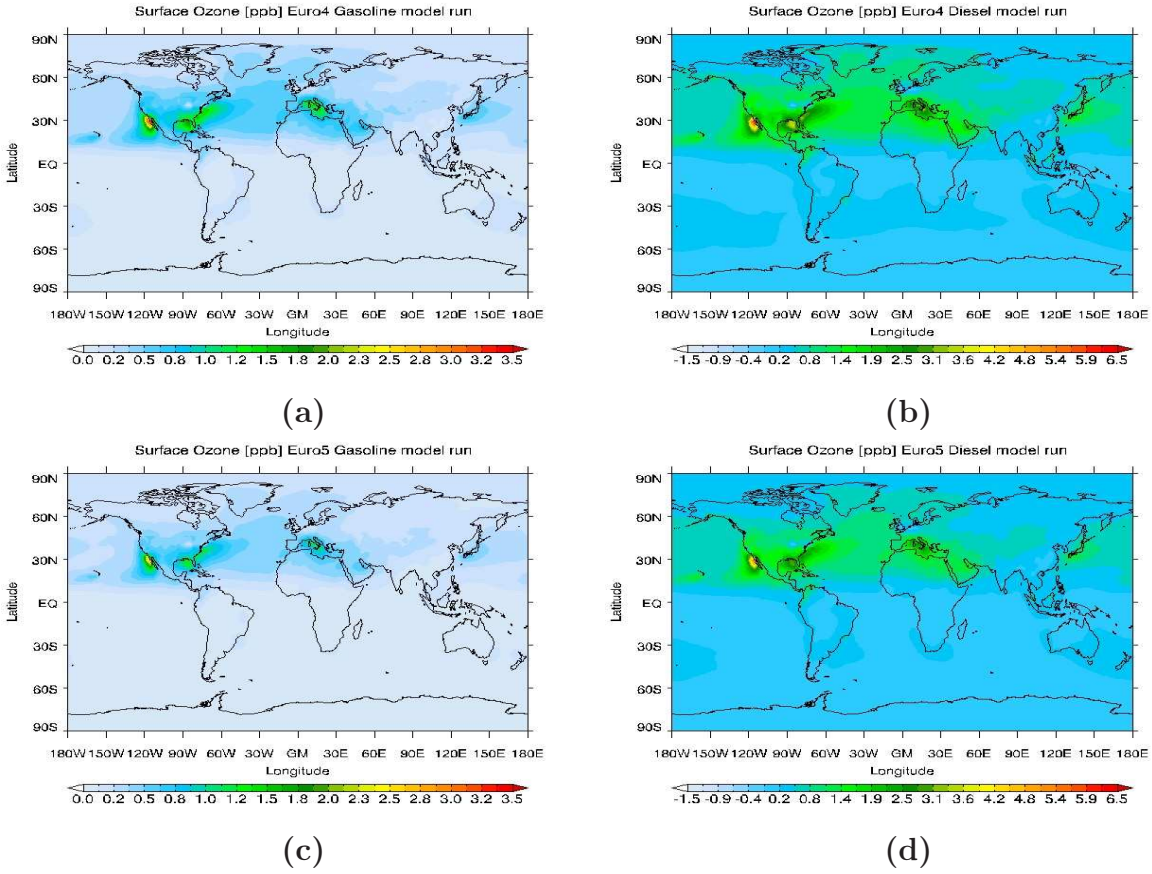

Figure 4.16: *Distribution of surface ozone concentration [ppb] from a monthly average from the one year the model was run. (a) Gasoline with Euro4 standards model run, (b) diesel Euro4 model run, (c) gasoline Euro5 model run, (d) diesel Euro5 model run, all with "Ref1" (with no traffic) subtracted so the effect of road traffic alone is shown. In the Euro4 and Euro5 model runs, total fuel consumption was sat to equal either gasoline or diesel, and to satisfy the EU legislation emission limits for Euro4 and Euro5, respectively. For emission limits, see table 2.5.*

The results from the Euro4 and Euro5 model runs are obtained by subtracting "Ref2", the reference run with no traffic present, from the Euro4 and Euro5 gasoline and diesel runs, so only the effect from road traffic emission, with the two legislation limits imposed is presented.

The surface ozone concentration induced by gasoline with Euro4 standards, figure 4.16 a, is only in the range of 1-4 ppb, with largest increase over California and the east coast of North America and southern Europe. A plume over the Atlantic ocean between the continents is present, with an increase of 1.5 ppb. Downwind of Japan and Hawaii an increase of about the same size is calculated. Euro4 standards, but with diesel emissions, produce more

surface ozone, with increased levels in the same areas as for gasoline Euro4. In the vicinity of California, a production of 7 ppb can be seen, while there is a somewhat smaller increase, around 4 ppb, on the east coast of USA, approximately around Florida, and a small decrease (1 ppb) of ozone is estimated near New York. A small decrease (1 ppb) is also found south in the UK, and an increase of about 2.5 ppb in the surrounding area of Italy. Over the Atlantic ocean, the enhancement is about 1.5 ppb. Also over Japan, an 1.5 ppb increase in ozone is estimated.

Figure 4.16 (c) and (d) shows the result in ozone from the model run with Euro5 standards for gasoline and diesel, respectively. It shows only small decreases, but the extent of ozone perturbations is smaller. For gasoline, the levels around the Mediterranean are 1 ppb, for Euro 4 standards it reached 4 ppb in the same area. In the vicinity of Florida 1.2 ppb is calculated for the Euro5, 2.5 ppb less than in Euro4, and in the vicinity of California, the concentrations in Euro5 reach 2.5 ppb, where it was up to 4 ppb in the Euro4 run. Diesel shows ozone levels of 4 ppb around California in the Euro5 model run, where it was 7 ppb in the Euro4 run. 2.5 ppb are found in the vicinity of Florida and the Mediterranean (4 ppb in Euro4). Levels of about 1.4 ppb are estimated over Japan and downwind of Hawaii, only slightly less than in the Euro4 run.

The response in ozone from the Euro4 and Euro5 runs for gasoline and diesel in January and July is shown in figure 4.17 a-h. Again the ozone titration is showing in January, while there is generally larger ozone enhancement in summer (July) than in winter. There is clearly more ozone production in the diesel model runs. Summer ozone levels are in the gasoline model run in the range of 1 - 5 ppb in the Northern Hemisphere, while the diesel run shows an increase up to 9 ppb. In the winter, ozone production from gasoline is around 2 ppb in the vicinity of California and Florida, while a decrease of 1 ppb is found east in North America and in Europe. Increase due to diesel has a maximum of 4.5 ppb in winter, and a maximum decrease of 3 ppb. From the EU legislation emission limits in Table 2.5, one can see that diesel emits over 3 times more NO_x than gasoline (Euro4 runs), but about half the amount of CO and hydrocarbons. In the Euro5 runs, the emissions have been reduced, from 2.5×10^{-4} $kg(NO_2)/km$ to 2.0×10^{-4} $kg(NO_2)/km$ for NO_x in diesel, and from 8.0×10^{-5} kg/km to 6.0×10^{-5} kg/km for gasoline. For CO, there is no reduction from Euro4 to Euro5 in diesel or gasoline, and neither for hydrocarbons in diesel, but for gasoline the reduction in hydrocarbons is from 9.0×10^{-5} kg/km to 6.8×10^{-5} kg/km. The reductions in emissions lead to a reduction of ozone in the range 0.3 - 2 ppb (gasoline) and 0.5 - 3 ppb (diesel), with the largest reduction located in the vicinity of the largest emission centers, as seen in figure 4.16 also.

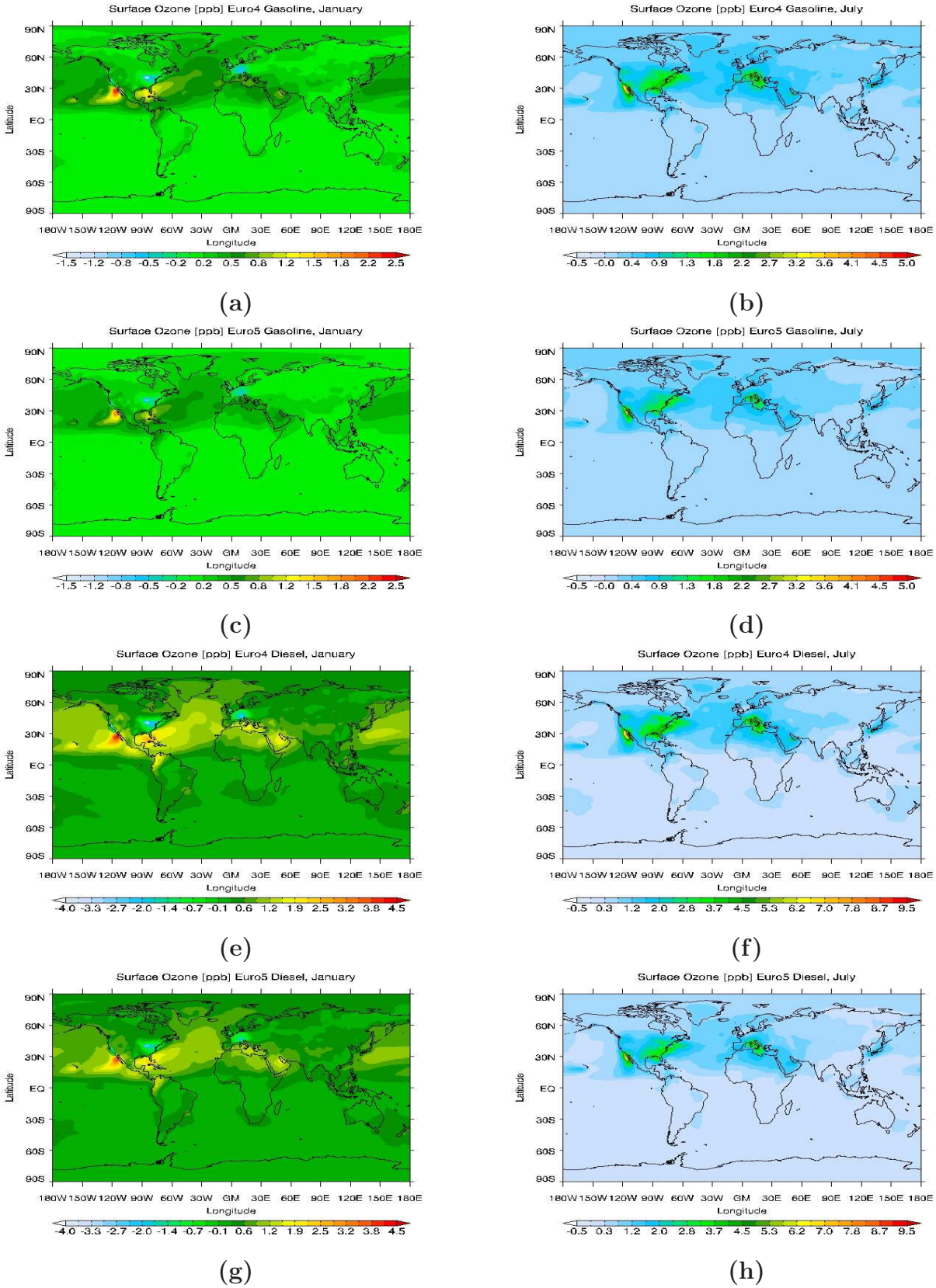

Figure 4.17: *Distribution of surface ozone concentration [ppb] from Euro4 and Euro5 model runs. For Euro4 gasoline in (a) January and (b) July. Euro5 gasoline in (c) January and (d) July. Euro4 diesel in (e) January and (f) July. Euro5 diesel in (g) January and (h) July. In these model runs total fuel consumption was sat to equal either gasoline or diesel, and to satisfy the EU legislation emission limits for Euro4 and Euro5, respectively. For emission limits, see table 2.5.*

4.3.2 Ozone - health perspective

Shortness of breath, dry cough or pain when taking a deep breath, tightness of chest, wheezing, and sometimes even nausea are common responses for humans exposed to high ozone levels (West et al., 2006). Ozone reacts with molecules in the airways, so that the lining of the airways loses some of its ability to serve as a protective barrier to microbes, toxic chemicals and allergens. Humans exposed to high levels of ozone have difficulties breathing because the airways respond by covering the affected areas with fluid and by contracting muscles. Ozone is also harmful for vegetation, by entering the plant's leafs through its gas exchange pores, the stomata, and dissolving in the water within the plant, reacting with other chemicals, which can among other consequences result in reduced photosynthesis, which in turn slows plant growth (Krupa et al., 2001). According to NILU (1995), Norwegian government notify the population when ozone concentrations exceed 160 μgm^{-3}, or 80 ppb.

In this section, surface ozone levels for three populated areas, North America, Europe and Asia , see figure 4.18 for the selected regions, are presented to examine the effect on air quality from the road transport sector. Ozone concentrations every hour, in the year the model was run for, in the first model layer were obtained to investigate the contribution from car exhaust emissions on occurrences of ozone concentrations in selected levels. The relative effects from present worldwide traffic, as well as gasoline and diesel separately are presented in this chapter. In addition, the relative effects from transferring to Euro5 from Euro4 are introduced.

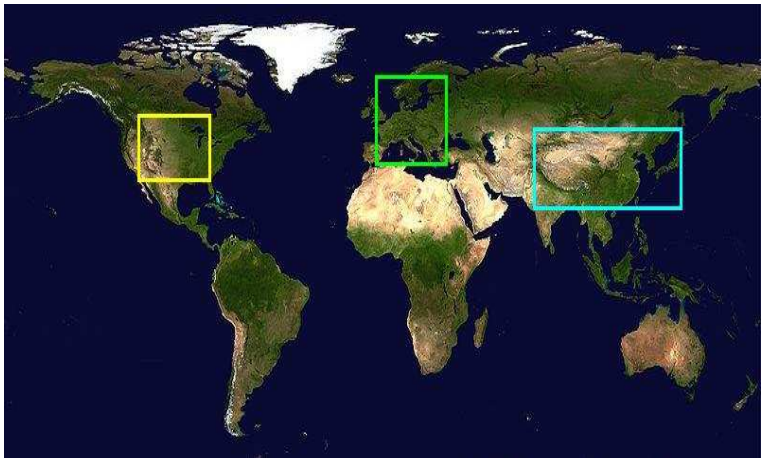

Figure 4.18: *The different boxes show the three areas which are emphasised in this section. Yellow box: parts of North America, green box : parts of Europe and turquoise box: parts of Asia, mainly China (figure adapted from Wikinews (2009))*

Day to day variability in ozone concentrations depend strongly on the alterations in meteorological conditions, such as solar radiation, temperature and stability. The presence of an inversion layer acts to prevent air from mixing vertically, and can trap accumulating ozone concentrations close to the surface. Relatively low wind speeds associated with weak horizontal pressure gradient around a surface high pressure and fair weather with high solar radiation (due to lack of clouds), could also lead to accumulating concentrations and high ozone levels. The focus in this study is, however, on the effect road transport emissions exert on the chemical production on tropospheric ozone, and the variability in meteorological factors is not investigated.

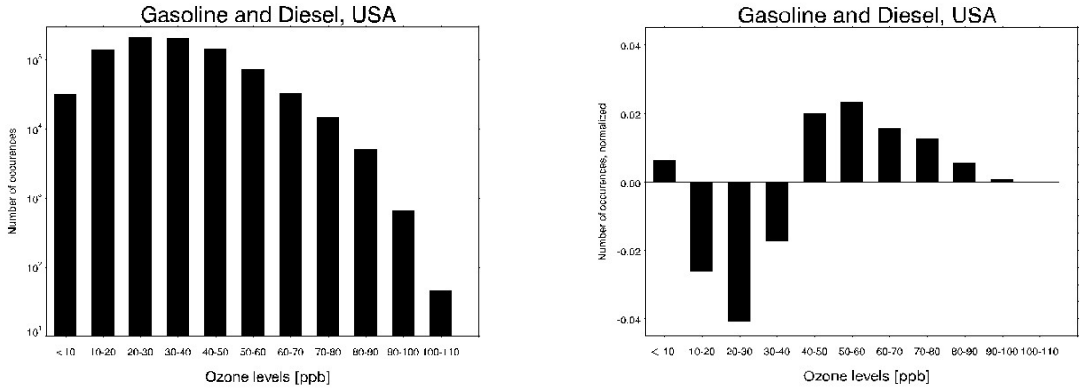

(a) **(b)**

Figure 4.19: *(a) Number of occurrences (logarithmic y-scale) of O_3 concentrations in specified interval levels calculated in the "Ref2" model run (with present worldwide traffic) in North America. (b) Change in occurrences of ozone levels [ppb] in specified intervals from North America, obtained from the model run "Ref2", relative to "Ref1" (with no exhaust emissions).*

Figure 4.19 (a) show the occurrences of ozone concentrations in different intervals from the run "Ref1", with present worldwide traffic, while figure 4.19 (b) shows the relative contribution on surface ozone concentrations from present worldwide traffic. The contribution in increased ozone levels from road traffic is roughly on the short side of 9 %, and extend from 40 to 100 ppb. The additional occurrences in the lowest interval, $<$ 10 ppb, originate from the titration of O_3 in wintertime, described in the theory chapter, 2.2.3, and discussed in chapter 4.3. Figure 4.20 displays the contribution from gasoline (4.20 a) and diesel (4.20 b) separately. In North America the shear of automobiles with diesel engines is small compared to automobiles with gasoline engines (cf. figures 3.3 and 3.4), so the the distribution from gasoline is the major contributor to the total effect (figure 4.20 a). Diesel (4.20 b) has only a small influence on ozone concentrations in North America.

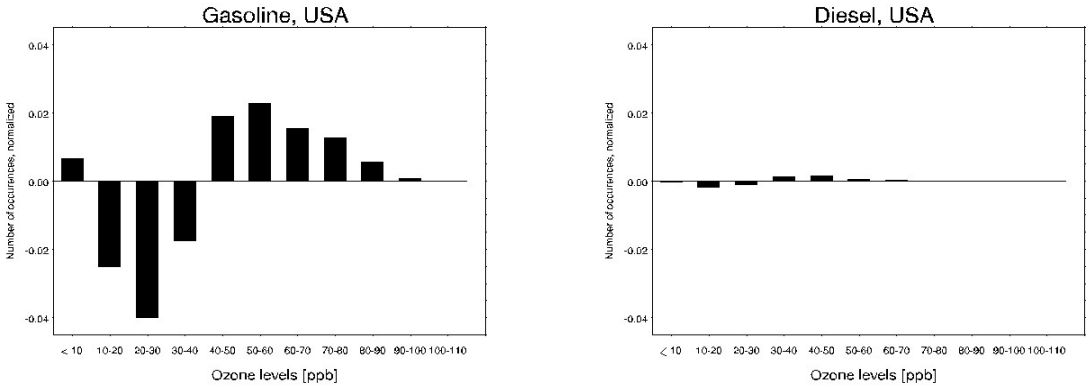

(a) **(b)**

Figure 4.20: *Change in occurrences of ozone levels [ppb] in specified intervals from North America. (a) Gasoline model run, relative to "Ref1" (with no exhaust emissions). (b) Diesel model run relative to "Ref1".*

The effect of transferring to a stricter emission legislation regime is shown for North America in figure 4.21, where the concentrations in the Euro4 standard model run are shown relative to the Euro5 model run, for gasoline and diesel in respectively 4.21 (a) and (b). The Euro4 and Euro5 model runs were executed by adopting total fuel consumption to either gasoline or diesel, with Euro4 and Euro5 legislation limits, respectively (see table 2.5 for emission limits). From the figure it is a noticeable shift from higher to lower ozone concentrations. Thus the Euro5 emission legislation leads to fewer occurrences of high ground ozone levels, which are the levels harmful to humans and vegetation. With Euro5 standards, ∼4 and 5.5 % reduction of the highest values can be expected for the legislation transition for gasoline and diesel, respectively. There is also a reduction in the lowest ozone interval level, which suggests a decrease in winter ozone titration due to reduced NO_x levels in Euro5.

In Europe, the relative effect from vehicle exhaust on surface O_3 levels is shown in figure 4.22 (b). Figure 4.22 (a) shows the occurrences of ozone concentrations from present worldwide traffic. Again the contribution to high ozone levels is evident (in the intervals from 40 to 90 ppb) in 4.22 (b), with a contribution of ∼8 %. There is a reduction in lower ozone levels, due to automobiles, but also here, a contribution in the lowest ozone level interval (about 1 %) due to ozone titration when sunlight is absent in winter, and during night. When separated into gasoline and diesel, the contributions are distributed as shown in figure 4.23. In Europe, diesel has a larger influence on total exhaust emissions than in North America, because of the larger diesel car fleet in Europe. The contribution is still less than from gasoline, which leads to a addition of around 7 % in ozone levels between 40 and 90 ppb,

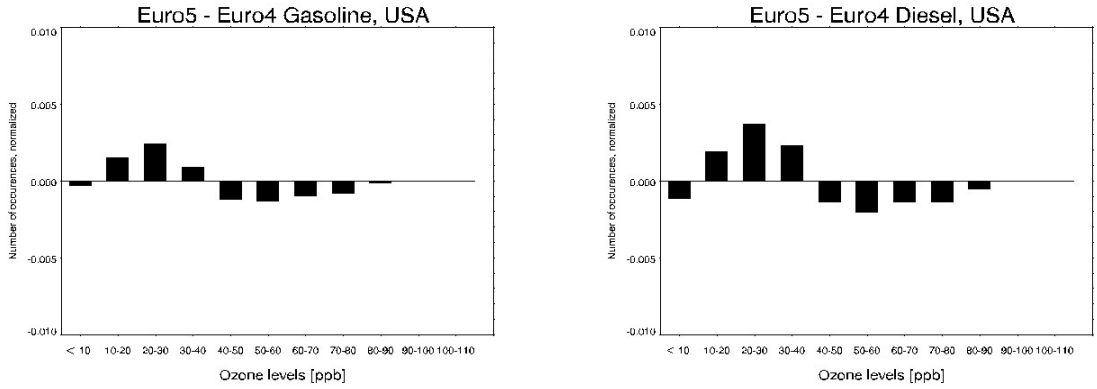

(a) **(b)**

Figure 4.21: *Change in occurrences of ozone levels [ppb] in specified intervals, from North America. Euro5 model relative to Euro4 model run for (a) gasoline and (b) diesel.*

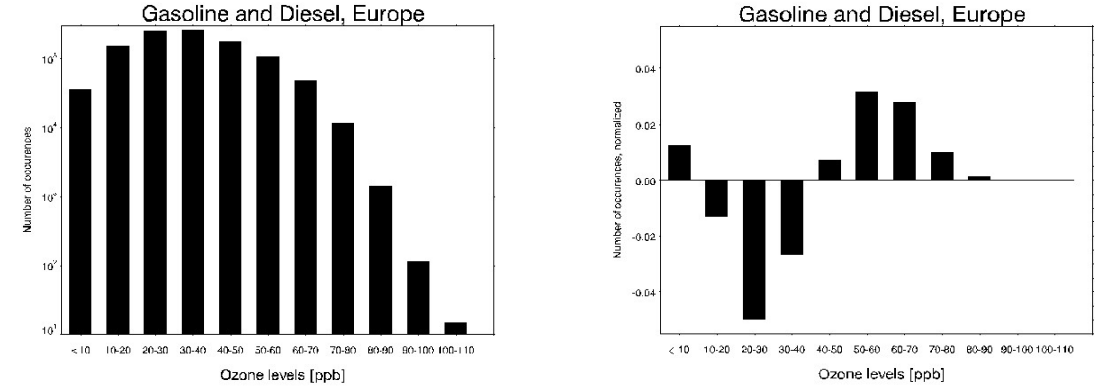

(a) **(b)**

Figure 4.22: *(a) Number of occurrences (logarithmic y-scale) of O_3 concentrations in specified interval levels calculated in the "Ref2" model run (with present worldwide traffic) in Europe. (b) Change in occurrences of ozone levels [ppb] in specified intervals from Europe, from the model run "Ref2" (with present worldwide traffic) relative to "Ref1" (with no exhaust emissions).*

while diesel leads to an increase just above 2 %. Gasoline in Europe leads to approximately 8 % less occurrences in the intervals between 10 and 40 ppb, than if there were no car exhaust at all.

The effect on shifting from Euro4 to Euro5 standards in Europe is shown in figure 4.24, for gasoline in (a), and diesel in (b). The effect is of a somewhat smaller extent for diesel than gasoline, but the trend for both propulsion

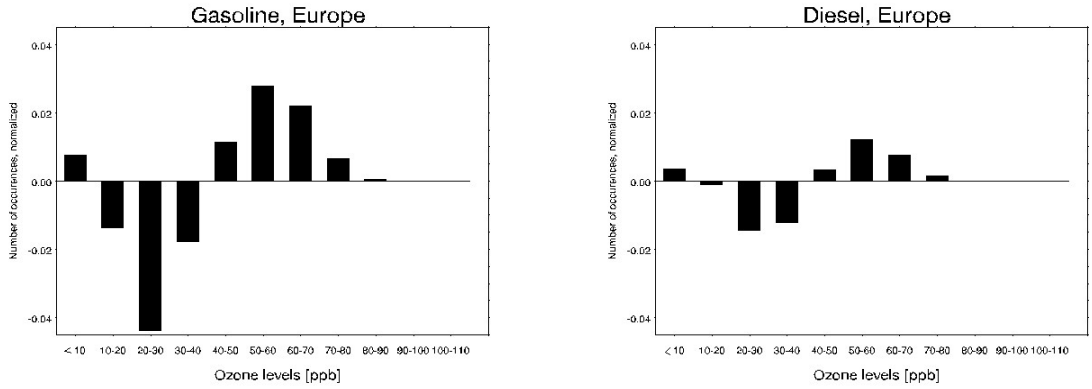

(a) **(b)**

Figure 4.23: *Change in occurrences of ozone levels [ppb] in specified intervals, from Europe, in (a) Gasoline model relative to "Ref1" (with no emission from automobiles) (b) Diesel model run relative to "Ref1".*

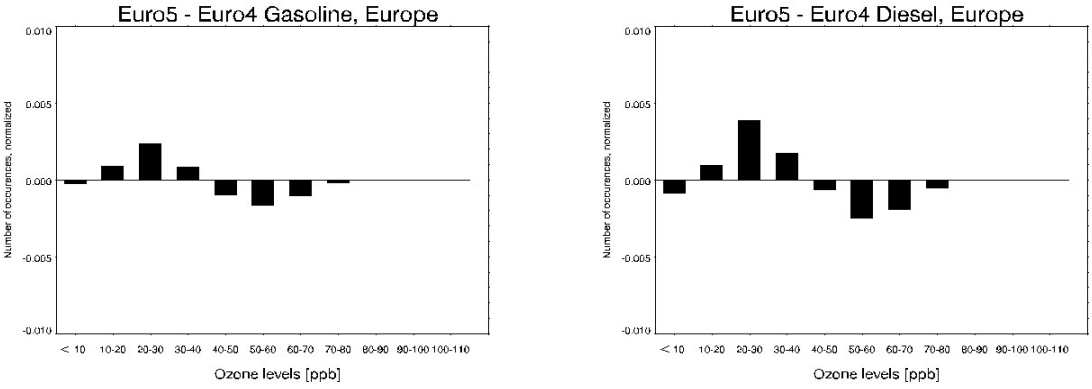

(a) **(b)**

Figure 4.24: *Normalized occurrences of ozone levels [ppb] in specified intervals from Europe, Euro5 model run relative to the Euro4 model run (a) gasoline and (b) diesel.*

types is towards larger occurrences of smaller values, and less occurrences of the highest values.

The calculations of hourly ground level ozone concentration in Asia are shown in figures 4.25 to 4.27. Figure 4.25 (a) shows the occurrences of ozone concentrations in specified interval levels from present worldwide traffic. Figure 4.25 (b) is the relative effect present traffic has on ozone concentrations, while 4.26 is for gasoline and diesel individually. As in North America, the distribution is mainly characterized by gasoline emissions, because of a higher number of gasoline cars in Asia. Here, as in the other two highly populated areas, road

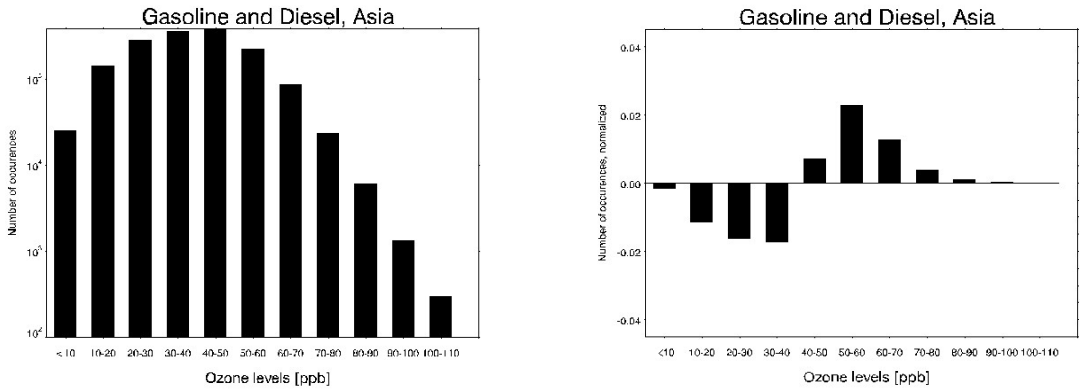

(a) **(b)**

Figure 4.25: *(a) Number of occurrences (logarithmic y-scale) of O_3 concentrations in specified interval levels calculated in the "Ref2" model run (with present worldwide traffic) in Asia. (b) Change in occurrences of ozone levels [ppb] in specified intervals, from Asia, from the model run "Ref2" (with present worldwide traffic) relative to "Ref1" (with no exhaust emissions).*

traffic emissions lead to a noteworthy increase in the highest ozone levels, of about 4%. In the case of Asia, there is a reduction of occurrences in the lowest interval, as opposed to the increase in this interval in North America and Europe. This can be due to the latitudinal difference between the regions, in that there is sufficient sunlight throughout the whole year in Asia, and ozone titration is not taking place. Changing from Euro4 to Euro5 leads to a reduction in the highest levels, as for North America and Europe, see figure 4.27. The relative change is to some extent larger for the transition in diesel.

Overall, for the three regions, road traffic plays a significant role in the production of high ozone concentrations. A transfer from Euro4 to Euro5 reduces the occurrences of the highest ozone levels. Thus a larger shear of the health intimidating levels is expected to decrease in transferring to Euro5.

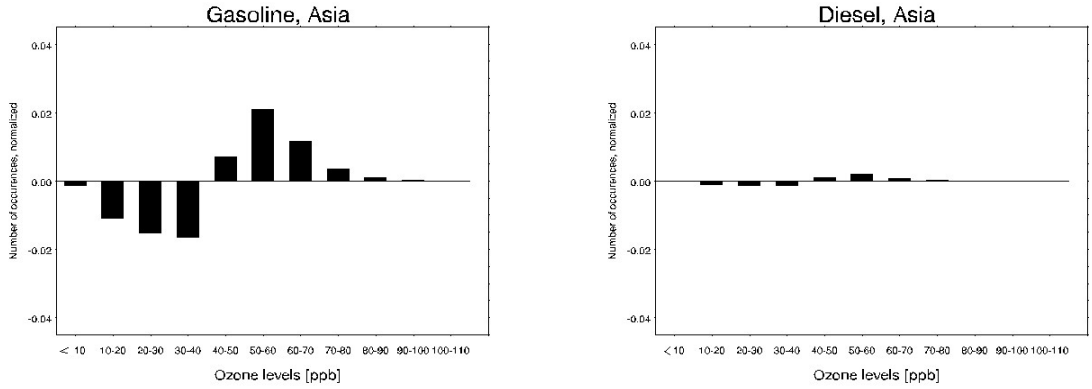

(a) **(b)**

Figure 4.26: *Change in occurrences of ozone levels [ppb] in specified intervals, from Asia. (a) Gasoline model run relative to "Ref1" (with no exhaust emissions) (b) Diesel model run relative to "Ref1".*

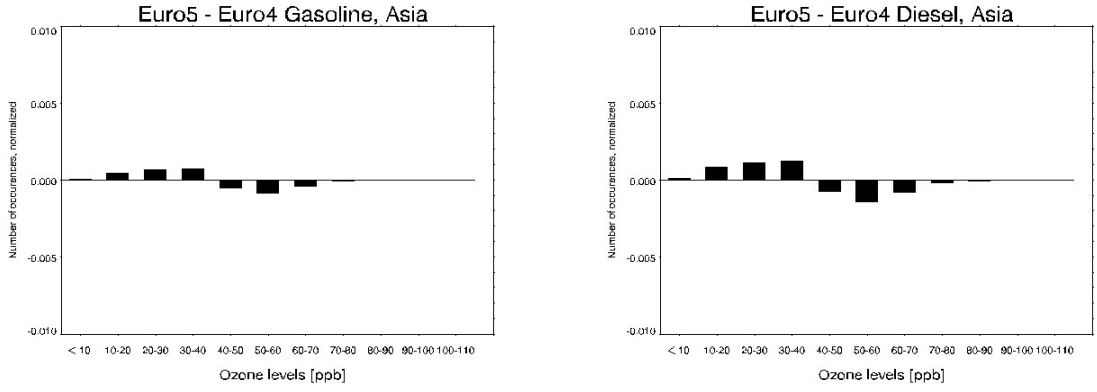

(a) **(b)**

Figure 4.27: *Change in occurrences of ozone levels [ppb] in specified intervals, from Asia. Euro5 model run relative to the Euro4 model run (a) gasoline and (b) diesel.*

4.4 Black Carbon

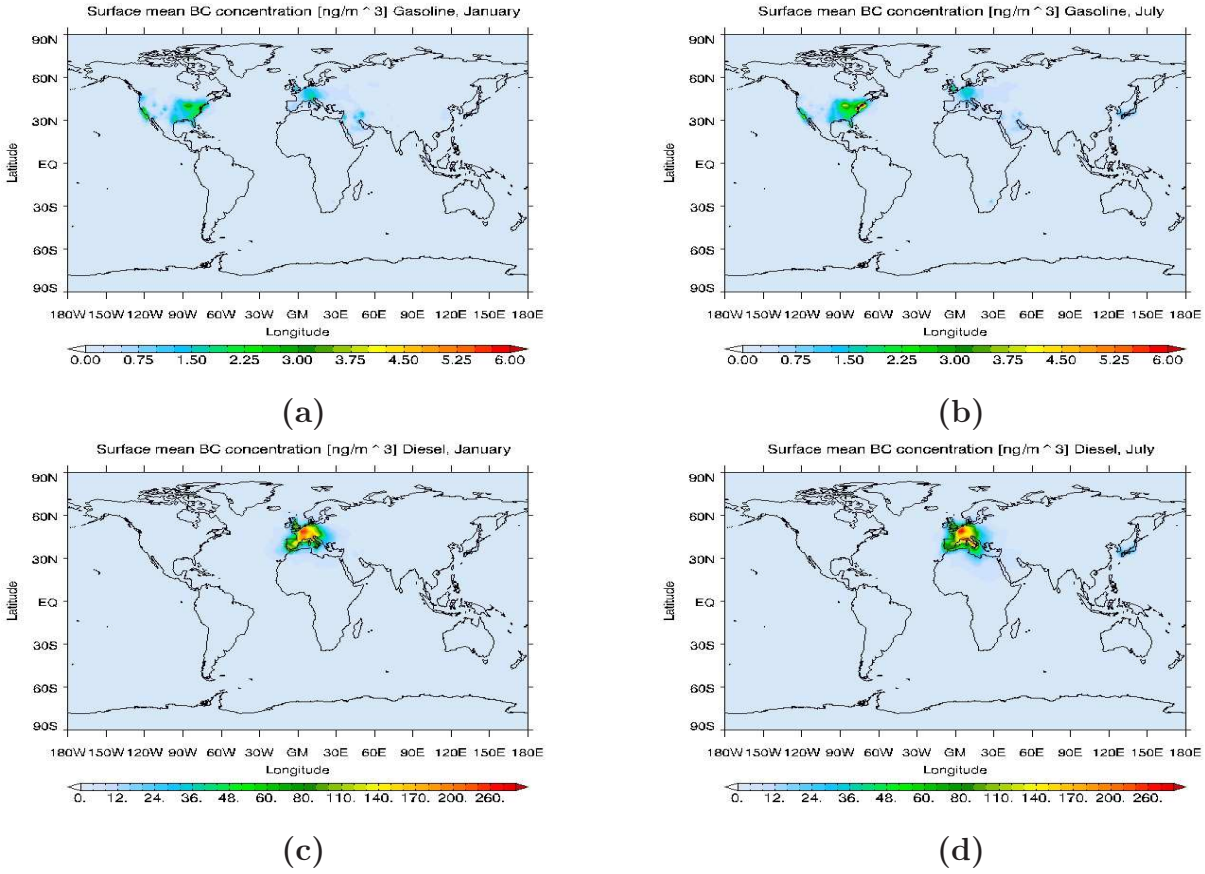

Figure 4.28: *Distribution of surface black carbon [ng/m^3] from gasoline in a) January and b) July, and diesel in c) January and d) July. Here, gasoline and diesel bc-runs are subtracted from the reference model run to get the effect of black carbon from gasoline and diesel exhaust emissions only.*

The surface distribution of black carbon is presented in figure 4.28, for gasoline in January and July (a and b, respectively), and for diesel in the same months (c and d). Vehicles fueled with gasoline have very low black carbon particle emissions. The burden from gasoline is quite similar in January and July, with slightly larger concentrations in July. The concentration over North America is ranging from 1 to 3 ng/m^3 (1-1.5 % of black carbon from fossil fuel, not shown) in winter, in summer up to 6 ng/m^3 (1.5 %). Over Europe and parts of the Middle East, concentrations of 1-2 ng/m^3 (< 1 %) are found.

The enhanced burden from automobiles with diesel engines is of a different size, with concentrations up to 250 ng/m^3 (30 %, figure 4.29) in January, and 275 ng/m^3 (35%, not shown) in July. The emissions are mainly distributed over Europe, but also emissions from Japan can be seen in July. The relative enhancement due to diesel emission in January is shown in figure 4.29. It

shows a plume of BC transported from Europe over the Atlantic ocean, with an enhancement of about 15 % nearest the continent, and decreasing further away from shore. What is also evident from the figure, is the transport to the Arctic, where there is an increase in BC concentrations of about 5 %. BC deposited in snow and ice is of considerably importance, because it is found to change the absorption of sunlight in snow, by snow grain aging which alters the optical properties of the grain, and contributes to move snowmelt to an earlier time of year (Flanner et al., 2007).

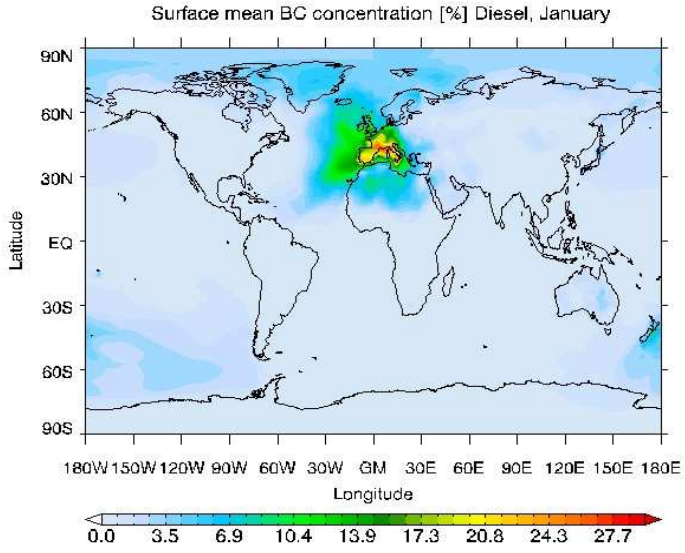

Figure 4.29: *Distribution of enhancement in surface black carbon from diesel in January, relative to the reference model run, without car exhaust emissions, given in per cent.*

4.4.1 Black Carbon Euro4 and Euro5

Figure 4.30 shows the calculations from the Euro5 standard model runs for gasoline (top row) and diesel (bottom row), for January (left) and July (right). Enhancements of black carbon from gasoline is up to 30 ng/m^3 (8 %), while for diesel it is approaching 40 ng/m^3 (14 %). The distribution is similar to the distributions of the other components presented in this theis, with enhancements close to the region of emission, naimly over urbanized areas.

Euro4 runs were not included, since the results would been equivalent, only by a factor larger, given from the legislation limits. I.e, diesel would be 5 times larger in Euro4 (1.4×10^{-5}) relative to Euro5 (2.8×10^{-6}) and gasoline 1.4 times larger in Euro4 (2.0×10^{-6}) compared to Euro5 (1.4×10^{-6}). Due to the fact that the model used in this thesis treats black carbon emissions

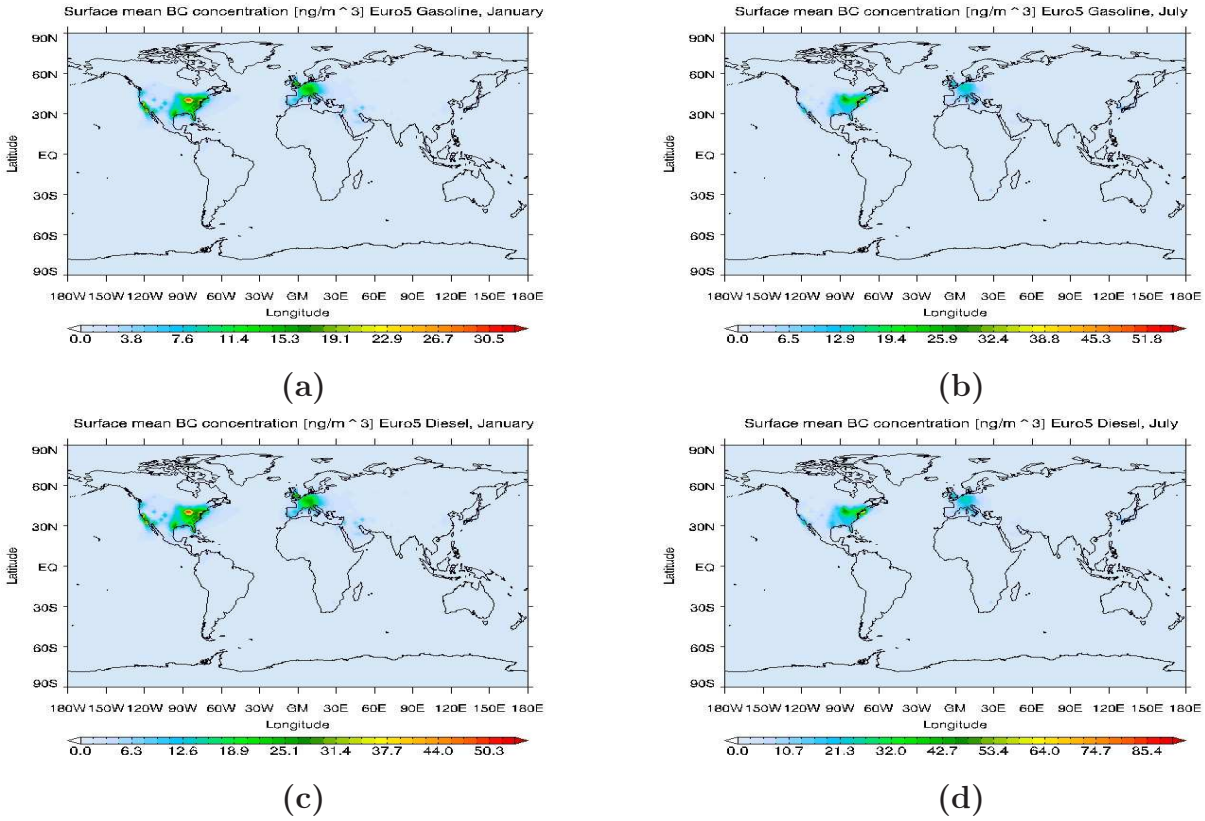

Figure 4.30: *Distribution of surface black carbon concentrations [ng/m^3] from Euro5 gasoline and diesel model runs. Gasoline in (a) January and (b) July. Diesel in (c) January and (d) July. In these model runs, total fuel consumption was sat to equal either gasoline or diesel, and to satisfy the EU legislation emission limits for Euro5. For emission limits, see table 2.5*

linearly, the distribution from transportation and deposition will be equal, only with larger concentrations for the Euro4 case.

4.5 Radiative Forcing

By the term "Radiative forcing" (RF) it is meant an externally imposed perturbation in the radiative energy budget of the Earth's climate system (IPCC, 2001). In equilibrium, the net global and annual mean radiative flux at the top of atmosphere equals zero. If, however, some factor, such as changes in solar irradiance, planetary albedo or the concentrations of radiatively active species acts to perturb the solar or emitted infrared radiation, it would lead to an imbalance in the radiation budget. This imbalance has the potential to lead to changes in climate parameters and result in a new equilibrium state of the climate system. The radiative forcing is the (hypothetical) instantaneous change in net (down minus up) irradiance, and is thus a measure of how the energy balance of the Earth-atmosphere system is influenced when factors that affect climate are altered.

In this section, estimates for radiative forcing due to road traffic are presented. The estimates are done for change in global and annual mean burdens of methane, ozone and black carbon, due to the exhaust emissions in the different model runs. Also estimates of RF for CO_2 from gasoline and diesel emissions, taken directly from the emission inventory, are done.

Estimates of radiative forcings from change in methane have been calculated with the simplified expression

$$\Delta F = \alpha(\sqrt{M} - \sqrt{M_0}) - (f(M, N_0) - f(M_0, N_0)) \tag{4.8}$$

where

$$f(M, N) = 0.47ln[1 + 2.01 \times 10^{-5}(MN)^{0.75} + 5.311 \times 10^{-15}M(MN)^{1.52} \tag{4.9}$$

and $\alpha = 0.036$, found in IPCC (2001), Table 6.2 in chapter 6, "Radiative Forcing of Climate Change", Boucher et al. (2001). M is the CH_4 perturbation in ppb, N is N_2O in ppb, and the subscript 0 denotes unperturbated concentrations. The second term on the right in 4.8 is a correction term for radiative overlap with N_2O.

Perturbations in methane were calculated with the assumption that a change in lifetime gives a corresponding change in concentration. Thus relative changes in CH_4 lifetime compared to Ref1 (reference run with no traffic), from each model run were calculated. This relative change (in %) was thereafter used to yield the perturbated CH_4 concentration. The unperturbated CH_4 abundance was assumed to be 1745 ppb, and 314 ppb for N_2O, from IPCC (2001) Table 6.1 (Boucher et al., 2001).

The different model runs mainly lead to a shorter mean methane lifetime. It is alterations in the hydroxyl radical, OH, that lead to change in methane lifetime, as mentioned in chapter 2.2.1. The sign in the OH perturbation

is dependent on the ratio between the degrees of strength of NO_x and CO perturbations. NO_x has a chemical lifetime of only a few days, so its ability to convert HO_2 into OH is considerable only near its emission sources. CO, which has a longer lifetime, about 1-2 months (in summertime), can be transported over larger distances, and OH can be destroyed further away from the source origin. Niemeier et al. (2006) found a zonal mean OH enhancement by up to 5 % due to road traffic in July, and remarks that while slightly increased in July, the level of OH should have decreased in January in the entire Northern Hemisphere in response to surface vehicle emissions. The model runs in this thesis simulated a shorter methane lifetime in the runs with exhaust emission, than in the one with road vehicle emissions turned off. This is most likely due to enhanced OH levels originating from NO_x emissions, as mentioned. The mean methane lifetime, and the radiative forcings calculated are listed for each model run in table 4.1.

Model run	$\overline{\tau}$	ΔCH_4 ppb	Radiative forcing (mWm^{-2})
Ref 1	6.73	-	-
Ref 2	6.57	41.1	-15.3
Gasoline	6.58	38.1	-14.9
Diesel	6.71	3.8	-1.4
E4 Gasoline	6.70	6.4	-2.4
E4 Diesel	6.64	21.7	-8.1
E5 Gasoline	6.71	4.2	-1.5
E5 Diesel	6.66	17.4	-6.5

Table 4.1: *Change in mean methane lifetime and radiative forcing [mWm^{-2}] calculated for each model run. Radiative forcings are calculated using a simplified equation (equation 4.8) from IPCC (2001). Change in methane abundance is calculated as the difference between the various model runs and "Ref1" (without any traffic present).*

The radiative forcing due to alterations in methane follows the curve: $\Delta F = RF_{ss}(1-e^{\frac{-t}{\tau}})$, where RF_{ss} denotes steady state. When considering the effect of emissions from one year, but over time, to a point H, we want take into account the effects from the above equation for one year, and then how the forcing from the methane perturbation decays over time:

$$\Delta RF = \int_0^1 RF_{ss}(1-\tfrac{-t}{\tau})dt + \int_1^H RF_{ss}(1-e^{\frac{-1}{\tau}})e^{\frac{-(t-1)}{t}}dt \qquad (4.10)$$

RF_{ss} is constant:

$$\Delta RF = RF_{ss} \int_0^1 (1 - e^{\frac{-t}{\tau}})dt + RF_{ss}(1 - e^{\frac{-1}{\tau}}) \int_1^H e^{\frac{-(t-1)}{t}} dt \tag{4.11}$$

solving the integral yields

$$\Delta RF = RF_{ss}[1yr - (-\tau)[e^{\frac{-1}{\tau}} - 1] + (1 - e^{\frac{-1}{\tau}})(-\tau)(e^{\frac{-H}{\tau}} - e^{\frac{-1}{\tau}})] \tag{4.12}$$

and when H is large:

$$\Delta RF = RF_{ss}(1 - \tau(1 - e^{\frac{-1}{\tau}}) + \tau(1 - e^{\frac{-1}{\tau}})) = RF_{ss} \times 1yr \tag{4.13}$$

Thus, the radiative forcings in table 4.1, are equal to the integrated radiative forcings.

Estimates of radiative forcing from change in ozone concentrations are given in table 4.2. 3-D ozone perturbation fields were converted from mixing ratio [mol/mol] to 2-D column ozone change in Dobson units (DU), and to obtain radiative forcing the ozone perturbation for each model run was multiplied by the radiative efficiency for ozone, 0.042 Wm^{-2} per DU (IPCC, 2001), which is the mean of several detailed model simulations.

Model run	Radiative forcing (mWm^{-2})
Ref 1	-
Ref 2	41,6
Gasoline	39,6
Diesel	2,6
E4 Gasoline	7,6
E4 Diesel	16,1
E5 Gasoline	6,0
E5 Diesel	13,2

Table 4.2: *Radiative forcings from changes in ozone concentrations, calculated using the radiative efficiency of 0.042 Wm^{-2} per DU (IPCC, 2001) for each model run. Ozone concentrations for each model run are the ozone concentrations in these runs, minus ozone concentrations in the reference run "Ref1" (with no traffic present).*

While the effect of today's fleet of cars has a larger RF from gasoline, the forcing from diesel when all automobiles are sat to equal either gasoline or diesel, with Euro4 and Euro5 standards, surpasses the forcing from gasoline, for ozone. The higher ozone concentrations from diesel cars will decay

with an e-folding time of 2-3 months if emissions where to stop. However, the additional OH, due to emissions of NO_x and increased O_3, will lead to a negative perturbation in CH_4, and this perturbation decays with a much longer e-folding time, around ∼12 years. Thus, while the initial RF from O_3 is positive, the negative perturbation in CH_4 leads to a net negative forcing over a longer time perspective (Wild et al., 2001). Wild et al. (2001) showed this for perturbations in NO_x. While this might be adequate for diesel emissions, it is not necessarily so for gasoline emissions, due to higher emissions of CO and VOC.

The radiative forcings for additional black carbon due to road traffic, are estimated by calculating the change in burden $[gm^{-2}]$ for the year the model was run for, for each model run, before multiplying this burden with a radiative forcing normalized to the change in global annual atmospheric burden, $[Wm^{-2}/gm^{-2}]$ or $[W/g]$, found by Berntsen et al. (2006). This normalized forcing is given for four different regions; Europe, China, South Asia and South America. Black Carbon are absorbing particles, and their radiative forcing depends on the amount of sunlight available, in addition to the albedo of the surface underneath. However, the estimated radiative forcing between the regions do not differ greatly, thus a mean of the four regions (1037.5 Wm^{-2}/gm^{-2}or W/g) is assumed to be adequate globally. Global and annual mean burden was multiplied with the normalized forcing, thus getting the global and annual mean radiative forcing, for the change in atmospheric black carbon burden from car exhaust, in $[Wm^{-2}]$. The calculated forcings are given in table 4.3 (given as $[mWm^{-2}]$).

Model run	Global Mean burden BC (gm^{-2})	Radiative forcing (mWm^{-2})
Gasoline	2.62420×10^{-6}	2.7
Diesel	5.69511×10^{-5}	59.1
E4 Gasoline	2.50659×10^{-5}	26.0
E4 Diesel	1.5272×10^{-4}	158.44
E5 Gasoline	1.75531×10^{-5}	18.2
E5 Diesel	3.05439×10^{-5}	31.7

Table 4.3: *Radiative forcings [mWm^{-2}] from changes in black carbon concentrations due to road traffic emissions. Calculated from burdens in the respective model runs, minus the reference run, so the global mean burden in BC (given in [gm^{-2}]) is from road traffic emissions alone.*

Based on the concept of Radiative Forcing, the Intergovernmental Panel on

Climate Change has employed the metric GWP (Global Warming Potential) as a tool to quantify and compare the potential impact of different climate change agents. GWP is a metric defined as the RF caused by a pulse emission of 1 kg of a trace gas, over a chosen time horizon, relative to the RF of 1 kg of the reference gas CO_2.

$$GWP(H)_t = \frac{\int_0^H RF_i(t)dt}{\int_0^H RF_{CO_2}(t)dt} \tag{4.14}$$

H here, is the chosen time frame. The absolute global warming potential, $AGWP$, for gas i, and for CO_2 is given by the numerator and the denominator, respectively. So the $AGWP$ for a gas i, is

$$AGWP(H)_t = \int_0^H RF_i(t)dt \tag{4.15}$$

	Integrated Radiative forcing ($mWm^{-2}yr$)					
H (yr)	Gasoline	Diesel	Euro4 Gasoline	Euro4 Diesel	Euro5 Gasoline	Euro5 Diesel
20	51.9	3.7	66.4	44.1	10.7	5.9
100	182.6	13.1	233.8	154.8	37.6	20.7
500	600.0	43.0	769.0	509.4	123.8	68.2

Table 4.4: *Integrated Radiative forcings [$mWm^{-2}yr$] from additional CO_2 from gasoline and diesel from today's fleet, and the two fuel types with Euro4 and Euro5 standards.*

The radiative forcings for O_3, CH_4 and BC presented here, are the AGWPs for one year, or more. Because we consider the effect of emissions in one year, the integral over any time frame, gives the same value.

Forcings from CO_2 from diesel and gasoline were calculated using $AGWP$ values from Forster et al. (2007). Thus, radiative forcings, from the additional CO_2 from gasoline and diesel in one year are found, over time perspectives of 20, 100 and 500 years. The values of the $AGWP$ are 2.47×10^{-14}, 8.69×10^{-14} and 28.6×10^{-14} $Wm^{-2}(kgCO_2)^{-1}$, respectively. The estimated forcings are given in table 4.4.

To conclude whether shifting the car fleet over to a fleet where diesel engines dominates is a good option or not is a difficult task, because gasoline and diesel have climate effects which differs in timescales. While diesel has the largest impacts on a short term perspective, the larger share of CO_2 in gasoline, means that on a longer timescale, the overall RF enhancement of diesel becomes less than for gasoline. The integrated radiative forcing in the Euro4 and Euro5 cases, for CH_4, O_3, BC and CO_2 are summarized and presented in tables 4.5 and 4.6. Here, one can see that while gasoline has a lower forcing for time frames of 20 and 100 years than diesel, on a scale of 500 years, the forcing from gasoline surpasses the forcing from diesel in the Euro4 case. While for Euro5, diesel also give a smaller forcing on the 100 years time frame (though only slightly). Euro5 generally gives forcings of significant minor scale for both gasoline and diesel.

	Sum of IRF, $(mWm^{-2}yr)$		
Model Case	20 yr	100 yr	500 yr
E4 Gasoline	97.6	256.0	800.2
E4 Diesel	210.4	321.1	675.7

Table 4.5: *Sum of Integrated Radiative Forcing, from CH_4, O_3, BC and CO_2 for time perspectives of 20, 100 and 500 years, for the Euro4 cases.*

	Sum of IRF, $(mWm^{-2}yr)$		
Model Case	20 yr	100 yr	500 yr
E5 Gasoline	33.4	60.3	146.5
E5 Diesel	44.3	59.1	106.5

Table 4.6: *Sum of Integrated Radiative Forcing, from CH_4, O_3, BC and CO_2 for time perspectives of 20, 100 and 500 years, for the Euro5 cases.*

Chapter 5

Summary and conclusion

In this thesis model simulations with the chemistry transport model Oslo-CTM2 were carried out to investigate the effects from road traffic emissions on tropospheric chemistry. The model was run for 4+12 months (the first 4 months included as spin-up). T42 horizontal resolution and 40 vertical layers were used. A up to date emission inventory was provided from Borken et al. (2007) through the EU project QUANTIFY. Several model runs were executed, with different emission scenarios, to investigate the difference in effects from automobiles equipped with gasoline and diesel engines. Further, the effects from the legislation emissions limits, Euro4 and Euro5 were studied. Components presented in the results were carbon monoxide (CO), nitrogen oxides (NO_x), ozone (O_3) and black carbon (BC). For the different components monthly means were studied, and seasonal differences from comparing January and July were presented. However, for ozone, surface level concentrations computed every hour were also assessed to examine the contribution from road traffic on health threatening levels.

The motivation for investigating effects from road traffic, and gasoline and diesel separately, is to quantify the relative impact such emissions exert on the tropospheric chemistry and the climate system. Automobile emissions effect climate through emissions of the greenhouse gas CO_2, and through emissions of O_3 precursors. O_3 is itself a greenhouse gas, in addition to being a component which alters the abundance of OH. NO_x and CO, which are ozone precursors, are also involved in altering the concentration of OH. OH abundance in the atmosphere is of importance because of its high reactivity, and thus plays the important role as the atmosphere's detergent. In that way, abundance of CH_4 is dependent on OH levels. Therefore, emissions from road traffic have an impact on tropospheric chemistry in several and diverse ways.

The model calculations show that the current fleet of road vehicles significantly affect the chemistry of the troposphere, particularly in the Northern Hemisphere. In the case of the ozone precursors, CO and NO_x, the concentrations increased most, and over largest spatial areas during winter, when

photodestruction is slow, and the components could be transported further from the emission sources. The largest enhancement in surface ozone concentrations is estimated to occur in the summertime (July) when photochemical activity is highest. In winter, there is a decrease in concentrations because of ozone titration. The model runs calculate the largest increase in ozone levels for gasoline, for today's fleet of cars. However, in the model runs where the total car fleet is sat to be either with gasoline or diesel engines and to obey Euro4 or Euro5 legislation emission limits, diesel emissions produce the largest enhancement in ozone concentrations. While gasoline produces enhancements up to 4 ppb in summertime, the production due to diesel has a maximum of 9 ppb.

Differences in emissions of ozone precursors from the two fuel types result in different spatial extent of ozone concentrations. Gasoline, which emits more CO and hydrocarbons than diesel, can be found to have an effect also in the Southern Hemisphere. Because CO has a longer lifetime than NO_x (which is a larger part of diesel emissions than gasoline), it is transported longer than NO_x, and can thus have an influence on ozone levels further away from the source of origin. Increase in ozone levels in Southern Hemisphere was found in the zonal mean plots from gasoline, thus indicating a transport of precursors over the hemisphere (emissions are mainly in the Northern Hemisphere). Diesel shows no sign of increasing ozone levels in Southern Hemisphere, because the main fuel to ozone production from diesel is not transported over as long distances. However, the model was only run for one year. Longer runs should be executed to determine the influence traffic emissions in Northern Hemisphere has on the Southern Hemisphere, since transport between the hemispheres takes 1-2 years.

It should be emphasized that the focus in this thesis mainly has been on global effects of traffic, with the exception of the ground level ozone concentrations obtained every hour to see the effect from traffic on ozone occurrences in populated areas. The resolution used in the model runs is however too coarse to resolve cities, and model simulations with a finer horizontal resolution could state more certainly the impact road traffic has on air quality in urbanized regions. There is in this thesis, nonetheless, shown strong implications that road traffic contribute in producing high ozone concentrations. In USA, Europe and Asia, respectively 9, 8 and 4 % of concentrations between 40 and 100 ppb is due to road traffic. In USA and Asia, the major contributor is gasoline, while diesel plays a somewhat larger part in Europe, but gasoline is still the main contributor. It is however important to remember the difference in sizes of the automobile fleets with gasoline and diesel engines. A transfer from Euro4 to Euro5 reduced the occurrences of the highest ozone levels, thus a larger shear of the health intiminating levels is expected to decrease when transferring to Euro5 legislation emission limits.

Estimates of radiative forcing from changes in methane levels, ozone perturbation and change in black carbon burdens were done. They show that for changes in CH_4, present worldwide traffic leads to a forcing of -15,3 mWm^{-2}. The negative forcing implies an increase in OH abundances due to road traffic, which leads to a higher reaction rate with methane. Gasoline leads to a forcing of -14,9 mWm^{-2}, and diesel - 1,4 mWm^{-2}. The Euro4/Euro5 runs give negative forcings of 2.4 and 1.5 mWm^{-2} for gasoline, and -8.1 and -6.5 mWm^{-2} for diesel, for Euro4 and Euro5, respectively.

Forcings from O_3 perturbations gives a estimate of 41.6 mWm^{-2} from road traffic as a whole, 39.6 mWm^{-2} and 2.6 mWm^{-2} for gasoline and diesel, respectively, when separated. From figure 1.1 tropospheric ozone is shown to contribute with a forcing around 0.4 Wm^{-2} (or $400mWm^{-2}$), thus the affect from road traffic stand for a significant share of the total forcing. With Euro4 standards, the forcing due to gasoline is 7.6 mWm^{-2}, and due to diesel 16.1 mWm^{-2}. With stricter emission limits, in Euro5, the forcings are reduced to 6.0 mWm^{-2} for gasoline and 13.2 mWm^{-2} for diesel.

For burdens in black carbon, today's car fleet imposes a radiative forcing of 2.7 mWm^{-2} from gasoline, and 59.1 mWm^{-2} for diesel. In the Euro4 case, forcings are 26.0 and 158.44 mWm^{-2} for the two fuel types (gasoline and diesel, respectively). In the Euro5 standard runs, the forcing from gasoline is 18.2 mWm^{-2}, and from diesel 31.7 mWm^{-2}. The level of scientific understanding is however very low (see figure 1.1) when is comes to forcing mechanisms from black carbon from fossil fuel burning.

When CO_2, the major contributor to warming of the climate system (cf. figure 1.1), is included, and the forcings from the different components are added up, the Euro4 case show that on the longest time frame (500 yr), gasoline imposed forcing exceed that of diesel. On the two shortest time frames (20 and 100 yr), diesel contributes the most. When the Euro5 emission standard is taken in use, diesel only contribute more than gasoline to RF on the shortest time frame. Thus, when policies are to be made regarding taxations on different fuel types, a determining factor is what legislation standard is in use (or will be used in the future), since Euro4 and Euro5 differ on which fuel type is the strongest contributor to RF on the 100 years time frame, and a future legislation might turn the table again. The decision on whether or not to encourage the larger taxation of automobiles with gasoline engines as a good measure to inhibit additional radiative forcing, necessarily depend on the time frame regarded.

Bibliography

Agency, U.S. Environmental Protection (1996) *A*ir Quality Criteria for Ozone and Related Photochemical Oxidants. Executive Summary. Available at http://cfpub.epa.gov/ncea/cfm/recordisplay.cfm?deid=2831.

Berntsen, Terje; Fuglestvedt, Jan; Myhre, Gunnar; Stordal, Frode and Berglen, Tore F. (2006) *A*batment of Greenhouse Gases: Does Location Matter?. Climate Change, Vol. 74(4): p. 377–411.

Berntsen, Terje; Fuglestvedt, Jan S. and Rypdal, Kristin (2009) *C*limate effect of passenger cars: Gasoline versus diesel. CICERO. (In preparation).

Berntsen, Terje K and Isaksen, Ivar (1997) *A* global three-dimensional chemical transport model for the troposphere, 1. Model description and CO and ozone results. J. Geophys. Res., Vol. 102: p. 21.239–21.280.

Borken, Jens; Steller, Heike; Merétei, Tamás and Vanhove, Philip (2007) *G*lobal and country inventory of road passenger and freight transportation, their fuel consumption and their emissions of air pollutants in the year 2000. Journal of the Transportation Research Board.

Boucher, O.; Haigh, J.; Hauglustaine, D.; Haywood, J.; Myhre, G.; Nakajima, T.; Shi, G.Y and Solomon, S. (2001) *C*limate Change 2001: The Scientific Basis. Contribution of Working Group I to the Third Assessment Report of the Intergovernmental Panel on Climate Change. [Houghton, J.T.,Y. Ding, D.J. Griggs, M. Noguer, P.J. van der Linden, X. Dai, K. Maskell, and C.A. Johnson (eds.)]. Cambridge University Press, Cambridge, United Kingdom and New York, NY, USA, 881pp.

Brasseur, G.P.; Orlando, J.J. and Tyndall, G.S. (1999) *A*tmospheric Chemistry and Global Change (Oxford University Press).

Colvile, R. N; Hutchinson, E. J; Mindell, J. S. and Warren, R. F. (2001) *T*he transport sector as a source of air pollution. Atmospheric Environment, Vol. 35: p. 1537–1565.

Dalsøren, Stig Bjørlow (2007) *C*TM studies on effects of various antropogenic emissions on tropospheric chemistry. Ph.D.thesis, University of Oslo.

Ernst, Armin and Zibrak, Joseph D. (1998) *C*arbon Monoxide Poisoning. The New England Journal of Medicine, Vol. 339(22): p. 1603–1608.

Flanner, Mark G.; Zender, Charles S.; Randerson, James T. and Rasch, Philip J. (2007) *P*resent-day climate forcing and response from black carbon in snow. Journal of geophysical research, Vol. 112.

Forster, P.; Ramaswamy, V.; Artaxo, P.; Berntsen, T.; Betts, R.; Fahey, D.W.; Haywood, J.; Lean, J.; Lowe, D.C.; Myhre, G.; Nganga, J.; Prinn, R.; Raga, G.; Schulz, M. and Dorland, R. Van (2007) *C*limate Change 2007: The Physical Science Basis. Contribution of Working Group I to the Fourth Assessment Report of the Intergovernmental Panel on Climate Change. [Solomon, S., D. Qin, M. Manning, Z. Chen, M. Marquis, K.B Averyt, M.Tignor and H.L. Miller (eds.)]. Cambridge University Press, Cambridge, United Kingdom and New York, NY, USA.

Fuglestvedt, Jan; Berntsen, Terje; Myhre, Gunnar; Rypdal, Kristin and Skeie, Ragnhild Bieltvedt (2008) *C*limate forcing from the transport sectors. Proceedings of the national academy of sciences of the United States of America, Vol. 105: p. 454–458.

Gauss, Michael (2003) *I*mpact of aircraft emissions and ozone changes in the 21st century: 3-D model studies. Ph.D.thesis, University of Oslo.

Granier, Claire; Niemeier, Ulrike; Jungclaus, Johann H.; Emmons, Louisa; Hess, Peter; Lamarque, Jean-François; Walters, Stacy and Brasseur, Guy P. (2006) *O*zone pollution from future ship traffic in the Arctic nothern passages. Geophysical Research Letters, Vol. 33.

Greenberg, J. P.; Helmig, D. and Zimmerman, P. R. (1996) *S*easonal measurements of nonmethane hydrocarbons and carbon monoxide at the Mauna Loa Observatory during the Mauna Loa Observatory Photochemistry Experiment 2. Journal of Geophysical Research, Vol. 101(D9).

Hauglustaine, D. A.; Brasseur, G. P.; Walters, S.; Rasch, P. J.; Müller, J.-F.; Emmons, L. K and Carroll, M. A. (1998) *M*OZART, a global chemical transport model for ozone and related chemical tracers 2. Model results and evalution. Journal of Geophysical Research, Vol. 103.

Hesstvedt, E.; Hov, Ø. and Isaksen, I. S. A. (1978) *Q*uasi steady-state approximation in air pollution modelling: Comparison of two numerical schemes for oxidant prediction. International Journal of Chemical Kinetics.

IPCC (2001) *C*limate Change 2001: The Scientific Basis. Contribution of Working Group I to the Third Assessment Report of the Intergovernmental Panel on Climate Change. [Houghton, J.T.,Y. Ding, D.J. Griggs, M. Noguer, P.J. van der Linden, X. Dai, K. Maskell, and C.A. Johnson (eds.)]. Cambridge University Press, Cambridge, United Kingdom and New York, NY, USA, 881pp.

Jacob, Daniel J. (1999) *I*ntroduction to Atmospheric Chemistry (Princeton University Press).

Jacobson, Mark Z. (2002) *C*ontrol of fossil-fuel particulate black carbon and organic matter, possibly the most effective method of slowing global warming. Journal of Geophysical Research, Vol. 107.

Jacobson, Mark Z.; Seinfeld, John H.; Carmicheal, Greg R. and Streets, David G. (2004) *T*he effect on photochemical smog of converting the U.S. fleet of gasoline vehicles to modern diesel vehicles. Geophysical Research Letters, Vol. 31.

Krupa, Sagar; McGrath, Margaret Tuttle; Andersen, Christan P.; Booker, Fitzgerald L.; Burkey, Kent O.; Chappelka, Arthur H.; Chevone, Boris I.; Pell, Eva J. and Zilinskas, Barbara A. (2001) *A*mbient Ozone and Plant Health. Plant Disease, Vol. 85(1): p. 4–12.

Liu, S. C.; Tranier, M.; Fehsenfeld, F. C.; Parrish, D. D.; Williams, E. J.; Fahey, D. W.; Hübler, G. and Murphy, P. C. (2001) *O*zone production in the rural troposphere and the implications for regional and global ozone distributions. Journal of Geophysical Research, Vol. 92(9): p. 1719–1722.

Lohmann, U. and Feichter, J. (2005) *G*lobal indirect aerosol effects: a review. Atmospheric Chemistry and Physics, Vol. 5: p. 715–737.

Matthes, S.; Grewe, V.; Sausen, R. and Roelofs, G.-J. (2007) *G*lobal impact of road traffic emissions on tropospheric ozone. Atmospheric Chemistry and Physics, Vol. 7(7): p. 1707–1718. ISSN 1680-7316. URL `http://www.atmos-chem-phys.net/7/1707/2007/`.

Mazzi, Eric A. and Dowlatabadi, Hadi (2006) *A*ir quality impacts of climate mitigation: UK policy and passenger vehicle choice. Environmental science & technology, Vol. 41: p. 387 –392.

Myhre, G.; Berglen, T. F.; Johnsrud, M.; Hoyle, C. R.; Berntsen, T. K.; Christopher, S. A.; Fahey, D. W.; Isaksen, I. S. A.; Jones, T. A.; Kahn, R. A.; Loeb, N.; Quinn, P.; Remer, L.; Schwarz, J. P. and Yttri, K. E. (2008) *R*adiative forcing of the direct aerosol effect using a multi-observation approach. Atmospheric Chemistry and Physics Discussions, Vol. 8.

Niemeier, Ulrike; Granier, Claire; Kornblueh, Luis; Walters, Stacy and Brasseur, Guy P. (2006) *G*lobal impact of road traffic on atmospheric chemical composition and on ozone climate forcing. Journal of Geophysical Research, Vol. 111.

NILU (1995) *E*n ulempe for helse og vegetasjon: Ozon ved bakken. URL `http://www.nilu.no/index.cfm?ac=topics\&folder\_id=4313\&text%\_id=7601\&view=text`, Norsk Institutt for Luftforskning (Norwegian Institute for Air Research).

Novelli, P. C.; Jr., J. E. Collins; Myers, R. C; Sachse, G. W. and Scheel, H. E. (1994) *R*eevaluation of the NOAA/CMDL carbon monoxide reference scale and comparisons with CO reference gases at NASA-Langley and the Fraunhofer Institut. Journal of Geophysical Research.

Novelli, P. C.; Steele, L. P. and Tans, P. P. (1992) *M*ixing ratios of carbon monoxide in the troposphere. Journal of Geophysical Research.

Olivier, J.; Peters, J.; Granier, C.; Petron, G.; Müller, J. F. and Wallens, S. (2003) *P*resent and future surface emissions of atmospheric compounds, POET report nr. 2. Technical report, EU project EVK2-1999-00011.

Oltmans, S.J. and Levy, H.II (1994) *S*urface ozone measurements from a global network. Atmospheric Environment, Vol. 28.

Pickering, K. E.; Wang, Y.; Tao, K.; Price, Colin and Müller, J.F. (1998) *V*ertical distributions of lightning NOx for use in regional and global chemical transport models. Journal of Geophysical Research, Vol. 103: p. 31,203–31,216.

Poisson, Nathalie; Kanakidou, Maria and Crutzen, Paul J. (2000) *I*mpact of Non-Methane Hydrocarbons on Tropospheric Chemistry and the Oxidizing Power of the Global Troposphere: 3-Dimensional Modelling Results. Journal of Atmospheric Chemistry, Vol. 36: p. 157–230.

Pope III, C. Arden; Bates, David V. and Raizenne, Mark E. (1995) *H*ealth Effects of Particulate Air Pollution: Time for Reassessment?. Environmental Health Perspectives, Vol. 103(5).

Prather, Michael J. (1986) *N*umerical Advection by Conservation of Second-Order Moments. Journal of Geophysical Research, Vol. 91: p. 6671–6681.

Price, Colin; Penner, Joyce and (1997a), Michael Prather (1997a) *N*Ox from lightning: 1. Global distribution based on lightning physics. Journal of Geophysical Research, Vol. 102: p. 5929–5941.

Price, Colin; Penner, Joyce and (1997b), Michael Prather (1997b) *N*Ox from lightning: 2. Constrains from the global atmospheric electric circuit. Journal of Geophysical Research, Vol. 102: p. 5942–5951.

Ramanathan, V. and Carmichael, G. (2008) *G*lobal and regional climate changes due to black carbon. Nature geoscience, Vol. 1.

Reich, Peter B. and Amundson, Robert G. (1985) *A*mbient levels of ozone reduce net photosynthesis in tree and crop species. Science, Vol. 230: p. 566–570.

Rypdal, Kristin; Berntsen, Terje; Fuglestvedt, Jan; Aunan, Kristin; Torvanger, Asbjørn; Stordal, Frode; Pacyna, Josef M. and Nygaard, Lynn P.

(2005) *T*ropospheric ozone and aerosols in climate agreements: scientific and political challenges. Environmental Science and Policy.

Sitch, S.; Cox, P. M.; Collins, W. J. and Huntingford, C. (2007) *I*ndirect radiative forcing of climate change through ozone effects on the land-carbon sink. Nature, Vol. 448: p. 791–U4.

Solberg, Sverre; Dye, Christian; Schmidbauer, Norbert; Herzog, Alex and Gehrig, Robert (1996) *C*arbonyls and nonmethane hydrocarbons at rural European sites from the mediterranean to the arctic. Journal of Atmospheric Chemistry, Vol. 25.

Sundet, Jostein Kandal (1997) *M*odel Studies with a 3-d Global CTM using ECMWF data. Ph.D.thesis, Dept. of Geophysics, University of Oslo.

Tiedtke, M. (1989) *A* Comprehensive Mass Flux Scheme for Cumulus Parameterization in Large-Scale Models. Monthly Weather Review, Vol. 117: p. 1779–1800.

Unger, Nadine; Shindell, Drew T.; Koch, Dorothy M. and Streets, David G. (2008) *A*ir pollution radiative forcing from specific emissions sectors at 2030. Journal of Geophysical Research, Vol. 113.

U.S. Environmental Protection Agency (2007) *O*zone and Your Patients' Health Training for Health Care Providers. http://www.epa.gov/03healthtraining/population.html, Last updated October 11th, 2007.

West, J. Jason; Fiore, Arlene M.; Horowitz, Larry W. and Muzerall, Denise L. (2006) *G*lobal health benifits of mitigating ozone pollution with methane emission controls. PNAS, Vol. 103(11): p. 3988–3993.

Wikinews (2009) http://en.wikinews.org/wiki/Portal:Weather.

Wild, Oliver; Prather, Michael J. and Akimoto, Hajime (2001) *I*ndirect long-term global radiative cooling from NO_x emissions. Geophysical Research Letters, Vol. 28(D4): p. 4191–4207.